TNO Defence, Security and Safety

TNO report

TNO-DV 2006 A459

MFP-REA follow-up 2002-2005

Date	March 2007
Author(s)	Prof Dr D.G. Simons
	C.A.M. van Moll, MSc
Classification report	Ongerubriceerd
Classified by	ltz 1 drs. R.P.A. Dekeling
Classification date	14-02-2007
	(This classification will not change)
Title	Ongerubriceerd
Managementuittreksel	Ongerubriceerd
Abstract	Ongerubriceerd
Report text	Ongerubriceerd
Appendices	Ongerubriceerd
Copy no	7
No. of copies	24
Number of pages	92 (incl. appendices, excl. RDP & distributionlist)
Number of appendices	5

20070817259

AQ F07-11-12090

MFP-REA follow-up 2002-2005

Het geluid van brekende golven weerkaatst aan de zeebodem. Door met een verticaal array van hydrofoons dit geluid te registreren, komt informatie over deze bodem beschikbaar. Kan hiermee de bodemsoort bepaald worden?
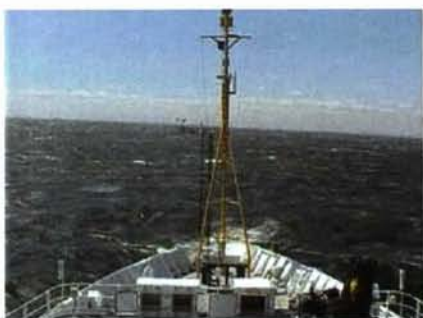
Probleemstelling

De Nederlandse marine heeft voor het gebruiken van sonardata kennis van de zeebodem nodig. Verschillende soorten bodems hebben namelijk heel andere effecten op de voortplanting van geluid onder water en daarmee op de prestaties van sonarsystemen. Door te meten hoe een uitgezonden signaal na weerkaatsing aan de bodem aankomt bij een ontvanger, kunnen de kenmerken van die bodem bepaald worden. Het heeft voor de marine echter grote voordelen als hiervoor, in plaats van een actief uitgezonden signaal, ruis veroorzaakt door wind aan het zeeoppervlak gebruikt zou kunnen worden. Dit heeft geleid tot de opdracht van de Nederlandse marine aan TNO Defensie en Veiligheid, locatie Den Haag, om te onderzoeken of omgevingsruis (ambient noise) gebruikt kan worden om snel de kenmerken van de omgeving, met name de zeebodem, te bepalen. Dit onderzoek is hiermee een

onderdeel van Rapid Environmental Assessment, REA.

Beschrijving van de werkzaamheden

Omdat het geluid van brekende golven voortdurend verandert en niet op voorhand bekend is, wordt het effect van weerkaatsing ervan aan de zeebodem gemeten door het verschil te bepalen tussen het geluid dat van boven en van onderen binnenkomt op een verticaal 'array' van hydrofoons. Het verlies aan intensiteit door de reflectie aan de bodem is afhankelijk van de hoek van ontvangst en van de frequentie (de toonhoogte) van de ruis. De manier waarop de kenmerken van de bodem inwerken op dit patroon van bodemverlies hebben wij beschreven met een model. De mate van detail van dit model is zo laag mogelijk gekozen, terwijl het patroon toch reproduceerbaar blijft. De combinatie van bodemparameters die het verschil tussen het gemeten en het berekende patroon zo klein mogelijk maakt gebruiken wij als schatter van de bodemkenmerken. Deze aanpak wordt Matched Field Processing (MFP) genoemd. Ondanks dat de bodem met slechts vijf parameters beschreven wordt, is het aantal mogelijke combinaties veel te groot om 'met de hand' de beste te zoeken. Daarom hebben wij een relatief nieuwe, zeer efficiënte, automatische zoekmethode verder ontwikkeld en

onderzocht. De combinatie van bodemverliesmodel en automatische zoekmethode is eerst toegepast op synthetische data en daarna op gemeten data. Speciale aandacht hebben wij besteed aan het statistisch interpreteren van de gevonden bodemkenmerken.

Resultaten en conclusies

Ook al zijn deze ideeën ongecompliceerd, toch is het op voorhand onzeker of ze ook werken. Internationaal is hier de afgelopen jaren veel onderzoek naar gedaan. In plaats van alles zelf uit te vinden, hebben wij ons met ons eigen onderzoek daar bij aangesloten. De resultaten van ons onderzoek in het kader van dit MFP-REA-project zijn gepresenteerd in artikelen in internationale tijdschriften. De daarin gegeven literatuur-verwijzingen geven een actueel overzicht van het onderzoeksterrein.

Toepasbaarheid

Het resultaat van ons onderzoek bevestigt dat - onder voorwaarden - de kenmerken van de zeebodem inderdaad met behulp van windruis bepaald kunnen worden. De voouitzichten zijn zelfs zo veelbelovend dat commerciële firma's operationele systemen ontwikkelen bestaande uit een kort verticaal array van hydrofoons, hangend aan een boei die de stroming van de zee volgt. Verwacht kan worden dat dergelijke

systemen binnen tien jaar op de markt
verschijnen, waarmee de kennis van de
zeebodem aanzienlijk toeneemt en daarmee
de gebruiksmogelijkheden van sonar.

PROGRAMMA	PROJECT
Programmabegeleider Itz 1 drs. R.P.A. Dekeling, DMO/DWS&B/RZS&B/S&W/OT	Projectbegeleider Itz 1 drs. R.P.A. Dekeling, DMO/DWS&B/RZS&B/S&W/OT
Programmaleider dr. ir. J.C. Sabel, TNO Defensie en Veiligheid	Projectleider ir. C.A.M. van Moll, TNO Defensie en Veiligheid
Programmatitel Onderwater propagatie en doelresponsie	Projecttitel MFP-REA
Programmanummer V029	Projectnummer 015.31956
Programmaplanning Start 01-01-2001 Gereed 31-10-2006	Projectplanning Start 01-01-2001 Gereed 31-10-2006
Frequentie van overleg Met de programma/project- begeleider werd regelmatig gesproken over de invulling en de voortgang van het onderzoek.	Projectteam prof. dr. D.G. Simons, ir. C.A.M. van Moll

Contents

Appendices
A Geoacoustic inversion of ambient noise: a simple method; IOA vol 23, 2001
B Geoacoustic inversion of ambient noise: a simple method; JASA vol 112, 2002
C Improved performance of global optimisation methods for inversion problems in underwater acoustics; ECUA 2004
D Inversion of shallow water ambient noise data by means of differential evolution as a global search method; ISCHIA 2004
E Sub-bottom profiling with ambient noise measured on a drifting vertical array; CRETE 2005

Abbreviations

DE	Differential Evolution
MFP	Matched Field Processing
PPD	Posterior Probability Distribution
REA	Rapid Environmental Assessment
VLA	Vertical Line Array

1 Introduction

For the assessment of sonar performance in shallow water, environmental knowledge is required. Increased deployment of navy units in shallow water areas therefore has made Rapid Environmental Assessment (REA) a hot issue. Combining this urgent need with the idea to make use of ambient noise data is too attractive to refuse. Bottom reflection loss can be derived from ambient noise received on a vertical array. By matching this loss to modeled loss, a method called Matched Field Processing (MFP), geoacoustic parameters can be estimated. This idea has been investigated in the research project MFP-REA. An overview of the ambient noise research is presented in this report.

The advantages of making use of ambient noise to get environmental information are obvious. No specialised sound source is needed and during the recording of the data even no ship is needed, allowing for covert operations. However, noise is an awkward phenomenon, difficult to grasp theoretically. A simple method to handle it would be a considerable advantage. Such a method is found and is the core of this research project. It is based on the idea of comparing the upward and downward received noise on a vertical array.

No REA devices are yet available for the navy's operations. But in depth research has resulted in state of the art knowledge of this research area. And, what is more, operational devices for REA are maturing fast.

This report discusses subsequent articles that present the research that has been performed for the MFP-REA project. A part of these articles is available in the appendix.

The first one presents the idea by means of the underlying physics. In the second paper five experimental datasets are used to elaborate these ideas and to discuss data quality issues. Environmental parameters can be derived by inversion methods, which require efficient global search methods. A relatively new method, called Differential Evolution, is shown to outperform existing methods by an order of magnitude in article number three and four. Number five discusses the limited information content of reflection loss data from ambient noise. Paper six presents a theoretical analysis of the effects of operational issues such as tilt in a vertical array, while number seven assesses the performance of a prototype freely drifting vertical line array buoy. An alternative method to derive sediment thicknesses directly from reflection loss data is described in article number eight, which method is compared with the inversion approach in the nineth paper. Number ten presents the efforts of a commercial firm to develop a buoyed array for rapid environmental assessment by means of ambient noise.

2 Overview of publications

To avoid violation of copyrights, not all the articles summarized in the following paragraphs are reproduced in the appendix. The full text of the papers of paragraph 2.1, 2.2, 2.3, 2.4 and 2.10 are in the appendices of this report. For the other papers we refer to their respective journals[1].

2.1 Geoacoustic inversion of ambient noise: a simple method (1)

C.H. Harrison, D.G. Simons, Proceedings of the Conference on Acoustical Oceanography, Southampton UK, 9-12 April 2001, (Proceedings of the Institute of Acoustics, Volume 23, 2001, pp 91-98).

Pioneering work on inverting ambient noise to deduce geoacoustic parameters has been successfully accomplished. This is done by comparing measured noise with that derived from a detailed noise model. This model requires as input a noise source distribution and environmental parameters such as bathymetry, sound speed profile and bottom reflection properties. It has been shown that, for range and azimuth independent environments and with uniformly distributed noise sources, geoacoustic parameters can be inverted by comparing measured and calculated noise, searching over a parameter space.

However, detailed and time varying input (such as sound speed profile) restricts the applicability of inversion with such a complicated noise model. This article, therefore, proposes an alternative approach, based on the strong influence of the seabed reflections on the vertical directionality of ambient sea surface noise.

Instead of matching a measured to a modeled noise signal, the proposed method matches reflection loss data. Seabed reflection loss can be derived relatively easy from noise received on a vertical array, by separating the upward from the downward field by means of beamforming. For a range independent environment and with uniformly distributed sea surface noise, a simple model suffices to reconstruct the plane wave reflection coefficient of the seabed. By matching this 'measured' and modeled bottom loss (i.e. the plane wave frequency and angle dependent reflection coefficient in dB units), inversion of geoacoustic parameters is possible.

The simplicity of the method to derive the seabed reflection loss (or bottom loss) can be understood by considering distant point sources, from which rays extend to the receivers after multiple surface and bottom reflections. For every ray arriving directly (i.e. most recently) from the surface, there is a corresponding ray arriving from the seabed with exactly one extra bottom reflection, the same number of surface reflections and almost the same horizontal wavenumber. So the intensity of the noise from all distant point sources, regardless of their strength, will appear weaker by the bottom reflection coefficient $R_b(\theta)$ for downward angle $-\theta$ than for equal upward angle $+\theta$. In addition the 'distant source' condition can be relaxed, to a source distribution that is close to uniform.

---

[1] For most of these papers a copy for personal use can also be acquired within a few days from the library of TNO Defence, Security and Safety. Phone +31 70 374 06 13 or e-mail gert.vis@tno.nl

The bottom reflection coefficient $R_b(\theta,f)$ not only depends on the elevation angle θ, but also on the frequency f. This frequency dependence not only comes from bottom interaction, but also from the beamforming required to measure the noise intensity arriving in the $+\theta$ and $-\theta$ directions on the vertical array. For low frequencies typically around 100 Hz, the angular resolution of the array degrades because of the limited length of the array. At frequencies above the design frequency of the array aliasing distorts the reflection loss pattern. Hence, a beam-smeared version $\hat{R}_b$ of the true reflection coefficient R_b is obtained.

Preliminary application of this method on experimental data gives promising results. For a moderately range dependent environment, in the absence of nearby shipping and for a nearly perfectly vertical array, the reflection loss for subsequent elevation angles can be derived accuralety, especially for higher frequencies. The technique is simple and requires little prior knowledge. Its performance needs to be demonstrated on experimental data under varying circumstances. Topics for further study are detailed inversion schemes to derive geoacoustic parameters from the bottom reflection loss pattern and counteracting the beam resolution problem at low frequencies.

2.2 Geoacoustic inversion of ambient noise: a simple method (2)

C.H. Harrison, D.G. Simons, Journal of the Acoustical Society of America, Volume 112 (number 4), October 2002, pp 1377 – 1389.

In principle it is possible to derive seabed properties from the bottom reflection loss of noise received on a vertical array. In this paper the potential of this method is demonstrated for experimental data from five sites (with water depths from 80 to 140 m). Special attention is given to data quality issues, while sophisticated techniques for searching parameter space are not applied. The main point is to demonstrate that a solution is possible.

The data are aquired with an experimental system, consisting of a moored 64 element vertical line array (VLA) roughly centered in the water column. Only the middle 32 regulary spaced hydrophones with half-meter separation were used for the noise calculations. The electronics provided a flat band between about 100 Hz and the design frequency of 1500 Hz. The sample frequency was 6 kHz. (These data are also used in the previous article.)

A theoretical analysis shows that the approach can tolerate arbitrary arrangements of distant ships and simultaneous local or distant wind noise, but that data containing nearby point sources that do not average out over time should be removed. Reflection loss versus frequency and angle is derived. Some propagation models can directly use this reflection loss, but if frequency-independent geoacoustic parameters are required, different analysis procedures can be applied. These procedures are not elaborated, since the main objective of this article is to focus on the derived (beam-smeared) bottom reflection loss data.

To take the effect of the finite beamwidth on the reflection loss into account a full noise model would be required. For demonstration purposes the derived (beam-smeared) bottom reflection loss data are compared here with reflection loss predictions under simplified assumptions. With uniformly distributed dipoles as noise sources and a range independent environment the directional noise can easily be calculated and the array

response can be estimated, knowing the beam pattern. These calculations are based on a three-layer (two boundary) model of the environment.

For several experimental datasets the up/down beamformed reflection loss is calculated and presented as an angle-frequency color plot. For comparison, 'correct' geoacoustic parameters for each specific site are taken from several reference sources.
These parameters are slightly adjusted to get a better agreement between the measured and the calculated beamformed reflection loss patterns. The calculated patterns are remarkably similar to the experimental plots, demonstrating the potential of the proposed method.

For each experimental data set the specific circumstances at the site had to be taken into account for generating the calculated reflection loss picture. In one case there was hardly any wind during the experiment. In this case anomalous patterns appear in the reflection loss picture, resulting from sidelobes of the beamforming to the remaining horizontal noise, while there is hardly any noise coming from up and down directions. However, if this happens, it is very obvious.

Several arguments indicate that the reflection loss derived with this method comes from the vicinity of the first bottom bounce, which is a function of angle. The consequence of this is that a drifting array could use this method to survey spatial bottom variations.

The article ends with an overview of analytical and experimental issues. Analytical matters are the effects of powerful directional sources, the consequences of sidelobes during beamforming and the inherent inversion ambiguity. Nonacoustic noise and array tilt are experimental issues. In spite of all conditions that have to be fullfilled, the method is still very promising and is now ripe for an automated search for geo-acoustic parameters.

2.3 Improved performance of global optimisation methods for inversion problems in underwater acoustics

Camiel van Moll, Dick G. Simons, Proceedings of the 7th European Conference on Underwater Acoustics, Delft, 5-8 July 2004.

Sometimes knowing reflection loss patterns does not suffice, but geoacoustic parameters are required. Matched field inversion problems in underwater acoustics relate to searching for that combination of environmental parameters that maximises similarity between a modelled and a measured pressure field. For instance, inversion of ambient noise looks for the best combination of sediment sound speed, sediment layer thickness, bottom attenuation and subbottom sound speed, that makes the calculated reflection loss similar to the measured loss.

Geoacoustic models mostly are strongly nonlinear, meaning that small parameter changes can cause big changes of the calculated model outcome. As a consequence, the best match between model and measurements is very unpredictable and global search methods must be applied. In essence these methods are random search methods: a combination of parameters is chosen at random and the distance of the resulting model outcome to the data is measured. The best combination is the one that minimises a distance function (also called energy function). To reduce the number of combinations that must be considered, a global search method applies certain rules to generate a new random combination of parameters.

Simulated annealing and genetic algorithms are well known and frequently applied global search methods. Differential evolution (DE) is a relatively new method, described in detail here, for which a better performance is claimed. DE resembles genetic algorithms in the sense that both improve a population of vectors during successive generations. In this article the claim is investigated by means of a complicated distance function with many local minima that the search algorithm has to escape from.

As performance criteria for optimisation methods, efficiency and robustness are considered. Since the forward model calculations take most of the computation time during optimisation, efficiency is measured by the required number of these calculations, typically a few tens of thousands. The stochastic nature of these methods causes that even a global search run can get stuck in a local minimum. Robustness is defined as the probability of an optimisation run to end in the global minimum. It is shown that with comparably high robustness (a probability of 0.99) DE requires only 2400 function evaluations instead of the 25600 of a genetic algorithm, an order of magnitude improved efficiency.

It is well known that the performance of optimisation methods depends on the specific energy function applied. Therefore it is not sure that DE is the best search method for geoacoustic inversion. However, since the energy function used has features similar to those known to be present in geoacoustic inversion - various local minima, parameter coupling and a varying sensitivity to the parameters, - the comparison of the methods suggests that DE is a very good method for geoacoustic inversion. Therefore DE will be used as the method for automated search of geoacoustic parameters by means of bottom reflection loss data derived from ambient noise.

Matched field inversion is an application of inverse theory. Addressing non-uniqueness and stability (a small perturbation to the data can lead to a large perturbation to the recovered model) are major issues in inverse theory. Because inverse theory estimates the best fitting model, the uncertainty of this estimate should be specified. These topics are not investigated in depth in this article.

2.4   Inversion of shallow water ambient noise data by means of differential evolution as a global search method

Dick G. Simons, Camiel van Moll, Chris H. Harrison, Proceedings of the 2nd Workshop on Experimental Acoustic Inversion Methods for Assessment of the Shallow Water Environment, Island of Ischia, 28-30 June 2004.

Deriving geoacoustic parameters from experimental data is far more difficult than from synthetic data. With experimental data a large part of control over the situation is sacrificed, especially the simplified description given by the bottom model leads to uncontrolled differences with the real world situation. However, using 'ground truth' geoacoustic parameter values derived from other sources (as in article 2), still gives some control over the situation. Sacrificing this prior knowledge leads to entering a huge parameter space - six dimensional in case the environment is modeled with six parameters - which is unsuited for investigating all parameter combinations. Automated global search methods are required. The main disadvantage of these methods is the introduction of ambiguous solutions; combinations of parameters that result in calculated bottom loss

that resembles measured bottom loss very well. From inverse theory it is known that these ambiguities are inevitable. Differential evolution is used as global search model.

This article gives a detailed description of the bottom loss models applied and of differential evolution. Experimental data from the 2000 Mapex experiment in the Mediterrenean are used. These data are inverted with a single sediment model, i.e. a single homogeneous sediment layer, overlying a uniform subbottom. Of 57 runs, 52 gave consistent results, allowing for an impression of the uncertainty of the parameter estimates. However, the bottom loss patterns derived from these parameter settings are much more in agreement with the measured bottom loss than that from the outcome of the hand-searching technique of article 2. The improved performance of differential evolution is demonstrated.

Since the experimental bottom loss pattern suggests the presence of a second sediment layer, the model is extended to two sediment layers overlying a subbottom half-space. Inversion of synthetic data made with this model was succesfully inverted, although also a second ambiguous solution was found. Inverting the experimental data with a two layer forward model is done 200 times, from which 114 succesful (low energy) runs are selected. These runs only show small differences between the first and second sediment layer, both in agreement with the single layer inversion results. This indicates that a single layer model suffices in this case.

2.5 Geoacoustic inversion of ambient noise reflection loss data

J. Dettmer, S.E. Dosso, M.K. Prior, C.H. Harrison, N.R. Chapman, Proceedings of the 7th European Conference on Underwater Acoustics, Delft, 5-8 July 2004

The information content of reflection loss data from ambient noise is limited. Therefore a full characterisation of the environment can not result from these data. With realistic synthetic reflection loss data - with similar characteristics as the experimental data of article 2 - the extent to which layer properties can be resolved is investigated. The minimum thickness of the top sediment layer and the maximum depth penetration are estimated.

To derive geoacoustic parameters, inversion is applied to synthetic ambient noise data. The parameter vector that makes the calculated reflection loss most similar to the synthetic loss gives a good estimate of the environment. However, an inversion problem can not be regarded solved as long as the parameter uncertainties are not determined. In Bayesian theory, the posterior probability distribution (PPD) is considered the complete solution of the inverse problem. This PPD gives credibility intervals for each of the estimated parameters and their correlation. In this way, confidence in the inversion solution can be expressed.

The forward model used during inversion, calculates the plane wave reflection coefficient R as a function of angle and frequency for an arbitrary set of fluid, homogeneous, horizontal layers. This reflection coefficient is applied to ambient noise due to breaking surface waves to model the upward and the downward field arriving at the vertical array. The effect of beamforming - required to separate both fields - is included, which smears out the reflection coefficient. Finally Gaussian distributed random noise is added to the synthetic data.

Each sediment layer is represented by 4 parameters: layer thickness, sound velocity, density and attenuation. The minimum layer thickness is resolved by using a single thin layer over a half-space. Several inversions with different layer thicknesses were performed. For each thickness the standard deviation of the upper layer parameters about their true values is determined. For synthetic data with a 200-1500 Hz frequency range, optimal resolution is reached around 0.7 m. For thinner layers, the method cannot resolve the sound speed of the layer.

The maximum penetration depth is derived by inverting two homogeneous layers above a half-space. The second layer is 1 m thick (exceeding the 0.7 m value) and its parameters can therefore be derived by inversion. The effect of increasing the thickness of the upper layer h_1 on the second layer parameter uncertainty is investigated. At $h_1 = 5$m the density of the second layer is no longer resolved for the synthetic data under consideration.

It should be kept in mind that frequency range and depth of penetration are determined by the array length and hydrophone density. However, this investigation has shown that it is possible to invert reflection loss data from ambient noise, where the depth penetration is in the order of a few metres.

2.6   Geoacoustic inversion of ambient noise: a modelling study

M.K. Donnelly, G.A. Matt, UDT Europe 2003

SEA, Systems Engineering & Assessment Ltd, is undertaking research with a dedicated ambient noise geoacoustic inversion system, based on a drifting VLA buoy. For this system a theoretical study aims at understanding key issues affecting performance. The system consists of a 32 hydrophone VLA suspended underneath a buoy. The design frequency of the array is 4 kHz, i.e. a hydrophone spacing of 0.1875 m. The sampling frequency is 12.288 kHz. In this way most of the frequencies of interest are covered. (Notice that the frequency range of this prototype system has shifted to frequencies higher than those of the experimental system of article number 2.). The environment taken into consideration is a range-independent 100 m deep isovelocity water layer overlying a two layer seabed.

For several situations synthetic data are generated, by successively modelling the vertically directed noise field for clearly defined environments (under simple conditions), calculating the response of the VLA (without array shading) and deriving the seafloor reflection coefficient. On such data a reflection coefficient analysis algorithm is applied, which resolves the first sediment layer thickness and sound speed, based on interference fringes which occur at high elevation angles. These parameter values are used as initial estimates for the inversion algorithm.

Theory states that the down-to-up in-beam noise power ratio resolves the seafloor reflection coefficient to within the angular resolution limits of the beamformer. This holds perfect for range-independent environments with a uniform sea surface noise source distribution. Modelled results indicate that the method still works with moderate range dependent environments and point sources in the far field. This sets the stage for three performance issues that need closer inspection. What is the effect of VLA tilt? What is the effect of an abrupt seabed change at a given range on the performance of the system? And what effect has a nearby point source (i.e. ship)?

Analysis of the consequences of array tilt shows that moderate tilt angles of up to 5° do not introduce significant errors. The rule of thumb is that errors introduced by tilt angles less than the beamwidth are tolerable.

With an abrupt change in the thickness of the first sediment layer from 1 m to 3 m at a range of 50 m the reflection coefficient analysis algorithm still gives acceptable estimates for sediment thickness and sound speed of the first layer. Since this algorithm makes use of the fringe pattern at steep angles, it inherently provides high spatial resolution and resolves the seafloor close to the VLA.

A strongly non-uniform noise source distribution violates the assumptions on which the method is based. With a ship at a range up to 3 km the method breaks down. But for the ship at 5 km distance the analysis algorithm still gives acceptable results (at 100 m water depth).

Attention must be given to the fact that the analysis is based on the outcomes of the reflection coefficient analysis algorithm and not on geo-acoustic parameter estimates resulting from full inversion. Analysis of the inversion results belongs to the next phase of work.

2.7 Measuring seabed reflection loss from ambient noise: an experiment in the north-west approaches to the UK

Marcus Donnelly, Proceedings of the 7th European Conference on Underwater Acoustics, Delft, 5-8 July 2004.

A data collection trial was conducted west of Scotland, a region for which several reference data (a borehole and seismic data) are available. The freely drifting VLA buoy mentioned in article 6 had the centre of the array at 58 m depth, approximately half way the water column of 137 m. Both ambient noise and noise from the trials vessel was recorded.

The seabed reflection coefficients derived from measured ambient noise are compared with modeled reflection loss from the reference acoustic data. The uncertainty margin for these reference data caused significant variation in the modelled reflection coefficients. The measured bottom loss from the ambient noise data agreed well with one of the modelled reflection loss figures, but this is no decisive confirmation that the so called 'measured bottom loss' is reliable.

As an extra check of this 'ambient noise bottom loss', it is used to calculate the modelled transmission loss over increasing ranges of the sound coming from the trial vessel. Because this sound was recorded at increasing ranges, the measured transmission loss is known. Both are broadly in good agreement. Also the modelled transmission losses are calculated for three seabed parameter combinations that are all within the reference uncertainty bounds. The transmission loss derived from the ambient noise bottom loss agrees very well with the modeled transmission loss for the 'High reflectivity' reference case.

From this investigation it was concluded that bottom reflection loss derived from ambient noise data, collected with a relatively short (6 m) VLA suspended from a freely drifting buoy, can provide useful and reliable information about the seabed.

2.8   Sub-bottom profiling using ocean ambient noise

Chris Harrison, Journal of the Acoustical Society of America, Volume 115
(number 4), April 2004, pp1505-1515.

Sound reflecting off a boundary experiences a reduction in amplitude as well as a phase
shift. Both effects are modeled in the reflection coefficient. The bottom reflection
coefficient inferred from directional ambient noise measured with a VLA, is derived as
a ratio of downward to upward received noise intensity. As a ratio of intensities
(incoming sound energy per square meter per second) this reflection coefficient only
contains amplitude information. What is normally called the reflection coefficient, is in
fact only its amplitude.

The missing phase information of the reflection coefficient can be restored from its
amplitude, under the condition that for a layered seabottom the first one of several
arrivals of noise reflected off multiple boundaries is also the strongest one.
The density difference between water and sediment normally takes care of this condition.
The phase of the reflection coefficient can then be reconstructed, using a technique
called spectral factorization.

Consider sound reflecting off the sea bottom under a single angle. In underwater
acoustics its reflection loss is usually treated as a frequency domain quantity.
The physical processes of sound reflecting at multiple boundaries can also be described
in the time domain, giving explicit arrivals from seabottom layers. Both descriptions are
related one-to-one by a Fourier transformation. The Fourier transform of the (frequency
domain) reflection coefficient (consisting of amplitude and phase) gives the (time
domain) impulse response of the seabed. This impulse response shows time arrivals of
the noise reflected off subsequent boundaries in the seabed. Multiplying these time
arrivals by the sound speed in water (1500m/s), instead of the true but unknown layer
sound speeds, gives approximate depths of the subsequent layers.

The way noise reflects off a boundary depends on its angle of incidence. Increasing angles
show increasing depths of the sea bottom layers, which can not be true. It appears that
only the higher grazing angles, say 70 - 90 degrees, give stable and reliable depths.
To derive a clear angle-depth picture, the amplitude of the reflection coefficient has to
be supplemented by its phase, since without the phase information the order of the
subsequent boundaries would be ambiguous.

Apart from an extensive explanation, this article describes the application of these
methods on experimental plane wave reflection coefficients derived from ambient noise
arriving on a VLA. The results look promising. With a drifting VLA buoy it was
possible to construct a bottom profile over 5 miles that agrees to some extent with a
sub-bottom profile obtained with standard seismic equipment.

2.9 Measurement of bottom layering and reflection using ambient noise

Chris H. Harrison, Proceedings of the International Conference on Underwater Acoustic Measurements: Technologies and Results, Heraklion, Crete, 28 June - 1 July 2005

This well written article gives a more extensive explanation of spectral factorization and investigates with simulated data the conditions for spectral factorization. The method performs well if the minimum phase assumption is met, which requires a high impedance contrast at the water sediment interface and relatively low contrast at subsequent layer boundaries.

More important is the following fundamental observation. To discriminate between upward and downward sea surface wind noise, a vertical line array is needed. By means of beamforming the reflection coefficient of the sea bottom for subsequent angles is derived. The more shallow grazing angles contain information about the upper sediment layers, but information about the deeper layers is contained in the reflection coefficients at steeper angles. However, every vertical array has the narrowest beams, and therefore the best resolving power, in the horizontal direction. At steep angles - the endfire of the VLA - the interference fringes become blurred because of the wide beam width. This limits the depth range of the method. Reduction of the beam width is possible by increasing the length of the array. However, operational requirements will restrict this length. Increasing the number of receivers does not result in narrower beams.

With this observation in mind, it is clear that a method that relies most on the steep angle reflection coefficients not only uses a small part of the information available in the total bottom loss picture, but even the part that is hindered most by the beam smearing effects at steep angles. In this respect it is sensible to consider the spectral factorization method as a preprocessing step for, for instance, an inversion method that makes use of the full bottom loss information at all grazing angles.

2.10 Sub-bottom profiling with ambient noise measured on a drifting vertical array

Simons Dick G., Snellen Mirjam, Weterings Ardien and Harrison Chris H, Proceedings of the International Conference on Underwater Acoustic Measurements: Technologies and Results, Heraklion, Crete, 28 June - 1 July 2005.

During an experiment in the shallow waters in the Mediterranean (near the Ragusa Ridge, south of Sicily), ambient noise is received on a drifting vertical array. From these experimental data a time series of bottom reflection loss is derived (using the up-down method), which is input to two different methods to infer the layering structure of the sea bottom. Both methods are compared by means of their resulting bottom profiles.

The first method uses a model to calculate the angle and frequency dependent reflection coefficient for a combination of geoacoustic parameters of the seabottom. For each geoacoustic parameter vector the difference between the calculated and measured reflection coefficient can be quantified. Inversion for the best parameter vector (the one with the smallest difference) is performed with Differential Evolution as global search method (cf article 4).

The second method obtains the seafloor layering in a direct manner. The calculations consist of supplementing the reflection loss with phase information and Fourier transforming the result, to derive the time arrivals of noise reflecting off subsequent bottom layers. Multiplying the time arrivals by the sound speed in water gives the layers thicknesses (cf article 8).

During the experiment the vertical array drifted 5 miles in 12 hours. With a footprint of order the water depth (130m) each method gives a considerable number of subsequent layer thicknesses. As a result one gets two bottom profiles each of which can be assessed for its consistency. Comparing both profiles shows considerable agreement, which gives confidence in both methods.

Although both methods use the same experimental reflection coefficients as input data, the time arrival method differs considerably from the inversion method in several ways. It derives its results directly and therefore needs far less computations than inversion does. Furthermore, inversion requires specification of the number of layers beforehand and it results in estimates of seabed parameters, such as layer thicknesses, sound speeds and densities. For the time arrival method the number of layers together with their estimated thicknesses are its outcome, without any other parameters. Since both methods are based on the same data they can supplement each other, with the time arrival method as a preprocessing step for the inversion. The random nature of the inversion method provides statistical information, such that the estimate for each of the parameters is accompanied by a confidence interval.

2.11 Seabed profiling with ambient noise

Marcus Donnelly, Sea Technology, June 2005.

The seabed properties can have a significant effect on the detection range of both passive and active sonar in shallow water environments. For sonar performance modelling, detailed acoustic characterisation of the seabed is not required; it suffices to have the correct acoustic reflection coefficient as function of grazing angle and frequency. In principle it is possible to derive this bottom loss by measuring the vertical directivity of sea surface noise received on a VLA. With such an array, the variation of noise intensity with vertical angle can be measured.

Based on this idea, Systems Engineering & Assessment Ltd. has the intention to make an operational system for rapid environmental assessment. As a prototype, a freely drifting VLA buoy has been demonstrated on three locations around the United Kingdom's coast. The environmental conditions during these experiments departed from those assumed during the set up of the theoretical approach. In spite of this, the derived reflection loss patterns agree with patterns to be expected from the known seabed types.

As soon as such a system has come to maturity, it is a highly attractive device. It derives its results quickly in terms of equipment deployability and data acquisition. It is able to resolve geophysical variability nearly real time and has minimal impact on the environment.

3 Conclusion

Using sea surface wind noise to derive environmental knowledge has big operational advantages for navies. No sound source is needed and no additional operational units are required during the recording of the data by the drifting VLA buoy.

In the proposed method, the angle and frequency dependent bottom loss is derived from the ratio of the downward and upward received noise intensity. For a range independent environment and with uniformly distributed sea surface noise, a simple model suffices to reconstruct this bottom loss. No complicated propagation or noise model is required and inversion methods can determine the unknown bottom parameters.

Both requirements of the bottom loss model can be mitigated. The method tolerates limited variability of the environment in range and azimuth. With a VLA, the footprint of the method is of the order of the water depth. The requirement of uniformly distributed sources is also relaxed. The method tolerates unknown source distributions and noise directionality, it is self compensating. Even distant point sources (ships) are acceptable. Although tilt of the vertical array causes smearing over the elevation angles, the method allows for a moderate tilt that stays within bounds set by the array's angle resolution.

The performance of the method depends on the hydrophone density and array length, which determine frequency range and depth of penetration. With half-meter separation of the hydrophones, the performance from 1000 to 1500 Hz is good and the method can complement low frequency active inversion techniques. The method explicitly shows the critical angles (and thus sediment sound speeds) and an indication of the number of layers. It is tolerant to poor quality data, although uncorrelated noise, such as quantization noise, reduces the dynamic range of the reflection loss. Nearby sound sources, however, lead to anomalous results and powerful directional sources can cause problems due to sidelobe leakage.

The method can give a good first assessment of the seabed. In those cases where only acoustical properties of the environment are needed, the method is even more promising, since it directly supplies accurate bottom reflection loss data. The strength of the method makes commercial firms eager to develop the required devices, suggesting that within several years operational systems can become available.
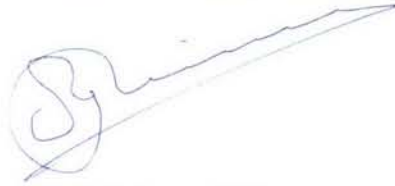
4 References

[1]   TUS SAS 03/B/EGS/PI/115-FFL,
       *LORA General Requirements - version 2, 'New Generation Long Range
       Classification'*,
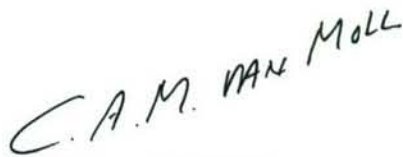   Brest, France, 21-08-03.

5   Signature

2509 JG The Hague, March 2007   TNO Defence, Security and Safety

F.P.G. Driessen, MSc   C.A.M. van Moll, MSc
Head of department   Author

A   Geoacoustic inversion of ambient noise: a simple method; IOA vol 23, 2001

Geoacoustic Inversion of Ambient Noise: A Simple Method.

C H Harrison[1], D G Simons[2]

[1]SACLANT Under Sea Research Centre, Viale S. Bartolomeo 400, 19138 La Spezia, Italy.
harrison@saclantc.nato.int
[2] TNO Physics and Electronics Laboratory, Oude Waalsdorperweg 63, 2509 JG The Hague, The Netherlands.
simons@fel.tno.nl

Abstract

The vertical directionality of ambient noise is strongly influenced by seabed reflections. Therefore, potentially, geoacoustic parameters can be inferred by inversion of the noise. In this approach, using vertical array measurements, the reflection loss is found directly by comparing the upward with the downward going noise. Modelling and parameter searching are minimised, and the method does not require a detailed knowledge of the noise source distribution.

1. Introduction

It is well known that in shallow water the coherence and directionality of ambient noise depend on the noise source distribution and environmental parameters such as bathymetry, sound speed profile and bottom reflection properties. In general, knowing the environment, one would require a detailed model to predict noise. Nevertheless pioneering work on inverting the noise to deduce geoacoustic parameters has been successfully accomplished [1,2,12] in environments that are range- and azimuth-independent, and where one can rely on the sources being uniformly distributed. In [2] a vertically separated pair of hydrophones was used to measure the broad band noise coherence, which was then compared with model calculations searching over geoacoustic parameter space.

In the Mediterranean, where shipping densities are high, the uniform source distibution assumption is frequently violated. Furthermore the source distribution may change over a period of hours, and there may be more dramatic changes associated with individual ships at short ranges. For this reason an alternative method (an extension of [12]) is investigated in this paper. It is shown below that it is indeed possible to make deductions about the seabed properties *without* knowing the detailed source distribution. In fact the reflection loss versus angle can be found directly by comparing the noise intensity arriving from equal up and down elevation angles. In some applications, particularly at high frequencies, a solution in the form of a reflection loss may be more appropriate or useful than the conventional geoacoustic parameters. An additional benefit is that we do not need a detailed noise model; the penalty is that we need a vertical array to resolve angles. Here we investigate this "inversion" technique using some experimental ambient noise data from south of Sicily. Ground truth is conveniently provided by some independent conventional geoacoustic inversion experiments carried out during the same trial.

2. Theory

The array response to a directional noise field and noise coherence can be represented as a wave integral of a Green's function (Equation 9.14 of [3]) or as an integral over ray arrivals [4, 5]. Here we choose the latter approach in order to allow for spatially varying environments and source distributions as has already been developed in [6]. Generally, given a noise directionality $D(\phi, \theta)$ (a function of elevation angle θ and azimuth ϕ) and the vertical array's beam pattern $B(\theta, \theta_s)$ for each steer angle θ_s, the array response $A(\theta_s)$ is given by

$$A(\theta_s) = \int \int D(\phi,\theta) B(\theta,\theta_s) \cos\theta \, d\theta \, d\phi \qquad (1)$$

It is shown in [6] that the directionality $D(\phi, \theta)$ can be expressed as two terms:

$$D(\phi,\theta) = Q(\theta) S(\phi,\theta) \qquad (2)$$

In the equivalent formula for coherence in [5,6] the beam pattern is simply replaced by a phase term. In equation (2), S is a complicated function of bathymetry, sound speed and noise source distribution including multiple arrivals, whereas Q is simply

$$Q(\theta) = \exp(-a\,s_p), \qquad\qquad\qquad \theta \geq 0$$
$$= R_b(\theta_b)\exp(-a(s_c - s_p)), \quad \theta < 0 \tag{3}$$

where $R_b(\theta_b)$ is the local (within one ray cycle of the receiver) bottom (power) reflection coefficient, and θ_b is related by Snell's law to θ at the receiver. The exponential terms represent respectively the attenuations along the residual parts of the ray directly from the surface (s_p) and directly from the bottom ($s_c - s_p$). If we could access the directionality itself, dividing the down D by the up D would give

$$\frac{D(\phi, -\theta)}{D(\phi, +\theta)} = \frac{Q(-\theta)}{Q(+\theta)} = R_b(\theta_b)\exp(-a(s_c - 2s_p)) \tag{4}$$

Since this is true for all azimuths ϕ it is also true for the azimuth integral $\int D(\phi, \theta)\,d\phi$. Assuming that the effects of absorption over one ray cycle are small we obtain

$$\frac{\int D(\phi, -\theta)\,d\phi}{\int D(\phi, +\theta)\,d\phi} = R_b(\theta_b) \tag{5}$$

Given appropriate angular resolution in (1) we can actually measure R_b as a function of θ and hence θ_b since the beam response tends to the noise directionality D.

The reason for this simplicity, despite inclusion of spatial variation of the environment and noise source distribution, can be seen as follows. Imagine a distant point noise source from which a single ray extends, after multiple surface and bottom reflections, to the receiver. For every such ray arriving directly (i.e. most recently) from the surface, there is a corresponding ray arriving from the seabed with exactly one extra bottom reflection, the same number of surface reflections and almost the same horizontal wavenumber. Provided the environment changes only slowly over one ray cycle, the slight shifts in position of reflection points have no effect. So all distant point sources, regardless of their strength, will appear weaker by $R_b(\theta_b)$ for downward θ than for upward θ. In addition we can relax the 'distant source' condition provided the source distribution is close to uniform as in the subsequent part of [6]. Thus this approach can tolerate arbitrary arrangements of distant ships and simultaneous local or distant wind noise.

For later reference we note that the function S in (2) reduces to

$$S(\phi, \theta) = \sin\theta_t\,/[1 - R_t(\theta_t)R_b(\theta_b)\exp(-as_c)] \tag{6}$$

with R_t and θ_t being surface loss and surface angle respectively, in the case where the noise sources are uniformly distributed dipoles.

3. Experiment

In May 1999 a set of experiments (ADVENT99) was carried out near the Adventure Bank, south of Sicily. An anchored 64-element vertical array was used for the noise measurements. The same array was used in conjunction with sound sources both fixed and towed by SACLANTCEN's ship, RV Alliance, for conventional geoacoustic inversion experiments (unpublished [7]). The 62 m array was centred in the 80m water depth, and although all 64 hydrophones were available only the middle 32 regularly spaced ones (at half metre separation) were used for these noise calculations. Noise was sampled at 6 kHz on an automatically repeated sequence of two roughly 15 second (90112 samples) windows every four minutes (at 0.5 and 3.5 min). The electronics provided a flat band between about 100 Hz and 2 kHz. Processing consisted of manually selecting portions without obvious contamination (unpublished [8]) and then beam-forming them in the frequency domain using MATLAB. The beam-formed array response can be determined conveniently by calculating the cross-spectral density between all pairs of channels, $C_{ij}(f)$, using a ready-made MATLAB routine including FFT averaging [9], then multiplying by the steer vectors $w_i(\theta_s, f)$, $w_j(\theta_s, f)$ for frequency f and summing

$$A(\theta_s, f) = \sum_i \sum_j w_i(\theta_s) C_{ij}(f) w_j(\theta_s) \tag{7}$$

An example of the beam-formed spectrum for the middle 32 hydrophones is shown in Figure 1. One can immediately see that there is more noise from above (top part of figure) than from below (bottom of figure) and that the picture is dominated by the poor angular resolution of the array at low frequencies. The design frequency of this middle part of the array is 1500 Hz and there is a clear grating lobe contribution arcing from $+90°$ at 1500Hz to $+40°$ at 2000 Hz. An anti-aliasing filter cuts the response off at about 2 kHz.
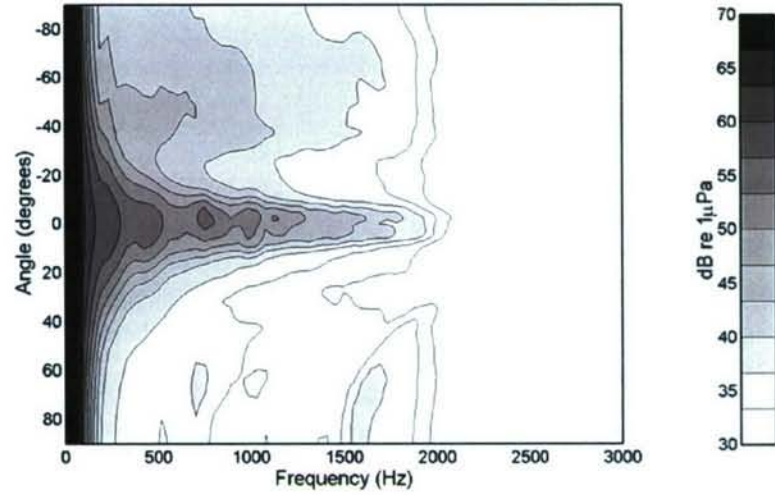
Figure 1 Beam-formed ambient noise spectrum measured on a 32-element vertical array.

The conventional geoacoustic inversion using low frequency sweeps (150-850 Hz) [7] led to the inferred optimum parameters at the ranges shown in Table 1. In the current context we regard these values as "ground truth".

Parameter	2 km	5 km	10 km
Sediment speed c_s (m/s)	1559±8	1568±7	1569±32
Sediment thickness h (m)	4.3±0.7	5.4±0.7	6.6±6.7
Attenuation α (dB/λ)	0.4±0.06	0.5±0.06	0.6±0.20
Density ρ (g/cm^3)	1.53±0.05	1.50±0.2	1.58±0.10
Sub-bottom speed c_b (m/s)	1637±17	1742±51	1702±68

Table 1: Ground truth – environmental parameter estimates taken from [7].

4. Simulation

Because of the problem of angle resolution it is wise to estimate its effect on the array response. Substituting (2) into (1) and dividing downward by upward array response we obtain the ratio of beam responses $\Re$, which is an approximation to R_b

$$\frac{A(-\theta_s)}{A(+\theta_s)} = \Re(\theta_s) \tag{8}$$

We note that, although S does not truly cancel out, its influence on the ratio $\Re(\theta_s)$ is weak. Therefore we assume that an estimate of S under the ideal conditions of a uniform noise source distribution, as in (6), will suffice. First we take the ground truth data (for 2 km) with an assumed sound speed of 1510 ms^{-1} just above the sediment, and we calculate the bottom reflection loss (RL=$10\log_{10}(R_b)$) versus angle using SAFARI [10]. Then we substitute this into (6) with $R_t=1$ and as$_c \to 0$, and we calculate the array response ratio $\Re(\theta_s)$ as distinct from the directionality ratio in (5).

Figures 2(a-d) show a set of comparisons between $\Re(\theta)$ and $R_b(\theta)$ at frequencies of 100, 300, 500, 1000 Hz. One can immediately see the smoothing effect of the beam pattern. The interference nulls (caused by the interference between the upper and lower boundaries of the sediment) are covered up, and more seriously, at low frequencies the beampattern averages so much that the high loss part of the RL curve (high angles) is biased towards a low value. The only solution is to improve the angle resolution by, for instance, adaptive beam forming, or to attempt to deconvolve the known beam pattern.
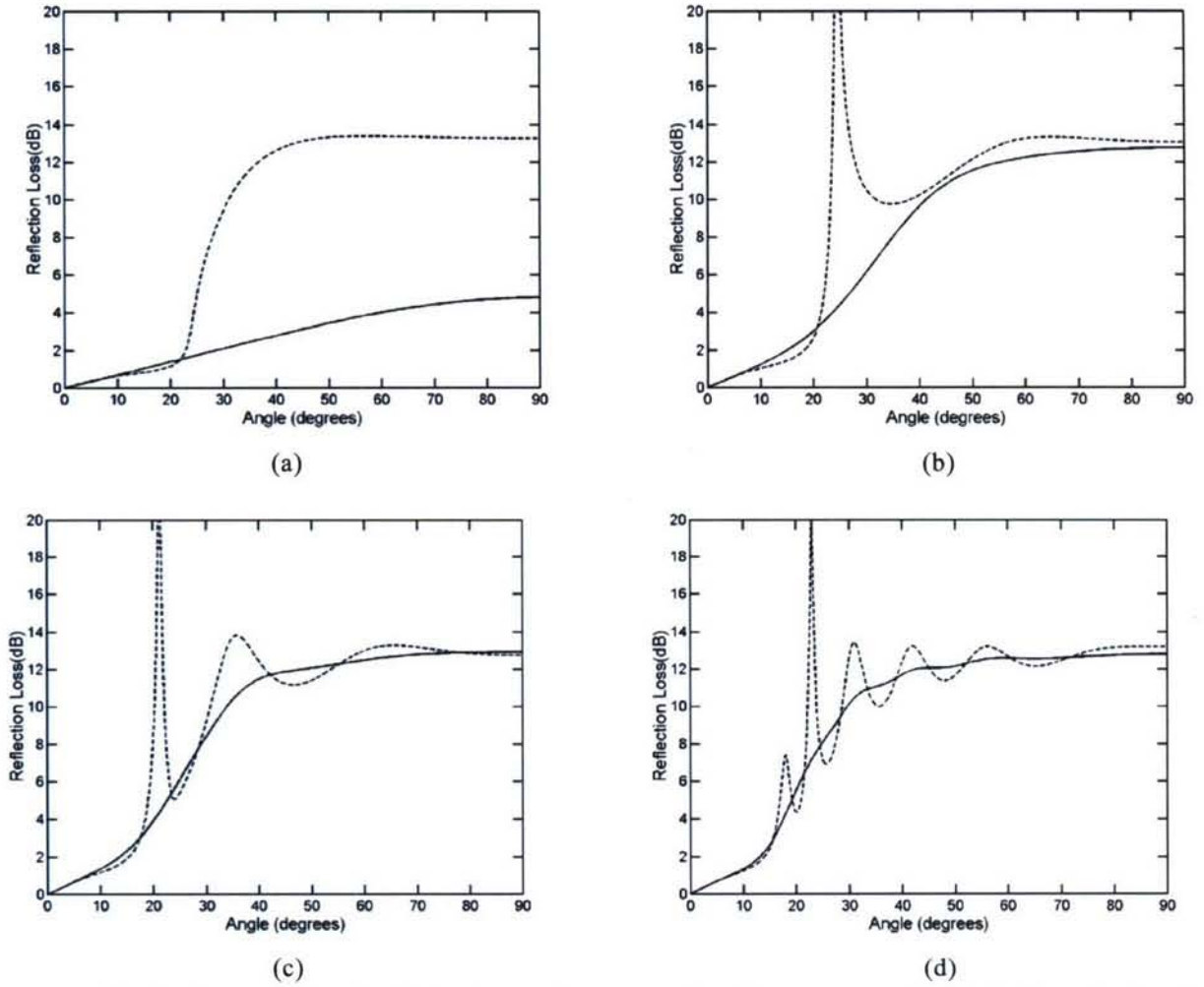
(a)   (b)

(c)   (d)

Figure2 Reflection loss calculated with SAFARI using 'ground truth' parameters, R_b (dashed), and ratio of array responses, $\Re$ (solid); at (a) 100 Hz, (b) 300 Hz, (c) 500 Hz, (d) 1000 Hz.

The 'before' and 'after' effect on the complete reflection loss *vs* angle and frequency can be seen conveniently by first taking the formulae in Section 1.6.3 of [3] to evaluate the three layer problem, and then applying the same beam spreading to it. This is shown in Figures 3(a,b).

5. Analysis of results

We have several options with the noise data. We can collect together the usable sections of noise with the aim of averaging out local changes in directionality. Alternatively we can look at 15 second blocks of noise gathered at different times of day with the aim of checking the sensitivity of the method to changes in source distribution. In a separate experiment in the vicinity, MAPEX2000 (unpublished [11]), noise measurements made with a 256 element horizontal array detected about 14 ships passing in 4 hours. It is thought that there were no ships close enough to spoil the 'distant ship' approximation of Section 3, although clearly a non-uniform and evolving distribution is to be expected. Invariance of the quantity $\Re(\theta)$ in (8) would provide some confidence in the theory.

Figure 4(a-d) shows the quantity $10 \log_{10}\Re(\theta)$ calculated from the VLA array response according to (8) for four separate 15 second blocks each about one hour apart. (The angle has been corrected from that at the receiver to that at the seabed on the assumption that the respective sound speeds are 1505 and 1500 ms^{-1}.) The array response is calculated for 181 steer angles from the cross-spectral density (128-point FFT, sampling at 6000Hz with averaging over the 15 seconds using the MATLAB function CSD)
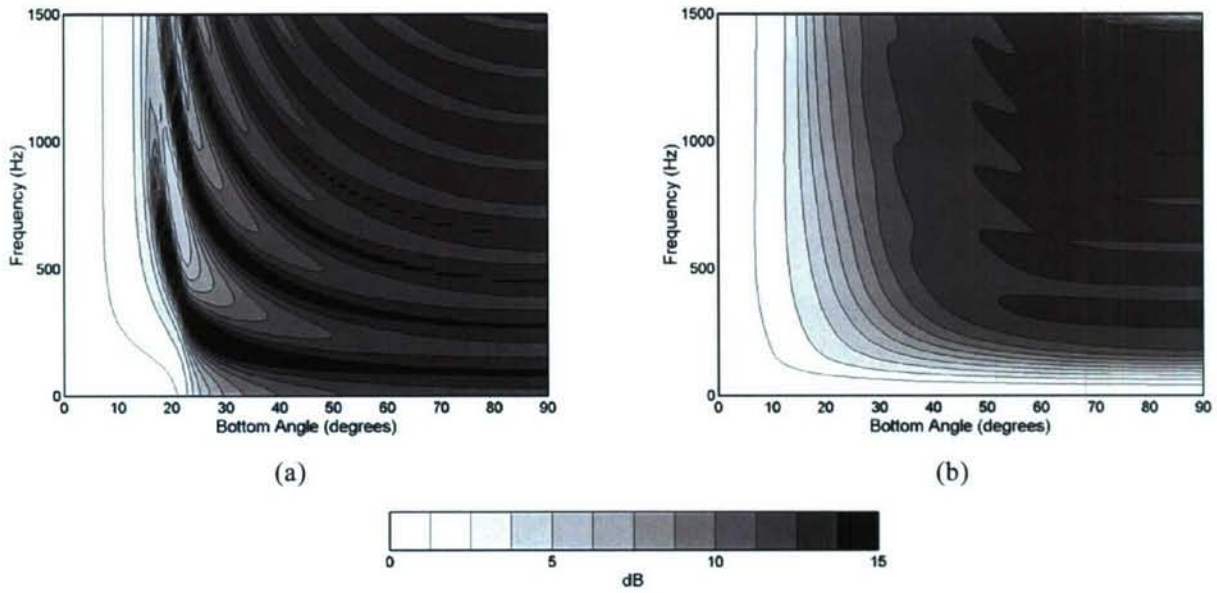
Figure3 Reflection loss (a) calculated with 3-layer formula from [3], (b) including simulated beam forming.

Although there are slight differences the main features appear not to change with time. In contrast the array response for these same times (Figure 5(a-d)) does show significant variation particularly near horizontal. This suggests, as we hoped, that $\Re(\theta)$ does not depend on source directionality and is simply a function of the array's position.

There are some additional interesting features in Figure 4. As expected from Figure 2, at low frequencies $10 \log_{10}\Re(\theta)$ is flatter than the true $10 \log_{10}R_b(\theta)$. For frequencies between about 200 Hz and 1500 Hz (the design frequency for this vertical array) the variation with angle resembles theory. There is a slow rise in loss up to the critical angle followed by a rapid rise to a plateau beyond, as we saw in Figure 2. However the peak is not at 90°, in fact Figure 4(a), in particular, shows a hint of fringe patterns following a law of the form $f \times \sin(\theta)$ = constant. Unfortunately we might expect such behaviour from modal phenomena, array side lobe phenomena or even sediment layer thickness phenomena, so we cannot use it to discriminate. Nevertheless the resemblance to the computed reflection loss versus angle and frequency shown in figure 1.24 of [3] and Figure 3 here is quite striking.

The peak value of $10 \log_{10}\Re(\theta)$ is around 10 dB, whereas the plateau in Figure 2 is at about 13dB. At these steep angles the Rayleigh reflection coefficient for a half-space simply depends on the density-sound-speed product, so there is limited scope for altering it. For instance, if we set $\rho c=2$ the bottom loss is 9.54dB. A more likely explanation for the discrepancy is the addition of non-acoustic noise to the hydrophones. This will have the effect of disproportionately boosting the weak upward-going signal, thus making the bottom appear to be a stronger reflector. It is also possible, though unlikely in these examples, that the upward-going signal is contaminated by the side lobes of the often much stronger horizontal noise.

In this experiment the data were transmitted via a radio buoy, offset horizontally from the array via a bottom cable at a nominal distance of 130 m. A potential complication is that splashes at the buoy would appear as spatially biased noise. However the direct elevation angle to the buoy is relatively small (17°). Also in Figure 5 there is no obvious single feature at a corresponding angle for all frequencies, which suggests that the buoy is not a problem.
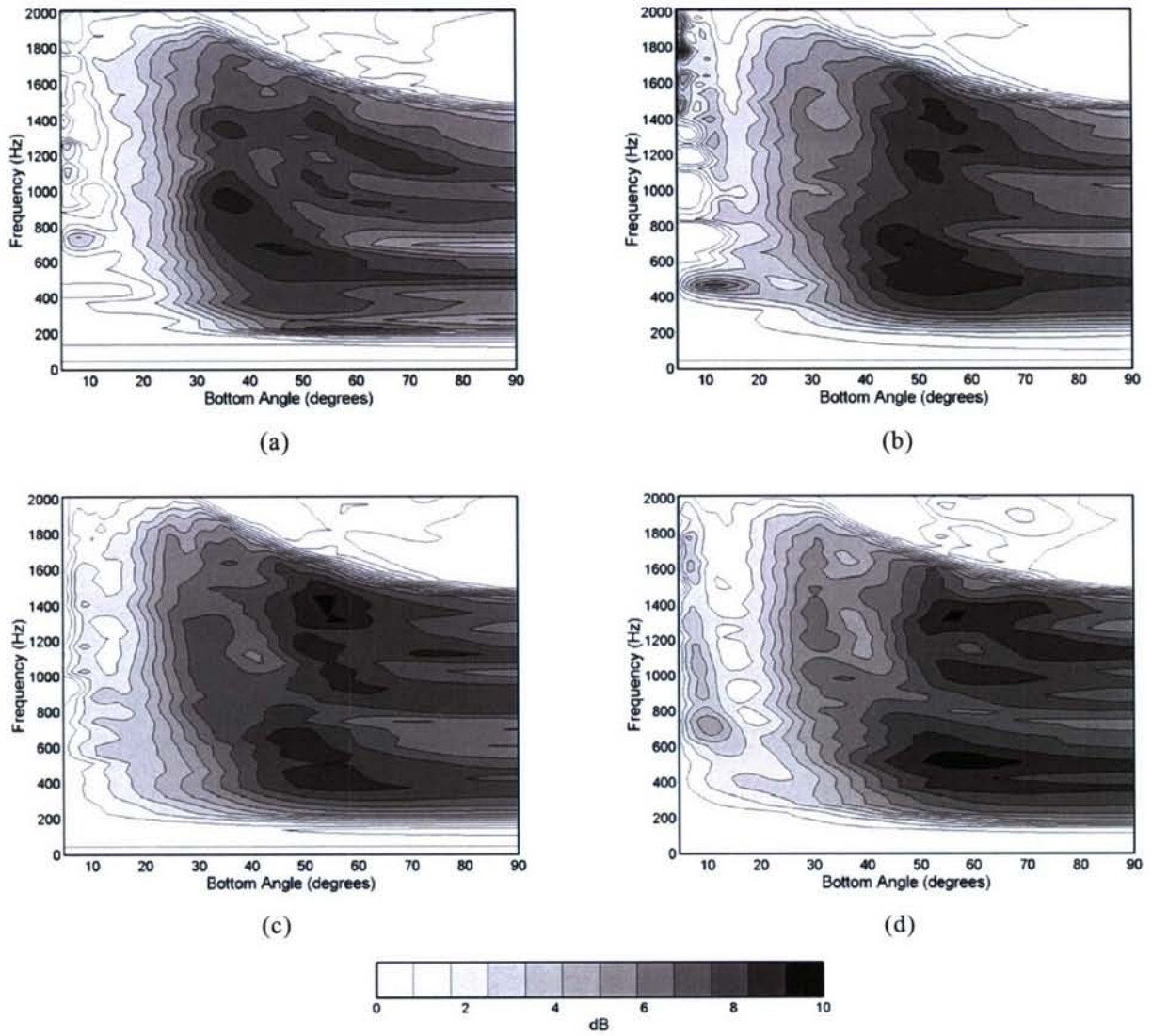
Figure 4 Inferred Reflection Loss versus angle and frequency at four times (a,b,c,d) roughly one hour apart.

Slight asymmetry of the peaks in Figure 5 will lead to an anomalous kink near zero grazing angle in reflection loss, as seen in Figure 4 (particularly (b) and (d)). A possible cause of this frequency dependent asymmetry could be that there are several distant ships contibuting from different azimuths to a slightly tilted array. Thus spectral lines from various azimuths in the horizontal plane are interpreted as deviating from horizontal in a complex manner.

Finally we form the average relection loss (Figure 6a) by first taking the power average of the four array response examples (Figure 6b).
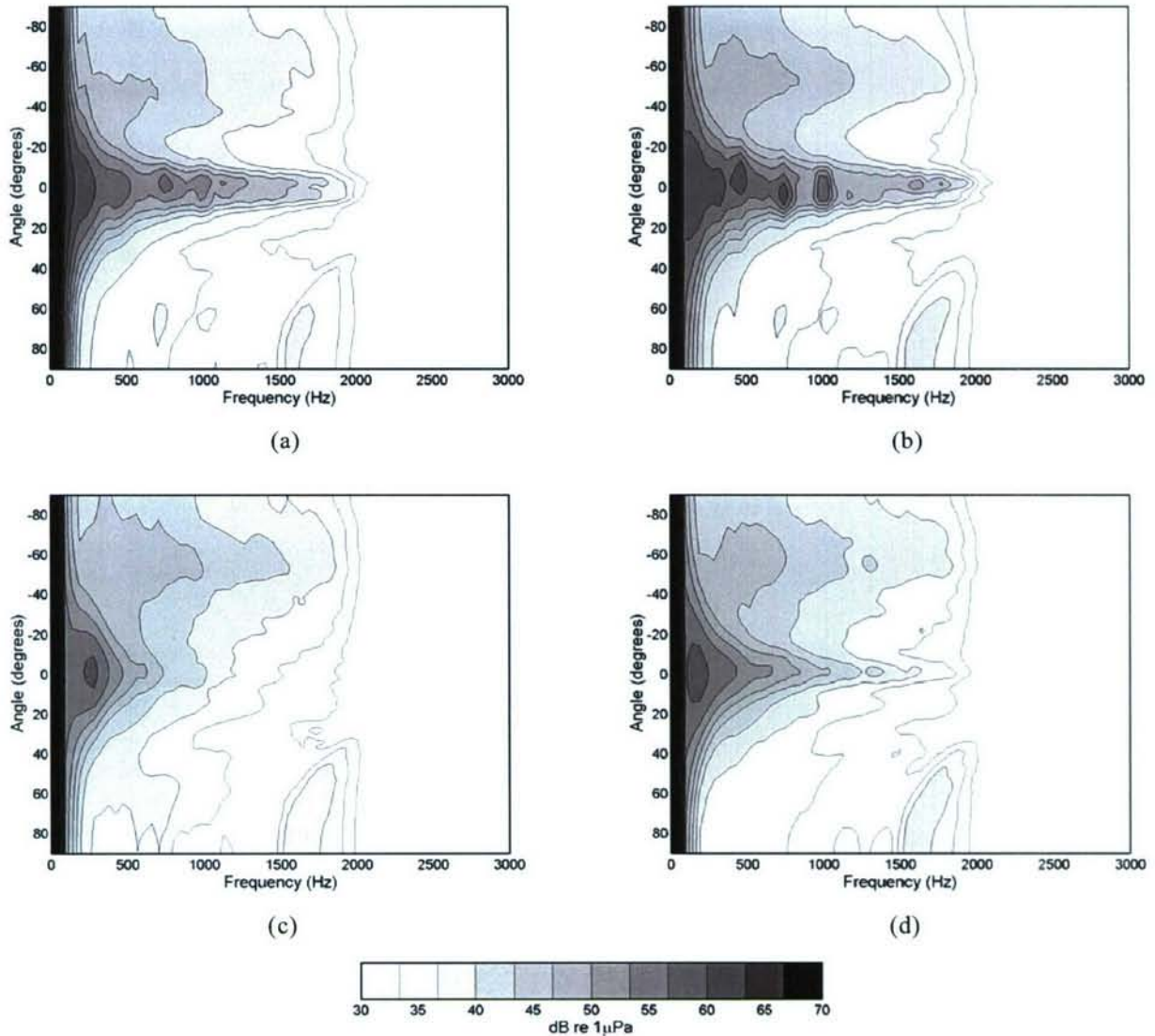
Figure 5 Beam-formed Array Response versus frequency at four times (a,b,c,d) roughly one hour apart.

6. Conclusions

A simple technique for extracting geoacoustic parameters from ambient noise measurements has been proposed and tried out with experimental data. Unlike coherence-based methods that use a hydrophone pair, this technique does not require a noise model. It can therefore still work when the noise directionality and bathymetry are unknown. The method works best at high frequencies because of the vertical array's limited angular resolution at low frequencies. Interestingly this complements conventional active inversion techniques where sound speed fluctuations impede model matching at high frequencies. It is suggested that the invariance of the inferred reflection loss (Figure 4) coupled with the variability of the array response (Figure 5) provides evidence that the method is sound. It is likely that some of the anomalies found are caused by poor quality data. For instance, the maximum value of reflection loss (at high angles) is often not as great as expected, but this can be explained by contamination with non-acoustic noise. Since first draft better quality data has been collected at several sites south of Sicily and near Elba.

Topics for further study might include detailed inversion schemes and possibly ways of counteracting the beam resolution problem.
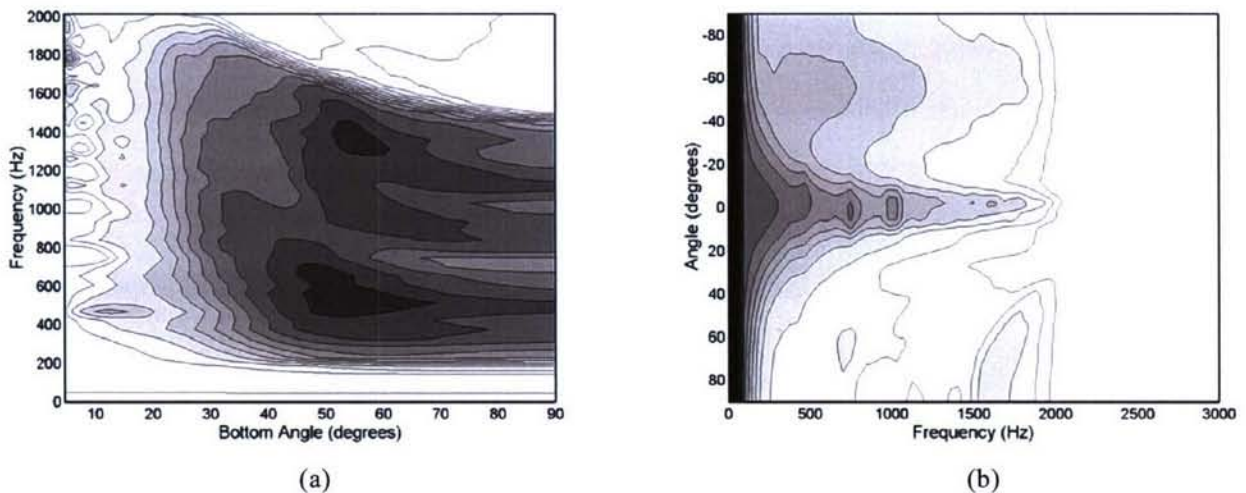
(a)

(b)

Figure 6 Reflection Loss (a) derived from the power averaged array responses (b) seen in Figs 4 and 5. Grey scales unchanged.

References

[1]   Buckingham MJ and Jones SAS. A new shallow-ocean technique for determining the critical angle of the seabed from the vertical directionality of the ambient noise in the water column. *J Acoust Soc Am* 1987; **81**: 938-946

[2]   Carbone NM, Deane GB and Buckingham MJ. Estimating the compressional and shear wave speeds of a shallow water eabed from the vertical coherence of ambient noise in the water column. *J Acoust Soc Am* 1998; **103**: 801-813

[3]   Jensen FB, Kuperman WA, Porter MB, Schmidt H. Computational Ocean Acoustics. AIP Press, New York, 1994, pp. 521

[4]   Chapman D. Surface-generated noise in shallow water: A model. *Proceedings of the IOA Conference* 1988, **9**: 1-11

[5]   Harrison CH. Formulas for ambient noise level and coherence. *J Acoust Soc Am* 1996; **99**: 2055-2066

[6]   Harrison CH. Noise directionality for surface sources in range-dependent environments. *J Acoust Soc Am* 1997; **102**: 2655-2662

[7]   Siderius Martin, Nielsen Peter, Sellschopp Jurgen, Snellen Mirjam, Simons Dick. Optimized sound propagation modeling in a time varying ocean environment. Submitted to *J Acoust Soc Am*

[8]   Harrison CH. Non-acoustic interference on the 64 element VLA. SACLANTCEN Report, submitted

[9]   MATLAB Signal Processing Toolbox. The Math Works Inc 1998

[10] Schmidt H. SAFARI User's Guide. SACLANTCEN Report SR-113, 1988.

[11] Harrison CH. Noise measurements during MAPEX2000, SACLANTCEN Report, submitted

[12] Aredov AA, Furduev AV. Angular and frequency dependencies of the bottom reflection coefficient from the anisotropic characteristics of a noise field. *Acoustical Physics* 1994; **40**: 176-180.

B   Geoacoustic inversion of ambient noise: a simple method; JASA vol 112, 2002

Geoacoustic inversion of ambient noise: A simple method

C. H. Harrison[a]

SACLANT Undersea Research Centre, Viale S. Bartolomeo 400, 19138 La Spezia, Italy

D. G. Simons[b]

TNO Physics and Electronics Laboratory, Oude Waalsdorperweg 63, 2509 JG The Hague, The Netherlands

The vertical directionality of ambient noise is strongly influenced by seabed reflections. Therefore, potentially, geoacoustic parameters can be inferred by inversion of the noise. In this approach, using vertical array measurements, the reflection loss is found directly by comparing the upward- with the downward-going noise. Theory suggests that this simple ratio is, in fact, the power reflection coefficient—potentially a function of angle and frequency. Modeling and parameter searching are minimized, and the method does not require a detailed knowledge of the noise source distribution. The approach can handle stratified environments and is believed to tolerate range dependence. Experimental data from five sites, four in the Mediterranean, one on the New Jersey Shelf, are described. Most of the Mediterranean sites had temporally varying noise directionality, yet yielded the same reflection properties, as one would hope. One site was visited in conditions of very low surface noise. This paper concentrates on an experimental demonstration of the feasibility of the method and data quality issues rather than automatic search techniques for geoacoustic parameters. © 2002 Acoustical Society of America. [DOI: 10.1121/1.1506365]

I. INTRODUCTION

It is well known that in shallow water the coherence and directionality of ambient noise depend on the noise source distribution and environmental parameters such as bathymetry, sound-speed profile, and bottom reflection properties. In general, knowing the environment, one could use a detailed propagation model to predict noise. Potentially, one could therefore deduce bottom properties from the noise without a specialized sound source or even a ship. Pioneering work on inverting the noise to deduce geoacoustic parameters has been successfully accomplished [Buckingham and Jones (1987); Carbone *et al.* (1998); Aredov and Furduev (1994)] in environments that are range- and azimuth independent, and where one can rely on the sources being uniformly distributed. Carbone used a vertically separated pair of hydrophones to measure the broadband noise coherence, which was then compared with model calculations searching over geoacoustic parameter space.

In the Mediterranean, where shipping densities are high, the uniform source distribution assumption is frequently violated. Furthermore, the source distribution may change over a period of hours, and there may be more dramatic changes associated with individual ships at short ranges. For this reason an alternative method [an extension of Aredov and Furduev (1994)] is investigated in this paper. A preliminary account of this work was given by Harrison and Simons (2001). It is shown below that it is indeed possible to make deductions about the seabed properties *without* knowing the detailed source distribution. In fact, the reflection loss versus angle can be found directly by comparing the noise intensity

arriving from equal up and down elevation angles. In some applications, particularly at high frequencies, a solution in the form of a reflection loss may be more appropriate or useful than the conventional geoacoustic parameters. An additional benefit is that we do not need a detailed noise model, but on the other hand we do need a vertical array to resolve angles. Here, we demonstrate the potential of the method with experimental data from five sites in the Mediterranean and one on the New Jersey Shelf. A future paper will discuss techniques for automatic geoacoustic parameter searching.

Ground truth is conveniently provided by independent conventional geoacoustic inversion carried out either during the same experiments or on different occasions. There are also a number of cores and geoacoustic models in most of the areas. Specific references will be made later.

II. THEORY

A. Noise theory

It is fairly obvious that the noise field depends on the reflection properties of the seabed, but not so obvious that the plane wave reflection coefficient is so simply related to the noise directionality. The array response to a directional noise field can be represented as an integral over ray arrivals [Chapman (1988), Harrison (1996)] or as a wave integral of a Green's function [Eq. (9.14) of Jensen *et al.* (1994)]. The ray approach for a range-dependent environment is spelled out in the Appendix. Here, we avoid these cumbersome derivations by choosing a simple energy flux argument to explain the effect in a more concise and convincing way.

Consider a block of sea water, Fig. 1, bounded by the sea surface, the seabed, and two vertical imaginary lines (planes) in an otherwise infinite horizontally uniform, vertically stratified environment. Insert an infinite source layer at

[a] Electronic mail: harrison@saclantc.nato.int
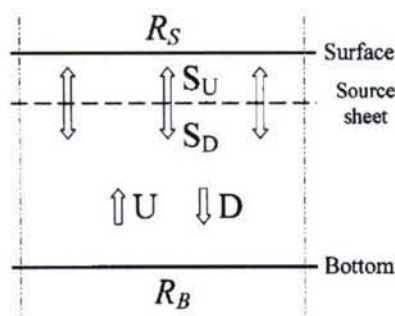[b] Electronic mail: simons@fel.tno.nl

FIG. 1. Diagram showing a finite block from an infinitely wide range-independent sea. Although sound may propagate obliquely the horizontal flux balances out, so here we only show the vertical components. Up- and down-going components of (plane wave) flux S_U, S_D emanate from a horizontal sheet source just below the sea surface. The vertical balance leaves components U and D in the body of the water, which are simply related to the bottom reflection loss R_B.

some small (finite) depth below the surface. Now, consider the balance of the upward and downward component of flux in the box (both above and below this source sheet). Note that because of the horizontal uniformity there is no net horizontal flux, so we can ignore the horizontal component. We regard the infinite source as emitting an incoherent plane wave (as a distant light bulb would!) at a given angle which subsequently obeys Snell's law at the various depths. Let the sheet source emit flux S_U upwards and S_D downwards (at the given angle). Beneath the source we define upward and downward fluxes (at the corresponding Snell angle) as U and D, respectively. Just below the source the total downward flux includes the surface reflected upward-going flux

$$D = S_D + R_s(S_U + U), \tag{1}$$

where R_s is the surface power reflection coefficient.

By the definition of the bottom power reflection coefficient R_b, we have

$$U = D R_b. \tag{2}$$

If we define an "effective" source strength S (since R_s may not be unity) as

$$S = S_D + R_s S_U, \tag{3}$$

then we find

$$D = S/(1 - R_s R_b), \tag{4}$$

$$U = R_b S/(1 - R_s R_b). \tag{5}$$

These are exactly the formulas obtained by Chapman (1988) and Harrison (1996) [also seen in Eqs. (A6) and (A3) of the Appendix and Harrison (1997a)] but with volume absorption set to zero. Including absorption in the flux argument is straightforward. Dividing Eq. (5) by Eq. (4), we obtain the up-to-down noise ratio which is evidently the same as Eq. (2). This is no surprise since it is the definition of reflection coefficient! If we now put a receiver in this field we can measure U and D, and hence deduce R_b, but clearly the original field consisted of plane waves so we will deduce a *plane wave reflection coefficient*. Also, the ratio depends on local bottom properties, i.e., within about one ray cycle for the angle in question.

Note that no matter where the sources are, as long as they are far enough away or large enough to be considered plane wave sources, Eq. (2) is always true. Therefore, the underlying tenet of this paper still holds. The plane wave condition reduces to being able to ensure that U, D at the receiver are substantially the same as at the bottom. Clearly, local point sources (that cannot, in some way, be spatially or temporally averaged out) violate these assumptions.

This is a powerful derivation for the following reasons:

(i)   We have made no assumption about rays, modes, or waves.

(ii) We have made no assumption about the dipole or monopole nature of the source.

(iii) We have made no assumption about the spectrum of the source.

(iv) Refraction makes no difference to the argument as long as energy gets from the surface to the receiver via the bottom (see the Appendix for more details).

(v)   A small net horizontal component of flux does not alter the vertical component. Therefore, neither non-uniform distant sources nor range-dependent environments spoil the argument (see the Appendix for more details).

Thus, this approach can tolerate arbitrary arrangements of distant ships and simultaneous local or distant wind noise. However, nearby point sources (with slight asymmetry in eigenray angles) that do not average out over time lead to problems that can nevertheless be anticipated and isolated by inspection of the array's beam response.

A dramatic demonstration of the correctness of the theory (at least for range-independent environments) is given by Harrison and Baldacci (2002). Within the confines of one wave model, one can construct both the "ground truth" reflection loss and the result of the proposed VLA processing technique. First, OASR [Schmidt (1999)] was used to calculate the bottom reflection loss for a given environment (similar to the Sand site, Sec. IV A later); a preview is shown in Fig. 2(a). Then, the array response to a sheet noise source was found from the correlation matrix option of OASN [Schmidt (1999)], and the up-to-down noise ratio was obtained from it [Fig. 2(b)]. In this example the array spans the full water column and these two plots are very nearly identical. Naturally, as the array size is reduced the deduced reflection loss gradually degrades.

B. Possible analysis procedures

There are several ways we can process this type of VLA data. First, it is possible to leave the output as reflection loss versus frequency and angle since this is exactly what is required for some propagation models, e.g., ray traces. Furthermore, it is possible to make comparisons with other reflection measurement techniques such as the "move-out" method where pulse travel times and known geometry allow direct measurement [Holland and Osler (2000)]. Second, it is possible to try to convert the data to frequency-independent geoacoustic parameters by using a search algorithm and a plane wave reflection formula or model (as opposed to a

noise model, i.e., one which needs to assume a complete environment and noise source distribution—precisely what we hope to avoid with this method). In the present paper we will venture no further than hand searches, the main point being to demonstrate merely that a solution is possible. The precise meaning of "hand search" will be explained during discussion of the examples in Sec. IV—the point is that there is a logical sequence in which one searches for one parameter at a time. A third possibility is to use amplitudes and fringe patterns to calculate layer thicknesses and velocities directly by methods more akin to those used in geophysical prospecting. By Fourier transforming from frequency to time it is, in principle, possible to convert the fringes (being a power spectrum) to the layers' autocorrelation function (a series of delta functions at delays corresponding to all layer separations). This time-domain information is then available as a function of angle.

In all three methods we first need to map the up-to-down ratio from the angle measured (by beamforming) at the receiver θ_r to the angle at the seabed θ_b. Thus, knowing the sound-speed profile, by Snell's law we have

$$\theta_b = \text{acos}((c_b/c_r)\cos(\theta_r)), \tag{6}$$

and with upward refraction, zero bottom grazing angle maps to a finite nonzero angle at the array. Conversely, with downward refraction, zero angle at the array maps to a nonzero angle at the bottom, and there will be a small range of angles at the bottom that is not detectable. It is also necessary that the path connect with the sea surface—otherwise, there could not be any measured surface noise at the given angle. If there is a sound speed higher than that at the receiver depth anywhere above the receiver c_m, there is a possibility of a "noise notch," a range of angles that is surface-noise-free. The edge of this range obviously corresponds to a nonzero angle at the receiver

$$\theta_m = \text{acos}(c_r/c_m). \tag{7}$$

Beyond this, the bottom angle may be greater or smaller than the angle at the receiver according to Eq. (6).

C. Simulated bottom reflection and beamforming

In the subsequent sections we make comparisons between measurements and predictions. Unless otherwise stated, the predictions are based on a three-layer (two-boundary) model with the bottom layer supporting shear waves. In some cases an extra intermediate fluid layer has been added. Theory is based on the analytical solutions from Jensen et al. (1994), Eqs. (1.49) (for shear), (1.57) (for three-layer), and (1.65) (for extension to m layer). The effect of the finite beamwidth could be estimated by using a full-noise model such as OASN [Schmidt (1999)] or CANARY [Harrison (1997b)]. This is taken up by Harrison and Baldacci (2002). Instead, for demonstration purposes we note here that, in the case where the noise sources are uniformly distributed dipoles and the environment is independent of range, the directional noise can easily be calculated (see the Appendix). We can therefore estimate the array response knowing the beam pattern. Dividing downward by upward array response we obtain the ratio of beam responses $\mathfrak{R}$, which is an approximation to R_b

$$\frac{A(-\theta_o)}{A(+\theta_o)} = \mathfrak{R}(\theta_b(\theta_o)). \tag{8}$$

Thus, for each experimental plot we can provide an unmodified layer model plot and also a beam-smudged version.

III. EXPERIMENTS

Experiments have been carried out at five sites in the Mediterranean Sea. Three sites are south of Sicily, near the Ragusa Ridge [Fig. 3(a)], one near the Adventure Bank during ADVENT99 in May 1999, and the other two on the Malta Plateau during MAPEX2000bis in November 2000. The other two are north and east of Elba [Fig. 3(b)] also during MAPEX2000bis. Bottom types include sand, silt, mud, and rock, and one of the sites was visited twice first
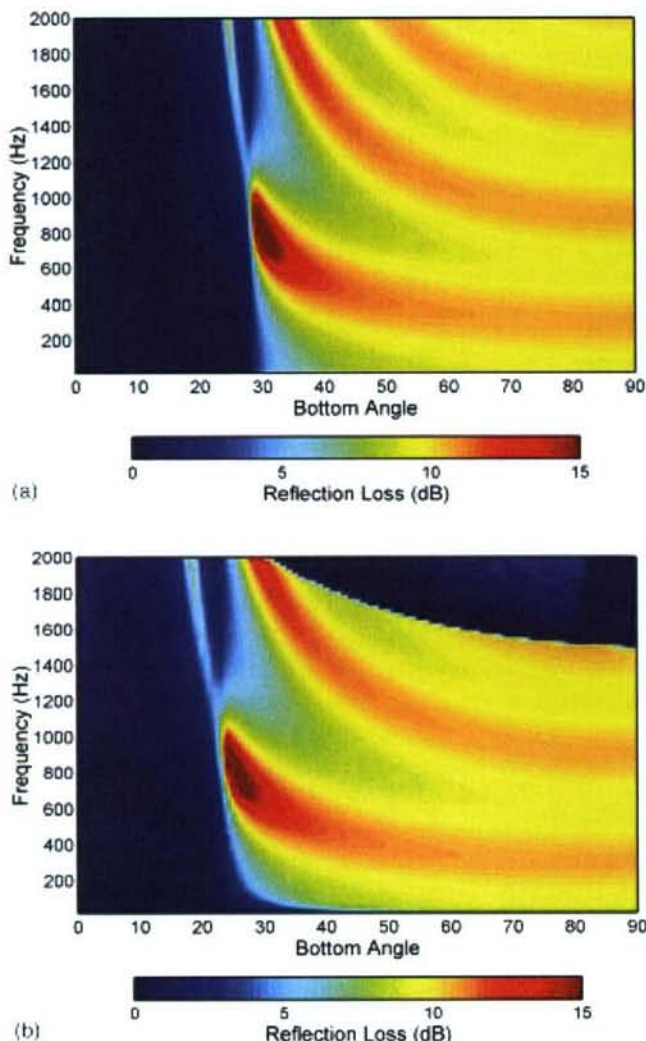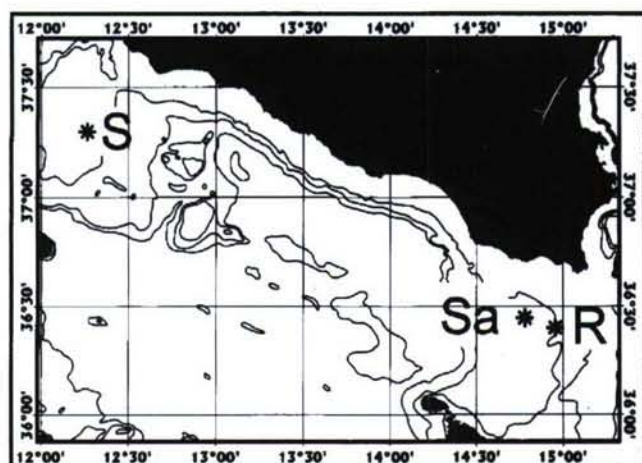

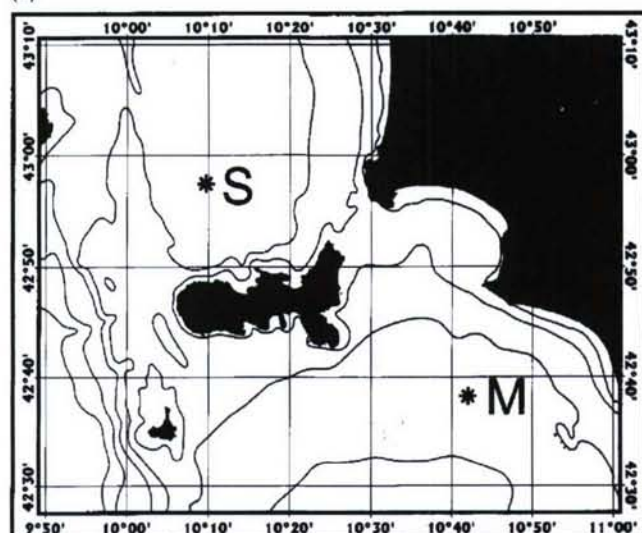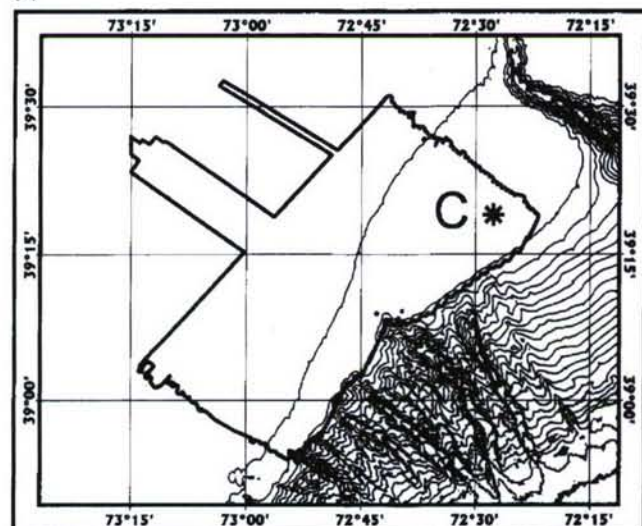FIG. 2. (a) Plane wave reflection loss for a hypothetical three-layer environment similar to the Sicily sand case modeled with OASR, and (b) the ratio of upward-to-downward noise for a 0.5-m-spaced vertical array spanning the water column calculated by OASN assuming a sheet source and the same environment.

J. Acoust. Soc. Am., Vol. 112, No. 4, October 2002

C. H. Harrison and D. G. Simons: Acoustic inversion of ambient noise   1379

FIG. 3. (a) Three experimental sites south of Sicily [Adventure Bank (labeled "S"), ADVENT99 and Ragusa Ridge (labeled "Sa" and "R"), MAPEX2000bis]; (b) two sites to the north ("S") and east ("M") of the Island of Elba (MAPEX2000bis); (c) one site on the New Jersey Shelf ("C"), BOUNDARY2001 showing the area extensively surveyed by Goff *et al.* (1999).

with, then without, significant wind noise. Another site was visited on the New Jersey Shelf during BOUNDARY2001 [Fig. 3(c)].

In all cases SACLANTCEN's moored 64-element vertical array (VLA) was used for the noise measurements (Troiano *et al.*, 1995). The same array was used in conjunction with sound sources both fixed and towed by SACLANTCEN's ship, RV ALLIANCE, for conventional geoacoustic inversion experiments (Siderius *et al.*, 2001). The 62-m array was roughly centered in the water column, and although all 64 hydrophones were available only the middle 32 regularly spaced ones (i.e., total length 16 m at half-meter separation) were used for these noise calculations.

Noise was sampled at 6 kHz on an automatically repeated sequence. During ADVENT99 the sequence consisted of two roughly 15-s windows every 4 min interlaced with active transmissions. This arrangement led to less than ideal gain settings for the noise measurements and a tendency to introduce quantization effects. In all the other cases noise measurements were taken for 10 s every 10 s while the RV ALLIANCE was quiet. The electronics provided a flat band between about 100 Hz and 2 kHz. Processing consisted of manually selecting portions without obvious contamination, and then beamforming them in the frequency domain.

IV. ANALYSIS OF RESULTS

The experimental beamformed array response can be determined conveniently by calculating the cross-spectral density between all pairs of channels, $C_{ij}(f)$, using a proprietary routine including FFT averaging, then multiplying by the steer vectors $w_i^*(\theta_o, f)$, $w_j(\theta_o, f)$ for frequency f, and summing

$$A(\theta_o, f) = \mathbf{w}^T \mathbf{C} \mathbf{w} = \sum_i \sum_j w_i^*(\theta_o) C_{ij}(f) w_j(\theta_o). \quad (9)$$

Each array response was calculated for 181 steer angles from the cross-spectral density matrix for the middle 32 elements (17–48) of the 64-element array. The bottom hydrophone (number 1) was moored at 11 m above the seabed in the Mediterranean cases and 14 m in the New Jersey case. The cross-spectral density used nonoverlapping 128-point FFTs, sampling at 6000 Hz, averaging over the 10 s of the file. Further power averaging was carried out over 10 to 30 files. In most cases a total of about 5 min of data (though carefully selected) proved adequate.

The Mediterranean sites have fairly heavy shipping, particularly those on the Malta Plateau and Adventure Bank. In a separate experiment in the vicinity (MAPEX2000), noise measurements made with a 256-element horizontal array easily detected about 14 nearby ships passing in 4 h (Harrison, 2001). It is thought that there were no ships close enough to spoil the "distant ship" approximation, although clearly a nonuniform and evolving distribution is to be expected. At the sites near Elba there tend to be occasional ferries and small fishing boats rather than container ships. In contrast,

C. H. Harrison and D. G. Simons: Acoustic inversion of ambient noise

TABLE I. Important sound speeds for angle mapping.

| Date dd-mm-yyyy | Site | Depths (m) | | Sound speeds (m/s) | | | Min. bottom angle (°) | Wind (kt) |
		Water	Array center	Array c_r	Bottom c_b	Max. c_{max}		
06-05-1999	Adv. Bank	80	39	1509.4	1511.2	1513.5	⋯	5–8
22-11-2000	S. Sicily	139	96	1512.0	1512.0	1524.2	0.00	20–22
23-11-2000	S. Sicily	99	56	1512.8	1511.4	1522.5	2.47	5–6
29-11-2000	N. Elba	121	78	1520.5	1512.1	1520.8	6.03	3–5
30-11-2000	E. Elba	125	82	1520.4	1508.8	1520.6	7.08	12–16
01-12-2000	N. Elba	121	78	1519.9	1513.9	1519.9	5.09	3–4
17-05-2001	N.J. Shelf	140	92	1499.3	1499.3	1500.5	0.00	10–14

there was hardly any nearby shipping at the New Jersey Shelf site. Wind speeds are shown in Table I. Sound-speed profiles at the various sites are shown in Fig. 4.

A. "Sand" site: S. Sicily (near Ragusa Ridge), 22 November 2000

The array response versus angle and frequency is shown in Fig. 5(a). There are various features common to all the following cases. On the right the intensity falls off rapidly because of a 2-kHz antialiasing filter. The general broadening towards the left is a manifestation of the poorer angle resolution at lower frequency. The double spikes near the horizontal span a noise notch caused, as explained earlier, by the sound-speed profile (see Fig. 4). Straight away we can see a considerable difference between up- and down-going intensity. The "up-to-down" ratio is shown in Fig. 5(b). Angles have been corrected from that at the receiver to that at the seabed according to the sound speeds shown in Table I. (Note that Table I also shows the minimum bottom angle for rays that connect with the sea surface; below this, data should be ignored.) Interpreting this picture now as a bottom reflection loss, the main features are low loss up to a critical angle and two interference lobes beyond this. This is classic behavior for a high sound-speed bottom (see, e.g., Jensen et al., 1994 and Nagl et al., 1982); once the critical angle is exceeded there is the possibility of simultaneous reflections from deeper layer boundaries which arrive later and therefore interfere. Indeed, this interference pattern is evidence that there is at least one other layer boundary present. Furthermore, in this case the regularity of the fringes with frequency suggests exactly two boundaries. The drop to low loss at the top of the picture is an artifact caused by the grating lobe that arcs from 90° at 1500 Hz (the design frequency) to 40° at 2 kHz in Fig. 5(a). Similarly, the low losses at low frequencies are caused by the inevitable poor angle resolution which degrades the up-to-down ratio. In fact, with this array the beamwidths to 3-dB points at 1500, 1000, 500, 200 Hz are, respectively, 6.7, 10, 20, 50 degs. In retrospect, all these features, particularly the two fringes, can be discerned by eye quite clearly in the original array response plot.

We can model these effects by applying the three-layer (two-boundary) model of Sec. II C with some appropriate geoacoustic parameters. Geoacoustic models for the vicinity are given by Max et al. (2000), core analysis by Tonarelli et al. (1993), and independent inversion results from MAPEX2000bis by Siderius et al. (to be published, 2002).

As shown in Table II, we take parameters from the first reference as a starting point and then make minor adjustments by hand; in particular, we adjust the layer thickness for agreement of fringe separation. The reflection loss is shown in Fig. 5(c). If we then simulate the effect of beamforming (see the Appendix), the result is remarkably similar to the experimental plot [Fig. 5(d)].

B. "Silt" site: N. Elba, 1 December 2000

Experimental array response (AR) and reflection loss (RL) curves for a silt bottom are shown in Figs. 6(a) and (b). There is now no noise notch because the array has no maximum sound speed above it. The most noticeable feature of the reflection plot is the irregularity of the interference fringes and the features at low grazing angles. In fact, we see superimposed fine and coarse fringes demonstrating that there must be more than two layer boundaries. Furthermore, since low frequencies tend not to be affected by thin layers, we can see that the lower part of Fig. 6(b) is dominated by fine fringes (200-Hz separation) caused by a thick layer with critical angle ~20°. In contrast, the coarser fringes seen starting at 1200 Hz, 90° must be caused by a thinner layer (a
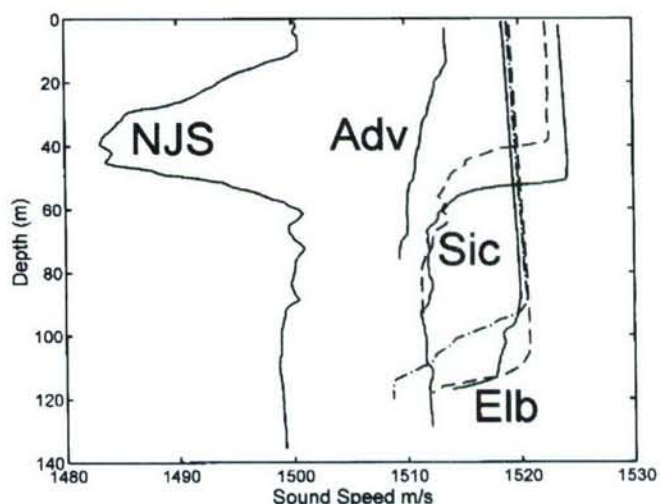

FIG. 4. Sound-speed profiles for all sites derived from near simultaneous CTDs for all sites except New Jersey, which was XBT. Labels indicate New Jersey Shelf (NJS), Adventure Bank (Adv), S. Sicily (Sic), "sand" site (solid), "rock" site (dashed), and Elba (Elb), "silt" site (solid), "silt" site without wind (dashed), "mud" site (dot-dash).
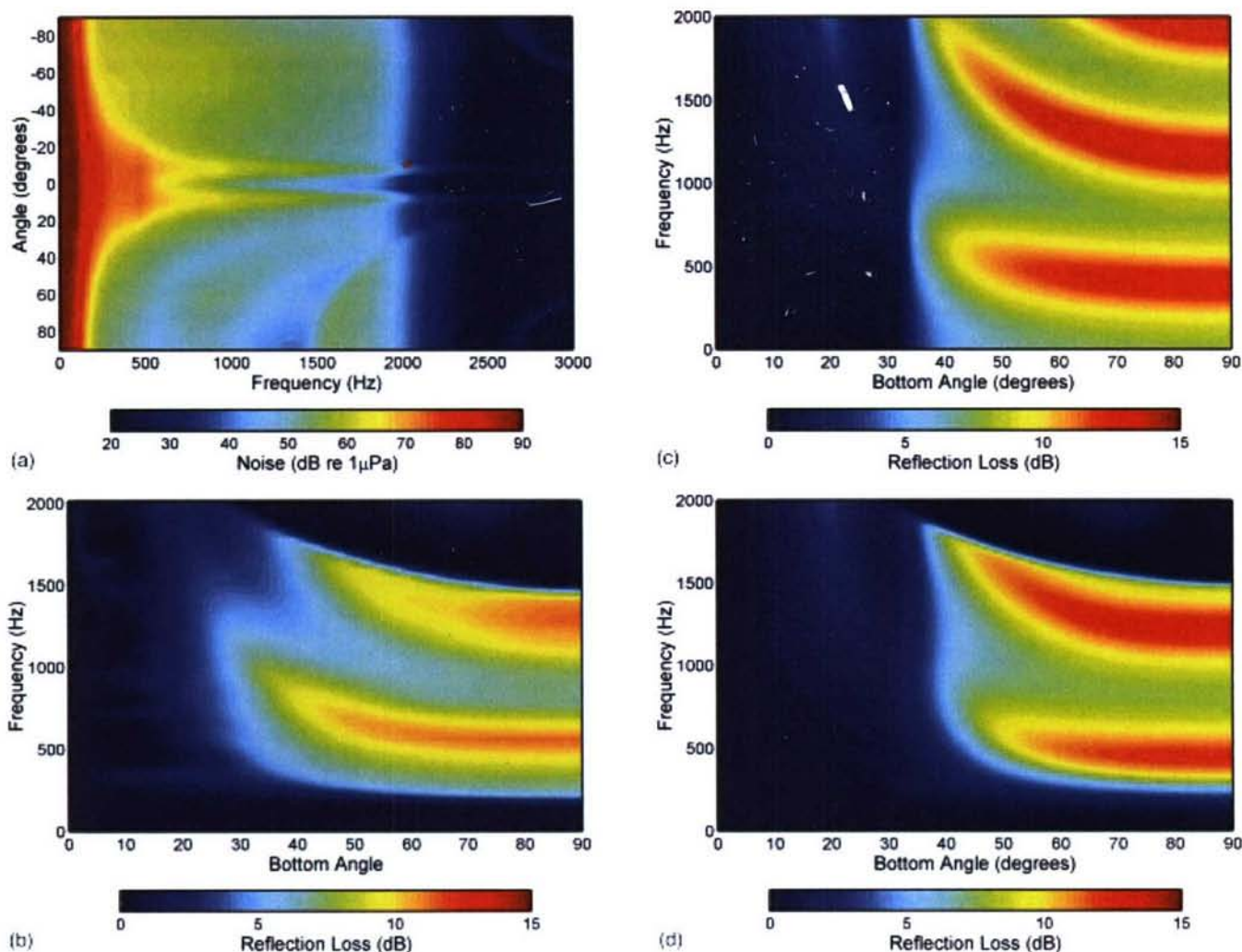
FIG. 5. (a) Experimental VLA beam response with 32 elements @ 0.5-m separation at the Ragusa Ridge, S. Sicily, "sand" site. (b) Reflection loss deduced from the up-to-down ratio of the beams from the VLA (min. bottom angle 0°). (c) Reflection loss from a simple layer model with parameters adjusted by hand as in Table II. (d) Beamformed noise resulting from the modeled reflection loss in a simple sheet noise model [Eqs. (A1), (A2), (A6)].

factor of 3 or 4 thinner, judging by the fringes) with a somewhat larger critical angle. This already provides strong clues to the bottom structure. Notice that the evidence for multiple layers is only manifest above about 900 Hz.

In earlier experiments at nearby sites, Jensen (1974) found a good two-boundary fit at low frequencies using normal-mode propagation modeling, and this was used as a starting point for subsequent inversion work by Gingras and

TABLE II. Geoacoustic parameters for all sites (initial from reference and final).

Site	Speed (m/s)[a]				Thickness (m)[a]		Density (gm/cc)[a]			Attenuation (dB/λ)[a]			Ref.[b]
	c1	c2	c3	c4	h2	h3	$\rho 2$	$\rho 3$	$\rho 4$	$\alpha 2$	$\alpha 3$	$\alpha 4$	
"silt"	···	1690	···	1750	4.3	···	1.9	···	2.0	0.4	···	0.4	TTMA
Adv. B.	1511	1630	···	1650	2.5	···	1.9	···	1.9	0.4	···	0.4	Fig 9
"sand"	···	1554	···	1950	5	···	1.3	···	2.0	0.18	···	0.3	MFHTB
Ragusa	1512	1554	···	1800	1.0	···	1.2	···	2.0	0.18	···	0.2	Fig 5
"silt"	···	1600	1530	1600	0.2	2.5	?	1.75	1.8	?	0.13	0.15	MWJ
N. Elba	1514	1600	1530	1600	0.7	2.1	1.8	1.75	1.8	0.13	0.14	0.15	Fig 6
"mud"	···	1645	1471	1600	0.3	6	?	1.5	1.8	?	0.06	0.15	MWJ
E. Elba	1509	1530	1471	1530	0.8	3.5	1.4	1.2	1.8	0.14	0.06	0.15	Fig 7
"clay"	···	1530	···	?	···	···	1.4	···	?	0.1	···	?	H
N.J. Sh.	1499	1695	···	1700	3.0	···	1.85	···	1.95	0.15	···	0.15	Fig 10

[a]Layers are numbered 1–4 from the top. Layer 1 is always water, but only the sound speed is shown. Layer 4 is always a half-space. Sometimes layer 3 is missing, i.e., zero thickness. A "?" indicates that no information was available from the reference cited.
[b]Bold characters indicate values actually used in the calculations for the figure indicated. Normal characters indicate values suggested by the references cited.
TTMA=Tonarelli et al. (1993); MFHTB=Max et al. (2000); MWJ=Murphy et al. (1976); H=Hamilton (1980).

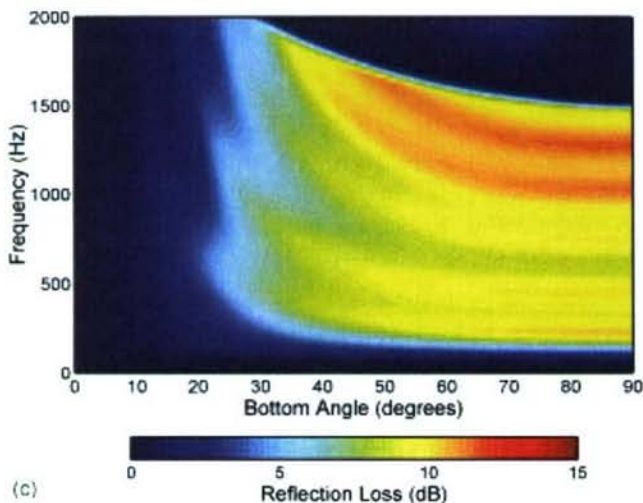C. H. Harrison and D. G. Simons: Acoustic inversion of ambient noise
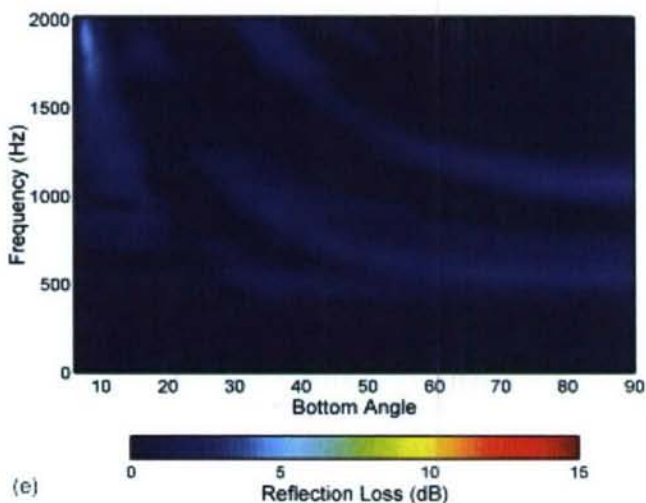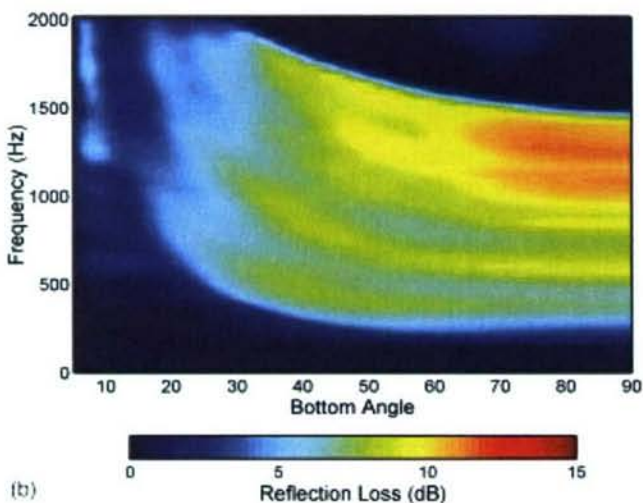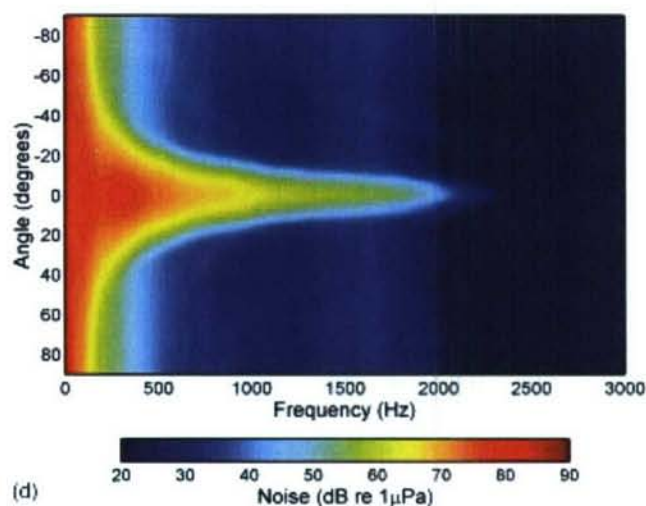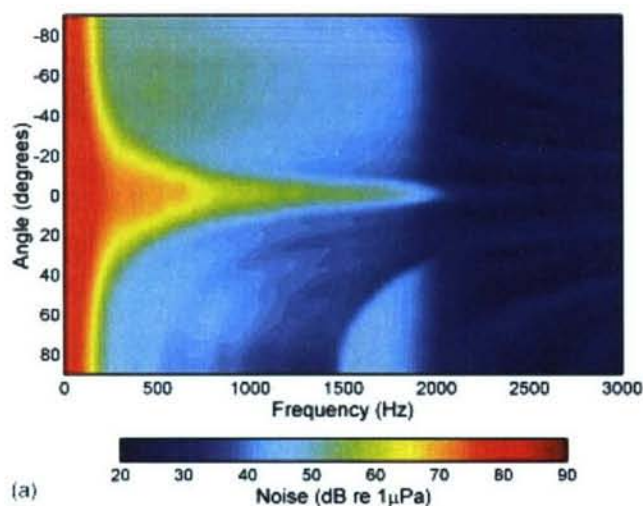
FIG. 6. (a) Experimental VLA beam response with 32 elements @ 0.5-m separation at the N. Elba "silt" site. (b) Reflection loss deduced from the up-to-down ratio of the beams from the VLA (min. bottom angle 5.09°). (c) Beamformed noise resulting from the reflection loss modeled using parameters adjusted by hand as in Table II. (d) Experimental beam response at the same site on a different occasion when there was no wind. Note extremely weak "up" and "down" contributions. (e) Anomalous reflection loss deduced from the up-to-down ratio of the beams from the VLA (min. bottom angle 6.03°). The ratio tends to unity since the up and down steered beams are in reality dominated by sidelobes of the strong "horizontal" noise seen in (d).

Gerstoft (1995). Parameters are given in Table II. These parameters, when inserted in the noise model, give good agreement with Fig. 6(b) at low frequencies, but to improve agreement at high frequencies we need to insert a thin layer with high sound speed (Table II). In fact, there is a lot of evidence from core analysis for such a thin, high-velocity layer sitting on top of the sediment near this site [Akal *et al.* (1972); Murphy and Olesen (1974); Jensen (1974); Murphy, Wasilj-

eff, and Jensen (1976); Holland and Osler (2000)]. In Fig. 6(c) we show a very good fit with a four-layer model.

C. "Silt" site, no wind: N. Elba, 29 November 2000

The silt site was also visited on an occasion when the sea was flat, calm, and there was hardly any wind (≤3 kt). There is a dramatic difference, visible immediately from the

(a)

0   5   10   15
Reflection Loss (dB)

(b)

0   5   10   15
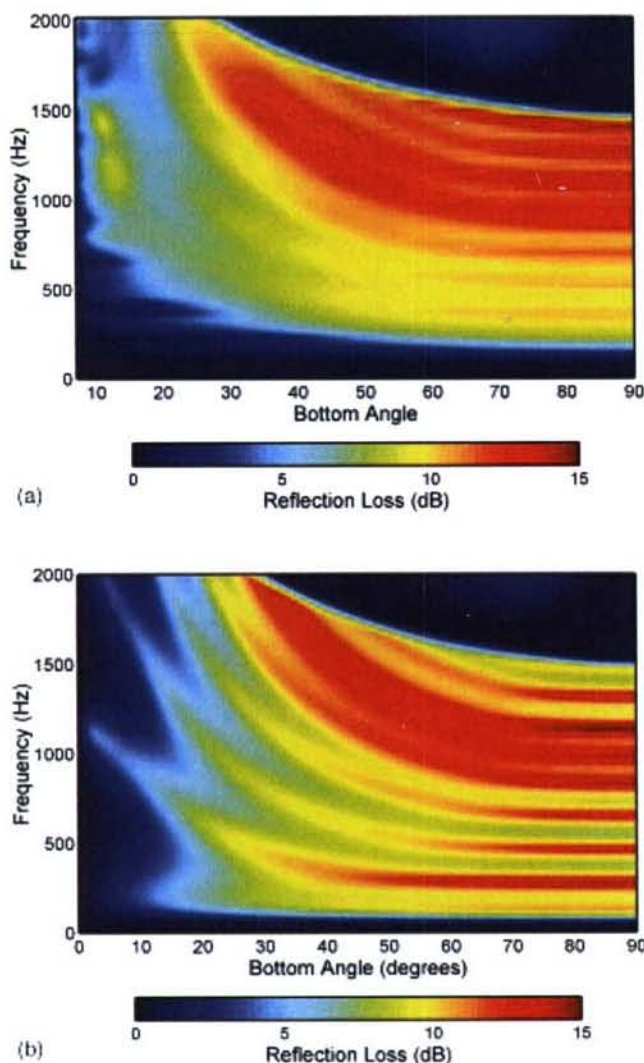Reflection Loss (dB)

FIG. 7. (a) Reflection loss deduced from the up-to-down ratio of the beams from the VLA at the E. Elba "mud" site (min. bottom angle 7.08°). (b) Beamformed noise resulting from the reflection loss modeled using parameters adjusted by hand as in Table II.

AR plot. The "up" and "down" levels are understandably both much weaker, but there are still sources near horizontal, probably distant shipping. On the assumption that there is no vertical noise at all, the beamformed responses are really responses of sidelobes to this horizontal noise. The response is therefore virtually the same up as down, and the ratio tends to unity (zero dB). This is essentially what we see in Figs. 6(d) and (e). Although there is structure it is mainly anomalous. However, it is very obvious from both the symmetry in AR plot and the differences in level between vertical and horizontal in the AR plot that this has happened, so the technique is reasonably robust from this point of view. It is stressed that it is the beamforming that is breaking down rather than the theory of this method; the up-to-down ratio is just difficult to measure in the presence of the loud horizontal sources.

D. "Mud" site: E. Elba, 30 November 2000

The mud site was expected to be lossy with sound speeds lower than that in water [Murphy, Wasiljeff, and

0   5   10   15
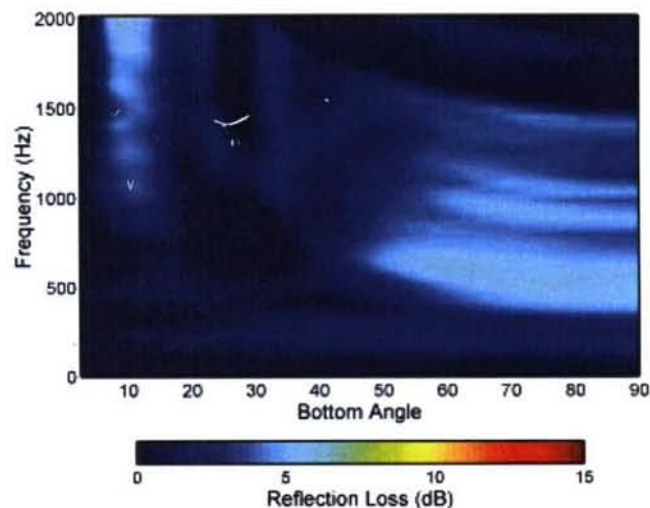Reflection Loss (dB)

FIG. 8. Reflection loss deduced from the up-to-down ratio of the beams from the VLA at the Ragusa Ridge, S. Sicily, "rock" site (min. bottom angle 2.47°).

Jensen (1976)]. In Fig. 7(a) there is evidence of higher losses at low angles, i.e., an absence of a clear critical angle. Again, there are two superimposed fringe patterns, one fine—with seven or eight loss maxima visible at, say 90°, and one coarse—with only one maximum and one minimum visible. This suggests three boundaries, two of which are wide apart and two of which are close together. Murphy, Wasiljeff, and Jensen (1976) demonstrate that there is again a thin, high-velocity layer at this site but now in the middle of the sediment layer. The result of a hand search with a three-boundary model, assuming a thin layer above the slow sediment layer, including beamforming, is shown in Fig. 7(b) (parameters are in Table II). By setting first sound speeds, then layer thicknesses, then density and absorption, it is possible independently to control the two sets of fringes, their relative amplitudes, and the low angle dependence. The search can be extended to a fourth boundary, simulating the position of the thin, fast layer within the main sediment layer, but this does not appear to improve the agreement.

### E. "Rock" site: S. Sicily (Ragusa Ridge), 23 November 2000

This site is included here for completeness, but we suspect that, as in Figs. 6(d) and (e), the wind was not strong enough to avoid artifacts, being 5–6 kts. Nevertheless, in Fig. 8 one can still see weak structure resembling that seen in earlier pictures and evidence of interference through layering, for instance an interrupted thin layer of silt above rock. Although one would expect rock to be a strong reflector, a half-space with impedance twice that of water would still have a reflection loss of 9 dB or so at high angles.

F. "Silt" site: SW Sicily (Adventure Bank), 6 May 1999

The peak values of reflection loss at this site [Fig. 9(a)] appear to be weaker than at the earlier ones. Suitable environmental data are provided by Tonarelli et al. (1993); Caiti et al. (1996); Caiti (1996); Snellen et al. (2001); Siderius et al. (2001) (see Table II). There is quite a spread of param-
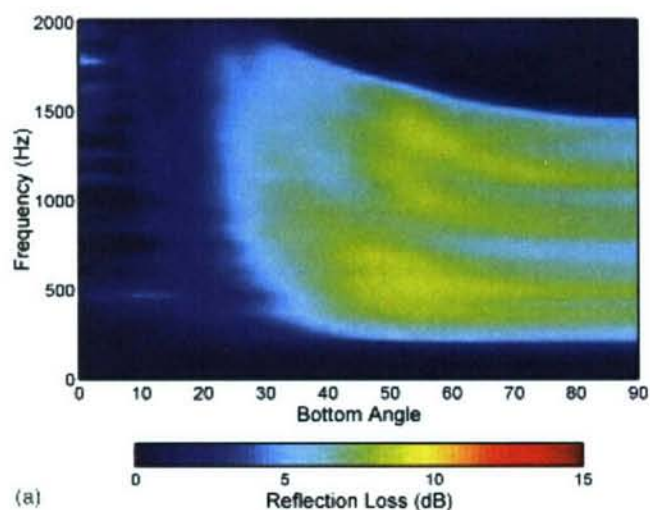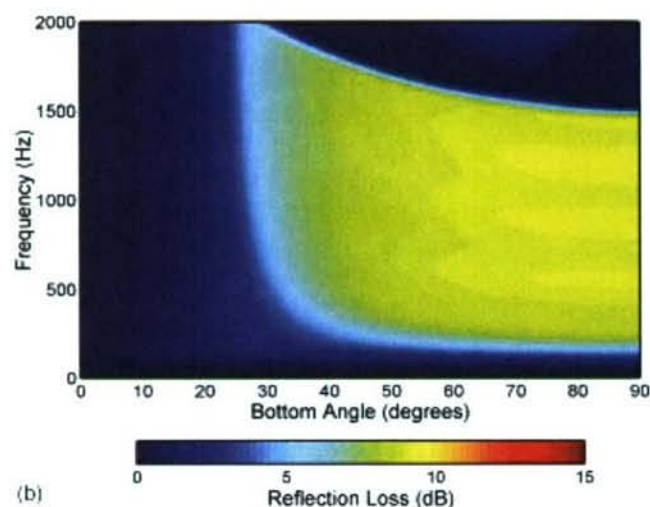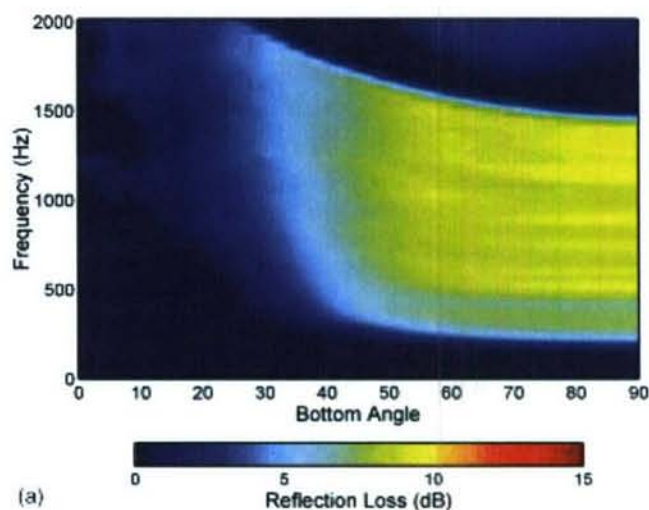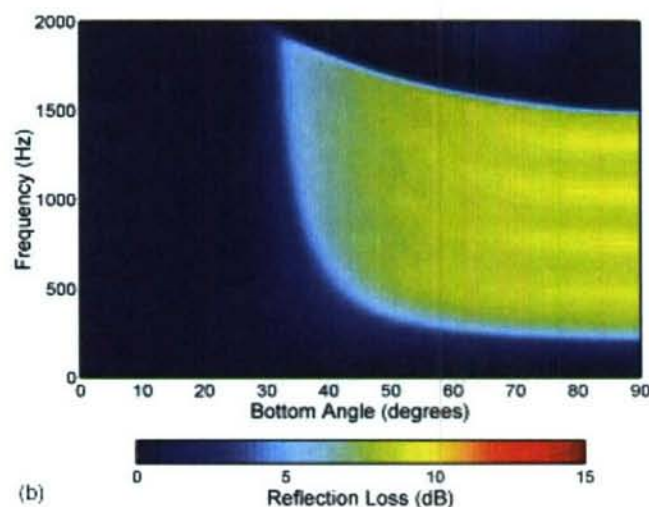
FIG. 9. (a) Reflection loss deduced from the up-to-down ratio of the beams from the VLA at the Adventure Bank, S. W. Sicily, "silt" site (zero bottom angle corresponds to 2.80° at the array). (b) Beamformed noise resulting from the reflection loss modeled using parameters adjusted by hand as in Table II.

FIG. 10. (a) Reflection loss deduced from the up-to-down ratio of the beams from the VLA at the New Jersey Shelf "stiff clay" site (min. bottom angle 0°). (b) Beamformed noise resulting from the reflection loss modeled using parameters adjusted by hand as in Table II.

eters between these references, partly because of real spatial variability, with sediment densities from 1.6 and 1.9 and sound speeds from 1670 and 1750 in the first few meters. The model fits shown in Fig. 9(b) are good but not quite as good as in the other cases. It is possible that deeper high-speed layers could account for the "lamb chop" shape of the experimental fringes (by providing loss peaks at the higher critical angle), but in retrospect these shapes look rather suspiciously unlike theoretical curves. The prime suspect is the addition of nonacoustic noise which artificially reduces the up-to-down ratio. It is known that these data were affected by a form of uncorrelated (pink) noise, namely, quantization noise when the gains had been set for experimental purposes other than gathering noise.

An interesting separate point, taken up in Harrison and Simons (2001), is that, although there are changes over several hours in noise directionality that are obvious in the beam response, the derived reflection loss is more or less immune to them.

G. "Stiff clay" site: New Jersey Shelf, 17 May 2001

There appears to be little quantitative geoacoustic data available for this site, although it is thought to be a stiff clay (Goff et al., 1999). Hamilton (1980, 1987) provides some average properties for "continental terrace (shelf and slope) environment." Between clayey silt and silty clay, sound speeds are 1546–1517 m/s and densities are 1.489–1.480 g/cc. Silt clays have a low loss of about 0.1 dB/wavelength. Initial parameters are shown in Table II.

The experimental reflection loss curve in Fig. 10(a) shows some layer structure, but the main feature is a simple step at around 35° up to about 10-dB loss. This can be modeled either as a half-space or as a multiple boundary. The sound speed in the basement is determined by the obvious critical angle, and the layer thickness is determined by the fringe separation. To get a good fit to the depth of modulation, while treating the layer as clay, it was necessary to choose a density close to that of water (1.05), but this conflicts with the assumption of a clay sediment. Equally convincing fits can be obtained by assuming either a half-space

of fine sand with sound speed 1700 m/s and density 1.8 g/cc (Hamilton, 1987), or a 3-m layer and basement of slightly differing properties close to that of fine sand. The effect of beamforming with the parameters of Table II is shown in Fig. 10(b). Note that this example happens to reveal an ambiguity or nonuniqueness in the inversion process which is common to many inversion methods. The experimental noise technique deduces a reflection loss which may indeed have measurement errors, but the reflection properties are not ambiguous in the same sense as the geoacoustic properties. A sensitivity analysis, particularly in this case, would be interesting but it is felt to be outside the scope of this paper. Some of these issues are discussed in Sec. V.

H. Data quality

The dynamic range of the reflection loss (i.e., depth of modulation of fringes) sometimes appears to be slightly smaller in the measurement than in the calculation. An obvious possible cause is the addition of (frequency-dependent) uncorrelated noise which potentially spoils the up-to-down ratio. It has the effect of disproportionately boosting the weak, upward-going signal, thus making the bottom appear to be a stronger reflector. In terms of the cross-spectral density matrix for the array, uncorrelated noise adds to the diagonal only. Adding the equivalent of 10% of the downward power to both up and down would result in a 10-dB ceiling in measured RL.

A form of uncorrelated noise (in the ADVENT99 data case only) was quantization noise. Another contender is rattling or knocking of hydrophones in their oil-filled pipe. The latter was found on several occasions and it has been possible to find, at one site (New Jersey Shelf), a morning with intermittent knocking [multichannel time series in Fig. 11(a)] and an afternoon without [Fig. 11(b)]. The surprising finding is that, although the noise directionality has changed between morning and afternoon, this degree of interference makes no visible difference to the corresponding derived reflection loss; Fig. 12 shows the equivalent of Fig. 10(a) but with knocking. Evidently, although the raw noise time series looks severely contaminated in the morning, the added absolute power is insignificant.

V. DISCUSSION OF PERFORMANCE

A. Strengths

The experimental data demonstrate a number of strengths of the noise inversion method.

(i) No sound source is required.
(ii) No propagation or noise model is required.
(iii) The method tolerates unknown source distributions and noise directionality. It is self-compensating.
(iv) The method tolerates distant point sources and ships.
(v) The method tolerates refracting environments.
(vi) The method tolerates range-dependent environments.
(vii) In contrast with most other inversion methods, high-frequency performance is good.
(viii) The method explicitly shows the critical angle and an indication of the number of layers; one can distin-
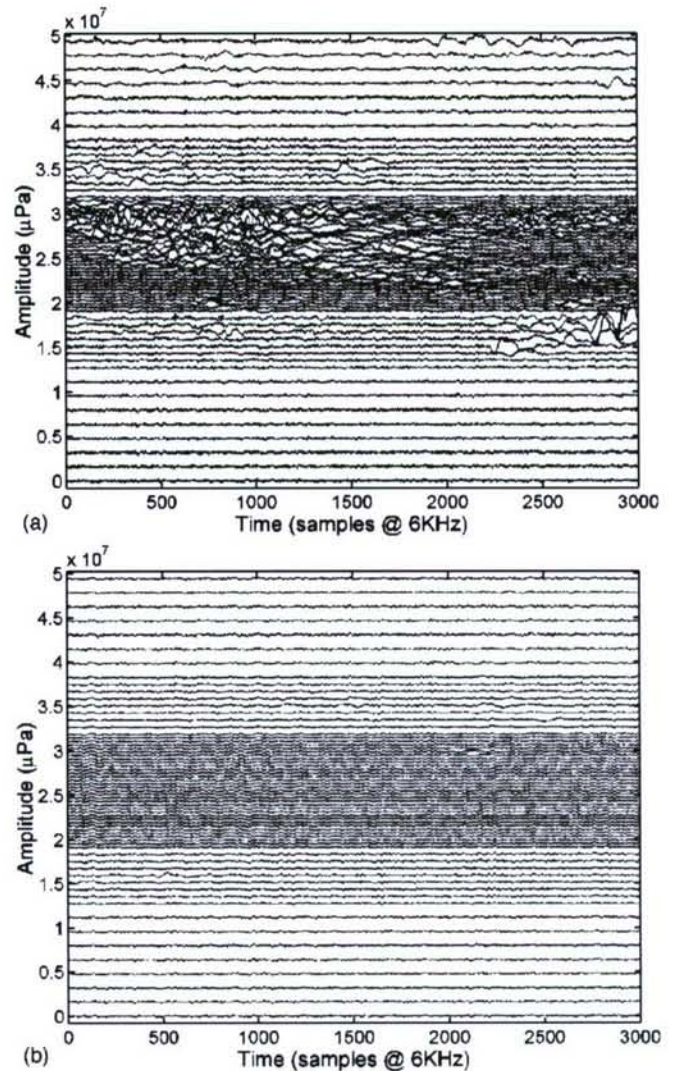

(a)

(b)

FIG. 11. (a) Complete 64 channels of time series (AM, 17-05-01) showing poor quality data with sound emanating from points on the array. Vertical channel separation is proportional to hydrophone separation. (b) Complete 64 channels of time series (PM, 17-05-01) showing good quality data.

guish by eye between one, two, and more than two bottom layers. Therefore, it is possible to isolate by hand the sound speed and thickness in the top few layers. The depth of modulation is controlled by the relative strengths of the boundary reflections, i.e., their impedance mismatches, so, having fixed the sound speeds one can determine the densities.

(ix) The method is tolerant to poor data quality.

An interesting question is, if the bottom loss varies with position, does this method measure a spatial average bottom loss or is it spatially biased? Ray theory (see the Appendix) suggests that the crucial bottom area is quite near to the receiver. In fact, it should be in the vicinity of the first bottom bounce which, of course, is a function of angle. This hypothesis has been confirmed by conducting a numerical experiment with a range-dependent wave model in which a variable size area beneath the array has distinguishable reflection properties from more distant points (Harrison and Baldacci, 2002). The corollary is that a drifting array could use this method to survey spatial bottom variations. Indeed,

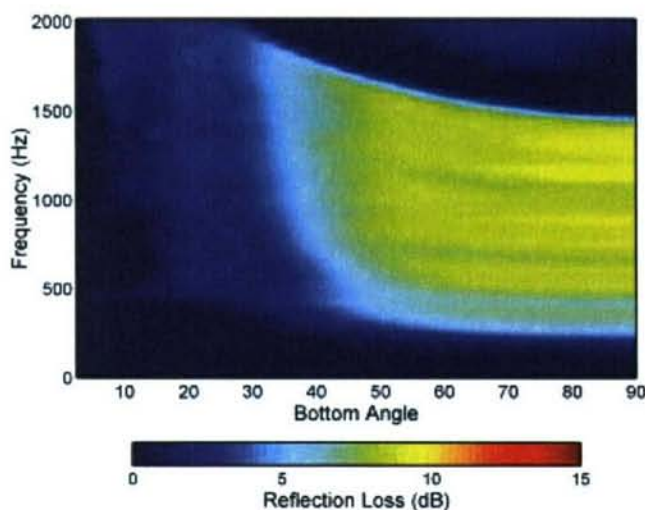C. H. Harrison and D. G. Simons: Acoustic inversion of ambient noise

FIG. 12. Reflection loss deduced from the up-to-down ratio of the beams from the VLA at the New Jersey Shelf "stiff clay" site but using *poor quality data* as shown in Fig. 11(a). Note that differences between this and the good quality data result [Fig. 10(a)] are barely perceptible.

this drift technique has been tried in a recent experiment (BOUNDARY2002, April 2002, unpublished), again using the 16-m central part of the VLA. Convincing bottom changes were seen during a several mile drift.

B. Analysis issues

1. Random errors

Assessing the impact of errors quantitatively is a difficult problem, and the purpose of Harrison and Baldacci (2002) was to investigate some of these problems by numerical simulation. Among the problems discussed elsewhere in this paper are: addition of uncorrelated noise to the hydrophones; deviation of the array from the vertical; sidelobe leakage in the presence of powerful directional sources; errors in up–down ratio for small angles where low losses are expected; resolvable eigenrays from nearby shipping.

2. Systematic errors

Two effects are obvious in all the comparisons between experimental and modeled reflection loss (including the OASR, OASN pair in Fig. 2). One is that, inevitably, at angles as small as the beam resolution the up-to-down ratio tends to unity. Thus, there is a predictable region near horizontal where the result is anomalous. The region gets wider as frequency lowers, but improvements are possible either by using techniques such as adaptive beamforming or by increasing the aperture. Another effect that depends on hydrophone separation rather than array size is the onset of a grating lobe at the design frequency. This typically results in anomalously low reflection loss.

3. Inversion problems

Even given an error-free measurement of (power) reflection loss, the geoacoustic properties that result from inversion are not necessarily unique. This is common and well known with many inversion techniques, and the usual solution is to introduce constraints on the magnitudes and behav-

ior of the physical parameters. An additional weakness in the noise case is that we have lost all *absolute* phase information, although we have retained some *relative* phase information in the form of the interference fringes. If we were to Fourier transform a complex (frequency-dependent) reflection coefficient we would, in principle, obtain an impulse response of the layers akin to standard geophysical displays [see the "move-out" technique in Holland and Osler (2000)]. The inversion ambiguity would therefore be the same as for those techniques. If, on the other hand, we Fourier transform the modulus square of the reflection coefficient we would obtain the autocorrelation function of the impulse response. Thus, layer spacing information is still there but it is mixed up to the extent that one cannot distinguish the order of, say, a thick layer and a thin layer. Nevertheless, even with a power reflection coefficient, the evident critical angle, intensity contrast, and fringe separation mean that sound speed, impedance mismatch, and layer thicknesses are fairly well determined as long as we assume a reasonably small number of layers.

C. Experimental issues

In general, there are a number of experimental issues.

1. Requirement for a VLA

It is true that the existing experimental arrangement using a 62-meter VLA is cumbersome and expensive. However, the aperture used in all the cases shown here is only 15.5 meters (32 elements @ 0.5-m separation), and one could contemplate two alternatives. One is an expendable VLA that is left to drift in much the same way as a sonobuoy. The other is a drifting or moored synthetic aperture, where one hydrophone is fixed in depth and the other moves up and down. In this way one could obtain vertical coherence, or rather, cross-spectral density for all necessary separations as required by Eq. (9).

2. Up–down beamforming contrast

Although the interference patterns seen in the experimental curves resemble those seen in theory, the theoretical reflection loss curves often contain taller spikes. This effect is, of course, highlighted by displaying in dBs, but there are various possible causes that could, in principle, be serious. Possibilities include addition of nonacoustic noise (electrical, quantization) or uncorrelated noise (strumming, knocking) or poor beamforming (incorrect assumptions on hydrophone gain, hydrophone separation or location, poor angle discrimination, poor knowledge of sound-speed profile). Most can be checked by inspection of ω-K plots, intensity histograms of individual channels, or the cross-spectral density matrix near the diagonal.

3. Array tilt

Even if the tilt is known, it is difficult to compensate mathematically without knowing the horizontal noise source distribution—but to know this defeats the object of this method, i.e., simplicity. Therefore, we need to make sure that the tilt stays inside some bounds set by the array's angle

resolution. However, fortuitously, when the resolution is poor (for low frequencies and steep angles) the reflection loss varies slowly with angle. This is no coincidence; the former depends on the *vertical* scale of the array, whereas the latter depends on the *vertical* scale of the layers. In fact, a glance at any of the reflection loss plots shows relatively gradual changes with angle, so that a tilt-induced spread of a few degrees cannot produce significant effects (Harrison and Baldacci, 2002).

4. Low-angle (near-horizontal) data

In this approach the reflection loss for very small angles depends on small differences between large quantities. It is therefore intrinsically unreliable. The true reflection loss must tend to zero at $0°$ so one could, perhaps, make use of this fact and loss values just inside the critical angle to deduce the absorption of the top sediment layer.

VI. CONCLUSIONS

A simple technique for extracting geoacoustic parameters from ambient noise measurements has been proposed and demonstrated with experimental data. Unlike coherence-based methods that use a hydrophone pair, this technique does not require a noise model. It can therefore still work when the noise directionality and bathymetry are unknown. The workable frequency range is determined by the array design frequency at high frequency, where grating lobes spoil the up-to-down beam ratio, and by its angle resolution at low frequency. In practical systems this complements conventional active inversion techniques where sound-speed fluctuations impede model matching at high frequencies (Siderius *et al.*, 2001).

A theoretical justification was given in terms of acoustic flux and also ray theory. This was supported by the results of a separate numerical study, using the wave models OASN and OASR, in which there was close agreement between the up-to-down beam ratio and the hypothesised "true" plane wave bottom loss.

A major point of the paper is that there are very clear variations from site to site that are unaffected by temporal changes in noise directionalities at those sites. In addition, the reflection loss interference patterns can be simply modeled with parameters close to those already found in other studies for the same sites. So far, the hand-searching technique has relied on inspecting the experimental plot for critical angle, fringe spacing, and depth of modulation to find a solution. It is felt that the method is now ripe for an automated search.

The method appears to be robust against most common forms of experimental data contamination except, of course, for absence of wind.

APPENDIX: REFLECTION LOSS RELATION TO NOISE DIRECTIONALITY IN A RANGE-DEPENDENT ENVIRONMENT

Here, we choose a ray approach in order to allow for spatially varying environments and source distributions as already been developed by Harrison (1997a). Given a noise directionality $N(\phi, \theta)$ (a function of elevation angle θ and azimuth ϕ) and the vertical array's beam pattern $B(\theta, \theta_o)$ for each steer angle θ_o, the array response $A(\theta_o)$ is given by

$$A(\theta_o) = \int \int N(\phi, \theta) B(\theta, \theta_o) \cos \theta \, d\theta \, d\phi. \quad (A1)$$

In a range-dependent environment the directionality $N(\phi, \theta)$ can be expressed as two multiplicative terms [Harrison (1997a)]; in the equivalent formula for coherence the beam pattern is simply replaced by a phase term

$$N(\phi, \theta) = Q(\theta) F(\phi, \theta). \quad (A2)$$

The function F is generally a complicated function of bathymetry, sound speed, and noise source distribution including multiple arrivals for each angle, although under certain conditions it can still be expressed in closed form [Harrison (1997a)]. For instance, it is a geometric series in a range-independent environment. The function Q is simply

$$Q(\theta) = \exp(-a s_p), \quad \theta \geq 0$$
$$= R_b(\theta_b) \exp(-a(s_c - s_p)), \quad \theta < 0, \quad (A3)$$

where $R_b(\theta_b)$ is the local (within one ray cycle of the receiver) bottom (power) reflection coefficient, and θ_b is related by Snell's law to θ at the receiver. The exponential terms represent, respectively, the attenuations along the residual parts of the ray directly from the surface (s_p) and directly from the bottom ($s_c - s_p$). If we could access the directionality itself, dividing the downward N by the upward N, we would eliminate the function F, leaving

$$\frac{N(\phi, -\theta)}{N(\phi, +\theta)} = \frac{Q(-\theta)}{Q(+\theta)} = R_b(\theta_b) \exp(-a(s_c - 2s_p)). \quad (A4)$$

Since this is true for all azimuths ϕ, it is also true for the azimuth integral $\int N(\phi, \theta) d\phi$. Assuming that the effects of absorption over one ray cycle are small, we obtain

$$\frac{\int N(\phi, -\theta) d\phi}{\int N(\phi, +\theta) d\phi} = R_b(\theta_b). \quad (A5)$$

Given appropriate angular resolution in Eq. (A1), we can actually measure R_b as a function of θ and hence θ_b, since the beam response tends to the noise directionality N.

From the ray point of view the reason for this simplicity, despite inclusion of spatial variation of the environment and noise source distribution, can be seen as follows. Imagine a distant point noise source from which a single ray extends,

1388   J. Acoust. Soc. Am., Vol. 112, No. 4, October 2002

C. H. Harrison and D. G. Simons: Acoustic inversion of ambient noise

after multiple surface and bottom reflections, to the receiver. For every such ray arriving directly (i.e., most recently) from the surface, there is a corresponding ray arriving from the seabed with exactly one extra bottom reflection, the same number of surface reflections, and almost the same horizontal wave number. Provided the environment changes only slowly over one ray cycle, the slight shifts in position of reflection points have no effect. So, all distant point sources, regardless of their strength, will appear weaker by $R_b(\theta_b)$ for downward θ than for upward θ. In addition, we can relax the "distant source" condition provided the source distribution is close to uniform as in the subsequent part of Harrison (1997a). The reasoning here is that with a sheet source there is no geometric spreading (it cancels out), so the only difference between an upgoing and a downgoing ray at exactly the same angle is the nearby bottom reflection. The same argument applies even if there have been several ray cycles between the surface source and the receiver.

In order to simulate the effects of beamforming on the directionality [see Eq. (A1)] we note that, in the case where the noise sources are uniformly distributed dipoles and the environment is independent of range, the function F in Eq. (A2) reduces to

$$F(\phi,\theta) = \sin\theta_s/[1 - R_s(\theta_s)R_b(\theta_b)\exp(-as_c)], \quad (A6)$$

with R_s and θ_s being surface loss and surface angle, respectively. We can therefore estimate the array response using Eqs. (A1) and (A2) knowing the beam pattern (from the array dimensions). Dividing downward by upward array response, we obtain the ratio of beam responses $\Re$, which is an approximation to R_b

$$\frac{A(-\theta_o)}{A(+\theta_o)} = \Re(\theta_b(\theta_o)). \quad (A7)$$

We note that, although F does not truly cancel out, its influence on the ratio $\Re(\theta_b(\theta_o))$ is weak. Therefore, we assume that an estimate of F under the ideal conditions of a uniform noise source distribution, as in Eq. (A6), will suffice.

Akal, T., Gehin, C., Matteucci, B., and Tonarelli, B. (1972). "Measured and computed physical properties of sediment cores: Island of Elba zone," SACLANT ASW Research Centre, La Spezia, Italy, Special Report No. M-82.

Aredov, A. A., and Furduev, A. V. (1994). "Angular and frequency dependencies of the bottom reflection coefficient from the anisotropic characteristics of a noise field," Acoust. Phys. 40, 176–180.

Buckingham, M. J., and Jones, S. A. S. (1987). "A new shallow-ocean technique for determining the critical angle of the seabed from the vertical directionality of the ambient noise in the water column," J. Acoust. Soc. Am. 81, 938–946.

Caiti, A., Ingenito, F., Kristensen, A., and Max, M. D. (1996). "Geoacoustic models for selected shallow water areas," SACLANT ASW Research Centre, La Spezia, Italy, Report No. SM-305.

Caiti, A. (1996). "Geoacoustic seafloor exploration with a towed array in a shallow water area in the Strait of Sicily," IEEE J. Ocean. Eng. 21, 355–366.

Carbone, N. M., Deane, G. B., and Buckingham, M. J. (1998). "Estimating the compressional and shear wave speeds of a shallow-water seabed from the vertical coherence of ambient noise in the water column," J. Acoust. Soc. Am. 103, 801–813.

Chapman, D. (1988). "Surface-generated noise in shallow water: A model," Proceedings of (UK) I.O.A. Conference 9, 1–11.

Gingras, D. F., and Gerstoft, P. (1995). "Inversion for geometric and geoacoustic parameters in shallow water: Experimental results," J. Acoust. Soc. Am. 97, 3589–3598.

Goff, J. A., Swift, D. J. P., Duncan, C. S., Mayer, L. A., and Hughes-Clarke, J. (1999). "High-resolution swath sonar investigation of sand ridge, dune, and ribbon morphology in the offshore environment of the New Jersey margin," Mar. Geol. 161, 307–337.

Hamilton, E. L. (1980). "Geoacoustic modeling of the sea floor," J. Acoust. Soc. Am. 68, 1313–1340.

Hamilton, E. L. (1987). "Acoustic properties of sediments," in Acoustics and Ocean Bottom, edited by A. Lara-Saenz, C. Ranz-Guerra, and C. Carbo-Fite (F.A.S.E. Conference, Madrid).

Harrison, C. H. (1996). "Formulas for ambient noise level and coherence," J. Acoust. Soc. Am. 99, 2055–2066.

Harrison, C. H. (1997a). "Noise directionality for surface sources in range-dependent environments," J. Acoust. Soc. Am. 102, 2655–2662.

Harrison, C. H. (1997b). "CANARY: A simple model of ambient noise and coherence," Appl. Acoust. 51, 289–315.

Harrison, C. H., and Simons, D. G. (2001). "Geoacoustic inversion of ambient noise: A simple method," Conference on "Acoustical Oceanography," Southampton, UK, 9–12 April 2001, edited by T. G. Leighton, Proc. Inst. of Acoust. 23, 91–98.

Harrison, C. H., Brind, R., and Cowley, A. (2001). "Computation of noise directionality, coherence, and array response in range-dependent media with CANARY," J. Computational Acoust. 9, 327–345.

Harrison, C. H. (2001). "Noise measurements during MAPEX2000," SACLANT ASW Research Centre, La Spezia, Italy, Report No. SM-391.

Harrison, C. H., and Baldacci, A. (2002). "Bottom reflection properties deduced from ambient noise: Simulation of a processing technique," SACLANT ASW Research Centre, La Spezia, Italy, Report No. SM-392.

Holland, C. W., and Osler, J. (2000). "High-resolution geoacoustic inversion in shallow water: A joint time- and frequency-domain technique," J. Acoust. Soc. Am. 107, 1263–1279.

Jensen, F. B. (1974). "Comparison of transmission loss data for different shallow water areas with theoretical results provided by a three-fluid normal-mode propagation model," in Sound Propagation in Shallow Water, edited by O. F. Hastrup and O. V. Olesen, Conference Proceedings CP-14 (SACLANT ASW Research Centre, La Spezia, Italy), pp. 79–92.

Jensen, F. B., Kuperman, W. A., Porter, M. B., and Schmidt, H. (1994). Computational Ocean Acoustics (AIP, New York), pp. 46, 50, 52, 54, 521.

Max, M. D., Fawcett, J., Hollett, R., Thomason, R., and Berkson, J. M. (2000). "Acoustic propagation and geoacoustic models for the Ragusa and West Malta Plateau geoacoustic terranes off SE Sicily," SACLANT ASW Research Centre, La Spezia, Italy, Report No. SM-337.

Murphy, E. L., and Olesen, O. V. (1974). "Broadband sound-propagation trials in shallow water near the island of Elba," SACLANT ASW Research Centre, La Spezia, Italy, Report No. SM-39.

Murphy, E. L., Wasiljeff, A., and Jensen, F. B. (1976). "Frequency-dependent influence of the sea bottom on the near-surface sound field in shallow water," J. Acoust. Soc. Am. 59, 839–845.

Nagl, A., Uberall, H., and Hoover, W. R. (1982). "Resonances in acoustic bottom reflection and their relation to the ocean bottom properties," IEEE Trans. Geosci. Remote Sens. GE-20, 332–337.

Schmidt, H. (1999). "OASES: Version 2.2. User's Guide and Reference Manual," Dept. of Ocean Engineering, Massachusetts Inst. of Technology. Obtained via http://acoustics.mit.edu/arctic0/henrik/www/oases.html

Siderius, M., Nielsen, P. L., Sellschopp, J., Snellen, M., and Simons, D. (2001). "Experimental study of geo-acoustic inversion uncertainty due to ocean sound-speed fluctuations," J. Acoust. Soc. Am. 110, 769–781.

Siderius, M., Nielsen, P., and Gerstoft, P. "Range-dependent seabed characterization by inversion of acoustic data from a towed array," J. Acoust. Soc. Am. (to be published).

Snellen, M., Simons, D., Siderius, M., Sellschopp, J., and Nielsen, P. L. (2001). "An evaluation of the accuracy of shallow water matched field inversion results," J. Acoust. Soc. Am. 109, 514–527.

Tonarelli, B., Turgutcan, F., Max, M. D., and Akal, T. (1993). "A comparison of shallow sediment properties in four locations on the Sicilian–Tunisian platform," SACLANT ASW Research Centre, La Spezia, Italy, Report No. SM-267.

Troiano, L., Guerrini, P., and Barbagelata, A. (1995). "SACLANTCEN towed and vertical array system characteristics," SACLANT ASW Research Centre, La Spezia, Italy, Special Report No. M-117.

C   Improved performance of global optimisation methods
         for inversion problems in underwater acoustics; ECUA
         2004

IMPROVED PERFORMANCE OF GLOBAL OPTIMISATION METHODS FOR INVERSION PROBLEMS IN UNDERWATER ACOUSTICS

Camiel van Moll and Dick G. Simons

TNO Physics and Electronics Laboratory, Underwater Acoustics Group, Oude Waalsdorperweg 63, 2509 JG The Hague, The Netherlands.
e-mail: vanmoll@fel.tno.nl

To invert for parameters of the seabed and the water column, global optimisation methods are used. These methods search for the best parameter combination, so as to make the difference between modelled and measured pressure fields as small as possible. Simulated annealing and genetic algorithms (GA) are commonly used as global optimisation algorithms for this inversion. Their efficiency depends on the tuning of the algorithm. For a bottom model with in the order of ten geo-acoustic parameters, a relatively new global optimisation method - Differential Evolution (DE) - is applied. We claim a ten times higher efficiency of DE, as it finds the optimal parameter combination with only one tenth of the number of model evaluations needed by GA. Apart from the tuning of the algorithms, the performance of DE in comparison with GA is investigated in terms of efficiency and robustness.

1. INTRODUCTION

In the last two decades global optimisation methods, such as simulated annealing (SA) and genetic algorithms (GA), have been applied to solve inversion problems in underwater acoustics. In this inversion a pressure field calculated by a model is compared with a measured pressure field, using a cost or energy function. The search is for that parameter combination that maximises similarity between modelled and measured field, i.e., giving the lowest energy value. In general, a fairly large amount of parameters are sought, typically 5 to 20. This is called 'matched field inversion'.

A purely random search would require too many forward model calculations. Search methods strongly reduce this number of function evaluations, but have the risk to fail by being trapped in a local minimum of the energy function. To overcome this problem, global optimisation methods, such as simulated annealing and genetic algorithms, have been designed.

Performance criteria for optimisation methods are efficiency, robustness and accurateness. Since the forward model calculations take most of the computation time during optimisation, efficiency is measured by the required amount of these calculations, typically a few tens of thousands. The stochastic nature of these methods causes that even a global search run can get stuck in a local minimum. Robustness is defined as the probability of an optimisation run to end in the global minimum, i.e., the probability of success of the optimisation method. Accurateness has to do with the distance between the outcome of a successful optimisation run and the precise location of the global minimum. In this article the attention is focused on robustness and efficiency.

Optimisation methods have a few setting parameters (e.g. crossover probability and mutation rate in GA), that have to be optimised themselves. It will be shown that these settings strongly influence the performance of the method. Although the optimal setting can be problem specific, we hope to find optimum settings that only need minor adjustments for other problems.

It is already well established that in matched field inversion GA outperforms SA. However, there is a need for methods even better than GA. A relatively new global search method, differential evolution (DE), is introduced. Its performance, in terms of efficiency and robustness, is shown to be better than that of genetic algorithms.

2. BASIC PRINCIPLES OF GENETIC ALGORITHMS AND DIFFERENTIAL EVOLUTION

In underwater acoustics the GA has been introduced by Gerstoft [1]. Its principle of operation is summarised as follows. To optimise an energy function E, GA improves populations of q parameter combinations during successive generations. A GA optimisation run starts by creating at random an initial population of q members. Each member represents a certain parameter value combination $\mathbf{m}$ and its energy E is calculated. A population member with a lower E (a higher fitness) has a higher probability to be selected in one (or more) of the pairs of parents to be formed. This results in $q/2$ pairs of parents with a larger proportion of fit members. From each pair of parents two children are created by a random exchange of parental values (steered by the crossover probability p_c), followed by random changes of individual parameter values (with mutation probability p_m). A set of q children vectors results. The next generation is established by taking at random $f_r q$ members of these children and selecting the $(1 - f_r)q$ most fit members of the current population. This process is repeated over several hundreds of generations.

GA's have the following setting parameters: population size q, crossover probability p_c, mutation probability p_m, reproduction size f_r and the number of generations N_G.

Differential evolution, just like GA, starts with an initial population of q randomly chosen parameter value combinations $\mathbf{m}$. These $\mathbf{m}$'s are improved during successive generations of constant size q, in the sense that a descendant replaces an $\mathbf{m}$, becoming its successor, if it has a lower energy. The distinctive feature of DE is the way in which these descendants are created. In [2] various ways to generate new $\mathbf{m}$'s are described. Here only the following procedure is considered. At the start of generation k the parameter vectors $\mathbf{m}_{k,1}, \ldots, \mathbf{m}_{k,q}$ are given and for each of them a descendant is created, being a potential successor. To create this descendant $\mathbf{d}_{k,i}$ of $\mathbf{m}_{k,i}$ first a partner $\mathbf{p}_{k,i}$ is constructed according to

$$\mathbf{p}_{k,i} = \mathbf{m}_{k,i_1} + F(\mathbf{m}_{k,i_2} - \mathbf{m}_{k,i_3})$$

with three different vectors $\mathbf{m}_{k,i_1}, \mathbf{m}_{k,i_2}$ and $\mathbf{m}_{k,i_3}$ chosen at random from the population and F a scalar multiplication factor between 0 and 1. The descendant $\mathbf{d}_{k,i}$ of $\mathbf{m}_{k,i}$ results from applying crossover to $\mathbf{m}_{k,i}$ and $\mathbf{p}_{k,i}$ with crossover probability p_c. A higher value of p_c leads (on the average) to more dimensions of $\mathbf{p}_{k,i}$ to be copied into $\mathbf{d}_{k,i}$, while the values for the remaining dimensions are taken from $\mathbf{m}_{k,i}$. $\mathbf{d}_{k,i}$ only replaces $\mathbf{m}_{k,i}$, becoming its successor, if its energy is lower.

The setting parameters of DE are population size q, multiplication factor F, crossover probability p_c and the number of generations N_G.

Comparing GA and DE, both show improvement of a fixed sized population of parameter combinations. However, in each generation of GA a fixed fraction of the population is replaced by children, whether they are better or not. In DE each member of the population will be replaced by its descendant only if this descendant has lower energy. On the other hand, the fitness of a member increases the probability of that member to play a role in the creation of children in GA, where in DE this fitness does not influence the probability of a member to be selected. Another difference is the way a partner $\mathbf{p}_{k,i}$ is found for $\mathbf{m}_{k,i}$. While in GA the partner is an element of the given generation, in DE it is constructed from the population and thus not an element of this generation. The partner creation process in DE is steered by the multiplication factor F and replaces the mutation mechanism of GA.

3. PERFORMANCE OF GENETIC ALGORITHMS AND DIFFERENTIAL EVOLUTION

A test function given in [3] is known to have characteristics that correspond to those of the geo-acoustic inversion problem. Its features are: number of parameters $N_p = 6$, various local minima, parameter coupling and a varying sensitivity to the parameters m_i. The global minimum is at the origin $m_i = 0$. The research on the performance of GA and DE presented here, is restricted to minimisation of this energy function called E_1.

To determine the probability of success multiple optimisation runs are needed, each run starting with a different randomly chosen population of q m's. The number of independent runs per setting is denoted N_r. N_c is the amount of these runs that have converged to the global minimum. The fraction of converged runs serves as an estimate for the probability of success p_s according to

$$p_s = \frac{N_c}{N_r} \quad \text{with} \quad \sigma_{p_s} = \frac{\sigma_{N_c}}{N_r} \quad \text{and} \quad \sigma_{N_c} = \sqrt{p_s(1-p_s)N_r}$$

When comparing the performance of different settings of the optimisation algorithms, also the statistical uncertainty on p_s, being σ_{p_s}, should be taken into account (where N_c has a binomial distribution). The efficiency is measured by the number of function evaluations or forward model calculations N, given by $N = f_r q N_G$ for GA and $N = q N_G$ for DE.

3.1. Settings for the Genetic Algorithm

GA is applied to E_1 with the following settings: ($q = 64$, $f_r = 0.8$) and ($q = 128$, $f_r = 0.4$), both with $N_G = 500$ (therefore both with $N = 25600$). p_c was varied in between 0.1 and 0.9 in steps of 0.2, whereas p_m was varied in between 0.025 and 0.25 in steps of 0.025. The number of independent runs N_r equals 50 for each combination of settings. The estimates of the success probabilities for the considered settings are presented in the figures 1 and 2.
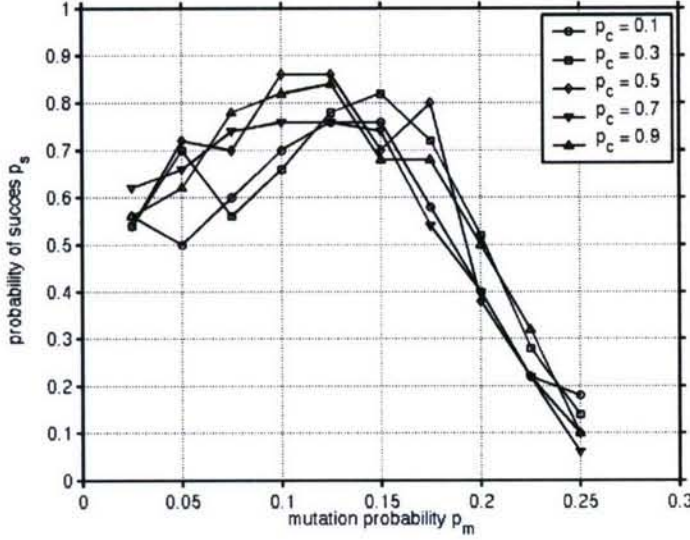

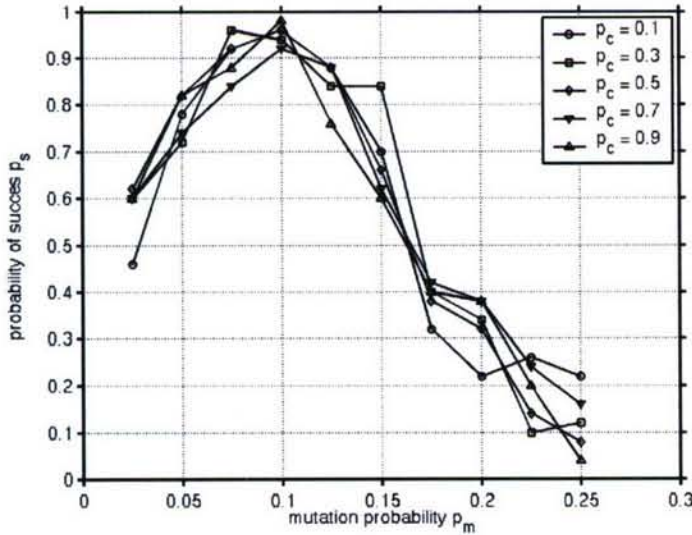Figure 1: GA with $q = 64$, $f_r = 0.8$; statistical error on p_s is about 0.06

Figure 2: GA with $q = 128$, $f_r = 0.4$; statistical error on p_s is about 0.06

It is observed that the attainable level of p_s hardly depends on p_c, while the choice of p_m is of major importance. There is a rapid fall off of p_s versus p_m for $p_m > 0.15$. The optimum setting of p_m is slightly larger than 0.1. The setting $q = 128$ and $f_r = 0.4$ (also with $N=25600$)

leads to higher levels of p_s, with the possibility of nearly 100 % success. Notice the need of taking the (statistical) error on p_s into account! Finally, Gerstoft's default setting [1] ($q = 64$, $N_G = 500$, $f_r = 0.5$, $p_c = 0.8$, $p_m = 0.05$) is not robust, leading to $p_s = 0.69$ (with N only 16000).

3.2. Settings for Differential Evolution

Applying DE to E_1, two combinations of q and N_G are considered: ($q = 16$, $N_G = 150$) and ($q = 32$, $N_G = 75$), both with $N = 2400$ (instead of the 25600 for GA). To provide more accurate estimates for p_s, the number of independent runs per setting is taken $N_r = 500$. p_s for different combinations of F and p_c is given in figures 3 and 4.

It is seen that the smaller number of generations $N_G = 75$ requires a lower setting of the contraction factor F. DE seems to be more sensitive to the choice of F than to that of the crossover probability p_c.
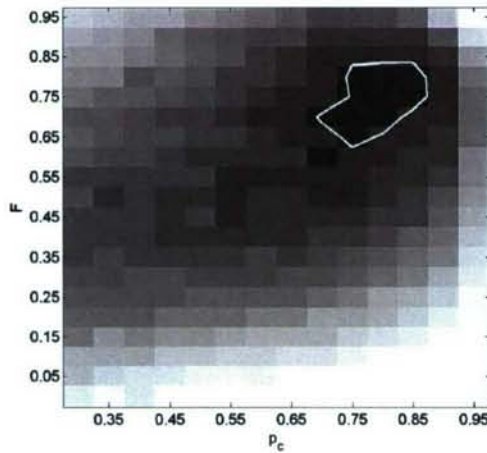

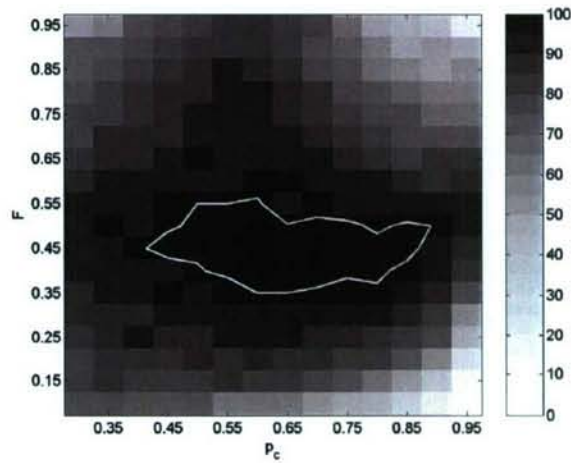
Figure 3: DE with $q = 16$, $N_G = 150$
90 % p_s contour

Figure 4: DE with $q = 32$, $N_G = 75$
97 % p_s contour

3.3. Comparing the performance of GA and DE

Table 1 gives the Gerstoft GA setting [1] and the optimum settings found for GA and DE.

	q	N_G	p_c	p_m	f_r	F	N	p_s
GA Gerstoft	64	500	0.8	0.05	0.5		16000	0.69 ± 0.05
GA best	128	500	0.9	0.1	0.4		25600	0.98 ± 0.02
DE	16	150	0.85			0.8	2400	0.91 ± 0.013
DE	32	75	0.75			0.5	2400	0.98 ± 0.007
DE	32	150	0.8			0.6	4800	0.99 ± 0.005

Table1: GA and DE best settings and corresponding performances.

With comparable robustness ($p_s = 0.98$) DE requires only 2400 function evaluations instead of the 25600 of GA, an order of magnitude improved efficiency.

How to explain this better performance? We suspect that the partner creation process of DE is a better way to escape from a local minimum. Therefore, the contraction factor F is an important setting parameter of DE. At the same time this partner creation process offers the

possibility to better explore the parameter search space, provided the mutual distances of the population members are sufficiently large.

4. SUMMARY AND CONCLUSIONS

In this paper a relatively new global optimisation method called differential evolution (DE) has been tested. This method can be applied for solving inversion problems in underwater acoustics. Its performance in terms of efficiency and robustness was compared with that of a genetic algorithm (GA). Efficiency is measured by the number of function evaluations. Robustness is defined as the probability of success. The fraction of runs that converge to the global minimum, out of a number of independent repetitions of the algorithm for a given setting (typically 50), estimates this probability.

The optimisation problem comprises the minimisation of an energy function depending on 6 parameters, featuring various local minima, parameter coupling and varying sensitivity to the parameters. Minimising this function with GA requires several tens of thousands of function evaluations. The performance of GA hardly depends on crossover probability, whereas it depends critically on mutation probability. Using 25600 function evaluations almost 100 % success probability was realised, provided a mutation probability of 10 % is taken. With DE the same success rate is obtained with 10 times less function evaluations. The performance of DE depends mainly on the multiplication factor and less on crossover probability.

The following question remains. Do the best settings found for the optimisation algorithms depend on the optimisation problem at hand? To this end we introduce another optimisation problem, i.e., geo-acoustic parameter estimation using matched field inversion [Snellen, 2004].

REFERENCES

[1] **Peter Gerstoft**, Inversion of seismoacoustic data using genetic algorithms and a posteriori probability distributions, *J. Acoust. Soc. Am.*, 95 (2) , pp 770 – 782, February 1994

[2] **Rainer Storn and Kenneth Price** , Differential Evolution – A simple and efficient adaptive scheme for global optimization over continuous spaces, *ICSI Technical Report*, TR-95-012, March 1995

[3] **Mark R. Fallat and Stan E. Dosso**, Geoacoustic inversion via local, global and hybrid algorithms, *J. Acoust. Soc. Am.*, 105 (6), pp 3219 – 3230, June 1999

[4] **Mirjam Snellen, Dick G. Simons and Camiel van Moll**, Application of Differential Evolution as an Optimisation Method for Geo-acoustic Inversion, *Proceedings ECUA 2004 Delft*, 5-8 July 2004

D   Inversion of shallow water ambient noise data by means of differential evolution as a global search method; ISCHIA 2004

Chapter 1

INVERSION OF SHALLOW WATER AMBIENT NOISE DATA BY MEANS OF DIFFERENTIAL EVOLUTION AS A GLOBAL SEARCH METHOD

Dick G. Simons

Department of Earth Observation and Space systems (DEOS)
Delft University of Technology, Kluyverweg 1, 2629 HS, Delft, The Netherlands
d.g.simons@lr.tudelft.nl
TNO Physics and Electronics Laboratory
Oude Waalsdorperweg 63, 2509 JG The Hague, The Netherlands
simons@fel.tno.nl

Camiel van Moll

TNO Physics and Electronics Laboratory
Oude Waalsdorperweg 63, 2509 JG The Hague, The Netherlands
vanmoll@fel.tno.nl

Chris H. Harrison

NATO Undersea Research Centre
Viale S. Bartolomeo 400, 19138 La Spezia Italy
harrison@saclantc.nato.int

Abstract   As the vertical directivity of ambient noise is dependent on the reflective properties of the seabed, geo-acoustic parameters can be inferred by inversion of the noise. This is clearly demonstrated in a paper by (Harrison and Simons, 2002). In this work the seabed reflection loss is directly found by comparing the upward- and downward-going noise. These are determined by beamforming the ambient noise field received on a vertical array of hydrophones. Geo-acoustic parameters were derived with a hand-searching technique that relies on inspection of the experimental (angle- and frequency dependent) reflection loss for critical angle, fringe spacing and modulation depth. In the current paper by applying a global optimisation technique as an automatic search method im-

proved estimates for the geo-acoustic parameters were obtained. For the global search method a relatively new technique, called "differential evolution", is applied (Storn and Price, 1995). Compared to a genetic algorithm a ten times higher efficiency is obtained, since differential evolution finds the optimal parameter setting with only one tenth of the number of forward model evaluations. For these inversions two different models for the seabed reflection loss were employed. First we assumed the seabed to consist of a single homogeneous fluid sediment layer on top of a homogeneous fluid subbottom. As the fringe pattern of some of the measured reflection loss data suggests the existence of at least two layers, the data were also inverted using a seabed model comprising two fluid sediment layers on top of a homogeneous fluid subbottom.

Introduction

As the coherence and vertical directivity of ambient noise depends on the reflective properties of the seabed, geo-acoustic parameters can be inferred by inversion of the noise. This is clearly demonstrated by, among others, (Carbone et al., 1998) and (Harrison and Simons, 2002).
Carbone measures the broadband noise coherence with a vertically separated pair of hydrophones, which was compared with noise model calculations searching over geo-acoustic parameter space.
In (Harrison and Simons, 2002) an approximation of the plane wave reflection coefficient of the seabed (as a function of grazing angle and frequency) is directly found by comparing the upward- and downward-going noise. These are determined by beamforming the ambient noise field received on a vertical array of hydrophones. Geo-acoustic parameters were derived with a hand-searching technique that relies on inspection of the experimental (angle- and frequency dependent) reflection loss for critical angle, modulation depth and fringe spacing. From these phenomena sound speed, impedance mismatch and layer thickness can already be determined fairly well. The potential of this method was demonstrated with experimental data from several sites in the Mediterranean. Pros and cons of the method are extensively discussed. Important strengths of the method are that no noise model is required and that it tolerates an unknown noise source distribution and noise from distant shipping. The paper of (Harrison and Simons, 2002) does not go further than hand searches for the geo-acoustic parameters, since the main point was to demonstrate merely that a solution is possible. It was concluded that by applying a global optimisation technique as an automatic search method, improved estimates for the geo-acoustic parameters should be obtained. It should however be emphasised that results from this inversion are not necessarily unique.
In this paper we compare the measured reflection coefficient with calculations using models for the plane wave reflection coefficient, searching over geo-acoustic parameter space. For these inversions we first assume the seabed to

consist of a single homogeneous fluid sediment layer on top of a homogeneous fluid subbottom. As the fringe pattern of some of the measured reflection loss data suggests the existence of at least two layers, the data are also inverted using a seabed model comprising two fluid sediment layers on top of a homogeneous fluid subbottom. These models are described in section 1. Also, the smearing effect of the beamforming is discussed in that section.

For the global search method a relatively new technique, called "differential evolution" (Storn and Price, 1995), is applied. A brief description of differential evolution, and a comparison with a genetic algorithm, is given in section 2. The ambient noise experiments and the data selected for this study are described in section 3. The inversion results are given and discussed in section 4. Section 5 presents a summary and some conclusions.

1. Ambient noise inversion - applied theory

A beam-smeared approximation of the bottom reflection coefficient is obtained by calculating the ratio of the downward and upward array response. Theoretically, this is given by (Harrison and Simons, 2001)

$$\hat{R}(\theta_s, f) = \frac{A_-}{A_+} = \frac{A(-\theta_s)}{A(\theta_s)} = \frac{\int_{-\pi/2}^{\pi/2} \frac{R(\theta,f)}{1-R(\theta,f)} B(\theta, \theta_s, f) \sin 2\theta d\theta}{\int_{-\pi/2}^{\pi/2} \frac{1}{1-R(\theta,f)} B(\theta, \theta_s, f) \sin 2\theta d\theta} \quad (1.1)$$

with

A_+	upward array response
A_-	downward array response
θ	grazing angle of incidence at the seabed
θ_s	steering angle of the beamformer
f	frequency
R	true bottom reflection coefficient
B	beam pattern of the vertical array

The real bottom loss BL is given by $BL = -20\log_{10}|R|$, whereas the beam-smeared bottom loss is given by $\hat{BL} = -20\log_{10}|\hat{R}|$. The effect of beamforming is to smear out features in BL, especially at the lower frequencies.

We search with an optimisation method for the geo-acoustic parameters by matching measured and modelled bottom loss $\hat{BL}$ using the following energy function

$$E(\mathbf{m}) = \frac{1}{C}\sum_{\theta,f}(\hat{BL}_{\text{cal}}(\theta, f, \mathbf{m}) - \hat{BL}_{\text{exp}}(\theta, f))^2 \quad (1.2)$$
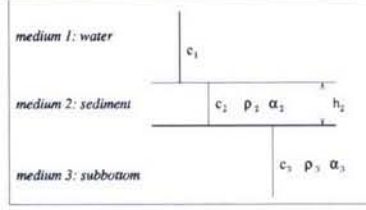
with

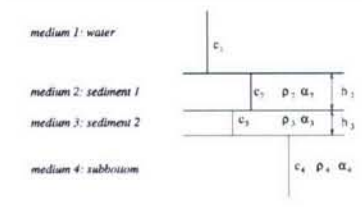*Figure 1.1a.* The single-sediment geo-acoustic bottom model.

Figure 1.1b. The two-sediment geo-acoustic bottom model.

m	the vector containing the unknown geo-acoustic parameters
C	a normalisation constant
$\hat{BL}_{cal}$	calculated or modelled bottom loss in dB (including smearing effect)
$\hat{BL}_{exp}$	experimental or measured bottom loss in dB

Two models for the seabed have been employed: a seabed consisting of a single fluid sediment layer on top of a homogeneous fluid subbottom (see figure 1.1a) and a seabed consisting of two fluid homogeneous sediment layers on top of a fluid subbottom (see figure 1.1b).

Each sediment and subbottom is assumed to have a constant sound speed, density and attenuation. To limit the size of the parameter search space, we do not invert for the densities ρ_2, ρ_3 and ρ_4. Density is coupled to sound speed according to one of the empirical relations given by (Hamilton and Bachman, 1982). Further, we assume $\alpha_4 = \alpha_3 = \alpha_2 = \alpha$, because the reflection co-efficient is less sensitive to attenuation in the deeper layers. For these layered structures analytical solutions for the reflection coefficient are given by (Jensen et al., 1994).

For the two-sediment layered structure the reflection coefficient R is given by

$$R = \frac{R_{12} + R_{24}\exp(2i\phi_2)}{1 + R_{12}R_{24}\exp(2i\phi_2)} \tag{1.3}$$

with

$$R_{24} = \frac{R_{23} + R_{34}\exp(2i\phi_3)}{1 + R_{23}R_{34}\exp(2i\phi_3)} \tag{1.4}$$

where R_{jk} is the (Rayleigh) reflection coefficient for the interface between medium j and k (medium 1 = water, medium 2 = sediment no.1 , etc., see figure 1):

$$R_{jk} = \frac{\frac{\rho_k c_k}{\sin\theta_k} - \frac{\rho_j c_j}{\sin\theta_j}}{\frac{\rho_k c_k}{\sin\theta_k} + \frac{\rho_j c_j}{\sin\theta_j}} \tag{1.5}$$

for $k = j + 1; j = 1, 2, 3$. Here $\theta = \theta_1$ and the vertical plane phase delays are given by $\phi_2 = k_2 h_2 \sin\theta_2$ and $\phi_3 = k_3 h_3 \sin\theta_3$.

Further, Snell's law applies: $k_4 \cos\theta_4 = k_3 \cos\theta_3 = k_2 \cos\theta_2 = k_1 \cos\theta_1$ where the wavenumber in medium j is given by $k_j = \frac{2\pi f}{c_j}$.

For the single-sediment situation the reflection coefficient is given by

$$R = \frac{R_{12} + R_{23}\exp(2i\phi_2)}{1 + R_{12}R_{23}\exp(2i\phi_2)} \tag{1.6}$$

In these equations the sound speed c_j is complex when the attenuation $\alpha_j \neq 0$. The imaginary part of c_j is then given by

$$\frac{c_j \alpha_j}{40\pi log_{10}(e)} = \frac{c_j \alpha_j}{54.575} \tag{1.7}$$

2. Description of differential evolution

In underwater acoustics genetic algorithms (GA) were introduced by (Gerstoft, 1994). Its principle of operation is summarised as follows. To optimise an energy function E, GA improves populations of q parameter combinations during successive generations. A GA optimisation run starts by creating at random an initial population of size q. Each member represents a certain parameter value combination **m** and its energy E is calculated. Because a population member with a lower E has a higher fitness, it attains a higher probability to be selected in one (or more) of the pairs of parents to be formed. This results in $q/2$ pairs of parents with a larger proportion of fit members. From each pair of parents two children are created by a random exchange of parental values, steered by the crossover probability p_c, followed by random changes of the N_p parameter values, with mutation probability p_m. A set of q children vectors results. The next generation is established by taking at random $f_r q$ members of these children and selecting the $(1 - f_r)q$ most fit members of the current population. This process is repeated over several hundreds of generations.

A GA has the following setting parameters: population size q, crossover probability p_c, mutation probability p_m, reproduction size f_r and the number of generations N_G. These have to be selected carefully and can be problem-specific, i.e., they depend on the optimisation problem at hand (see e.g. (van Moll and Simons, 2004)).

Differential evolution (DE), just like GA, starts with an initial population of q randomly chosen parameter value combinations **m**. These **m**'s are improved during successive generations of constant size q, in the sense that a descendant replaces an **m**, becoming its successor, if it has a lower energy. The distinctive

feature of DE is the way in which these descendants are created. In (Storn and Price, 1995) various ways to generate new m's are described. Here only the following procedure is considered. At the start of generation k the parameter vectors $\mathbf{m}_{k,1}, ..., \mathbf{m}_{k,q}$ are given and for each of them a descendant is created, being a potential successor. To create this descendant $\mathbf{d}_{k,i}$ of $\mathbf{m}_{k,i}$ first a partner $\mathbf{p}_{k,i}$ is constructed according to

$$\mathbf{p}_{k,i} = \mathbf{m}_{k,i_1} + F(\mathbf{m}_{k,i_2} - \mathbf{m}_{k,i_3}) \tag{1.8}$$

with three different vectors $\mathbf{m}_{k,i_1}$, $\mathbf{m}_{k,i_2}$ and $\mathbf{m}_{k,i_3}$ chosen at random from the population and F a scalar multiplication factor between 0 and 1. The descendant $\mathbf{d}_{k,i}$ of $\mathbf{m}_{k,i}$ results from applying crossover to $\mathbf{m}_{k,i}$ and $\mathbf{p}_{k,i}$ with crossover probability p_c. A higher value of p_c leads (on the average) to more dimensions of $\mathbf{p}_{k,i}$ to be copied into $\mathbf{d}_{k,i}$, while the values for the remaining dimensions are taken from $\mathbf{m}_{k,i_3}$. $\mathbf{d}_{k,i}$ only replaces $\mathbf{m}_{k,i}$, becoming its successor, if its energy is lower. The setting parameters of DE are population size q, multiplication factor F, crossover probability p_c and the number of generations N_G.

Comparing GA and DE, both show improvement of a fixed sized population of parameter combinations. However, in each generation of GA a fixed fraction of the population is replaced by children, whether they are better or not. In DE each member of the population will be replaced by its descendant only if this descendant has lower energy. On the other hand, the fitness of a member increases the probability of that member to play a role in the creation of children in GA, where in DE this fitness does not influence the probability of a member to be selected. Another difference is the way a partner $\mathbf{p}_{k,i}$ is found for $\mathbf{m}_{k,i}$. While in GA the partner is an element of the given generation, in DE it is constructed from the population and thus not an element of this generation. The partner creation process in DE is steered by the multiplication factor F and replaces the mutation mechanism of GA.

In (van Moll and Simons, 2004) and (Snellen et al., 2004) it was demonstrated that, compared to a GA, a ten times higher efficiency is obtained with DE, as DE finds the global optimum with only one tenth of the number of forward model evaluations.

3.   The selected ambient noise data

For this study we selected the North Elba case (silt bottom, water depth 121 m) from the five sites in the Mediterranean where ambient noise measurements were carried out. The motivation for selecting the North Elba data is the irregularity of the interfering fringes in the observed bottom loss, which might be evidence for the presence of two sediment layers. This is considered to be a challenging situation for inversion. The experiments were described in great

detail by (Harrison and Simons, 2002). They were carried out with a moored 64 element vertical array with an acoustic aperture of 62 m roughly centred in the water column. Only the middle 32 regularly spaced hydrophones (aperture 16 m, element spacing 0.5 m) were used for the processing, which consisted of beamforming of manually selected portions of noise data. Each portion comprises a few seconds of ambient noise data. The resulting array responses versus angle and frequency were averaged over many portions of data. The up-to-down ratio of the array response is thus based on a few minutes of data in total.

4.   Inversion results

4.1   Single sediment layer inversions - the North Elba data

We discuss the inversion results of the bottom loss data obtained from the North Elba ambient noise data (see figure 1.5a) assuming a single sediment model for the seabed (see figure 1.1a). As explained in section 1 we do not invert for density, hence the number of parameters sought amounts to 4. The search bounds of the parameters to be inverted are given in table 1.1. A constraint in the inversion algorithm is $c_3 > c_2$ ($c_1 = 1514$ m/s).

Table 1.1.   Parameters to be inverted for: single-sediment inversions of the North Elba data.

Parameter	Search range	Inversion result
c_2 [m/s]	1400-1700	1520.4 ± 0.6
ρ_2 [g/cm^3]	N.A	1.562 ± 0.002
h_2 [m]	0.1-5	3.40 ± 0.03
α [dB/λ]	0-2	0.00031 ± 0.00004
c_3 [m/s]	1500-1900	1538.4 ± 1.5
ρ_3 [g/cm^3]	N.A.	1.620 ± 0.004

DE was run 57 times. In the following we perform a statistical analysis of the final parameter estimates of 52 successful runs. Parameter correlation is illustrated in figure 1.2 showing the magnitude of the linear correlation coefficient calculated for all combinations of the parameter estimates. The statistical significance of each of the correlation coefficients was also determined: the red stars in the figure indicate for which parameter combination the confidence of the observed correlation coefficient exceeds 95%.

In figure 1.3 parameter estimates are plotted against each other for combinations with strong coupling. There is no correlation between the sediment geo-acoustic parameters (c_2, c_3 and α) and the sediment thickness h_2.

Histograms of the parameter estimates are given in figure 1.4. The corresponding mean and standard deviations for each parameter are given in table
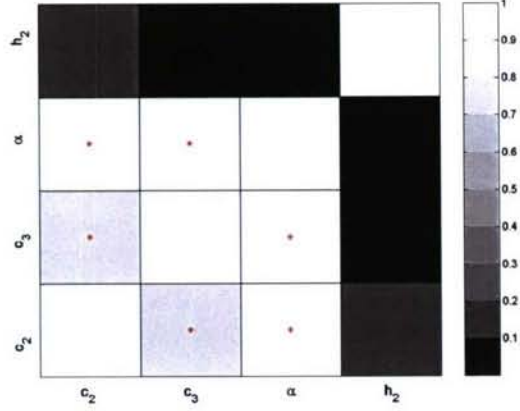
Figure 1.2. Single-sediment inversions of the North Elba data: magnitude of the correlation coefficient for all parameter combinations. A red star is plotted if the correlation is statistically significant.
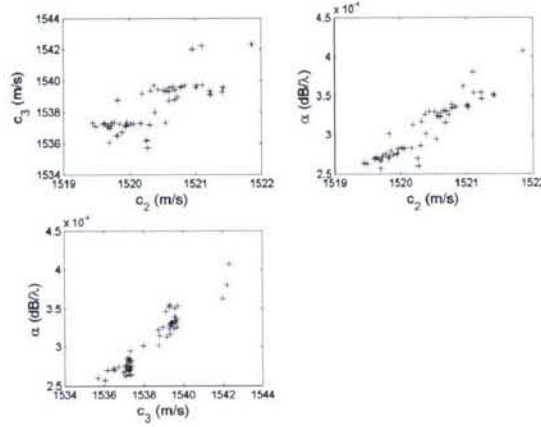

Figure 1.3. Single-sediment inversions of the North Elba data: The 52 parameter estimates plotted against each other for those combinations with strong coupling.

1.1. It can be concluded that all parameters are accurately determined. The parameter values obtained are further assessed in section 4.2.2 where we discuss inversions of the same data with a two-sediment layer model.

Using equation 1.1 we have calculated the beam-smeared bottom loss $\hat{BL}$ for the mean values of the inversion results as given in table 1.1, the result of which is given in figure 1.5d. The deviation from the measured (beam-smeared) bottom loss, as presented in figure 1.5a, is given in figure 1.5e. The
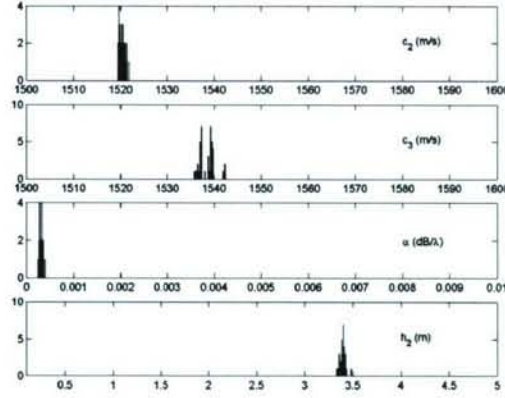
Figure 1.4. Single-sediment inversions of the North Elba data: histograms of the 52 estimates for each parameter.

same is done for the parameters reported in (Harrison and Simons, 2002), which were obtained using the hand-searching technique (see figures 1.5b and 1.5c). We observe that a considerable improvement is obtained with an automated search technique

4.2 Inversions with two sediments

4.2.1 Synthetic case. First, the performance of the inversion with two sediments is assessed using a synthetic reflection coefficient created for the parameter values given in table 1.2. Again, we do not invert for density (see section 1), hence the number of parameters sought amounts to 6. Constraints in the inversion algorithm are: $c_4 > max(c_2, c_3)$ and $h_2 + h_3 < 5$ m ($c_1 = 1514$ m/s).

The inversion was run 171 times. On the basis of the energy function values obtained for these runs, two solutions to the inversion problem can be distinguished, see figure 1.6.

First, we select the best solutions for which $E < 0.01$ (111 out of 171). For these solutions parameter correlation is illustrated in figure 1.7, which shows the magnitude of the linear correlation coefficient calculated for all combinations of parameter estimates. Again, we indicate for which parameter combination the confidence of the observed correlation coefficient exceeds 95 %. As in the case of the single sediment inversions of measured data (see previous paragraph), the geo-acoustic parameters of the two sediments (c_2, c_3, c_4 and α) are strongly coupled. Also, the thicknesses of the sediments, h_2 and h_3, are
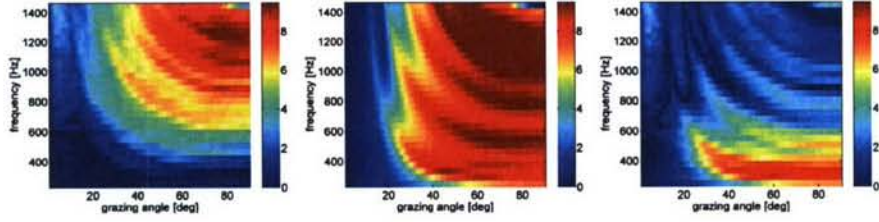
Figure 1.5a.
Measured bottom loss
$\hat{BL}$

Figure 1.5b.
Modelled $\hat{BL}$ using geo-
acoustic parameters from
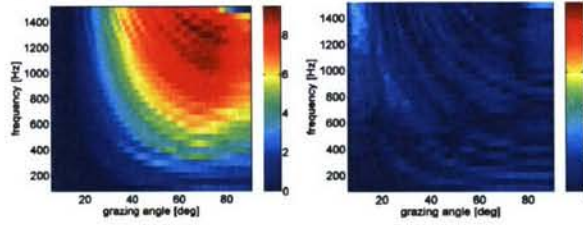(Harrison and Simons, 2002)

Figure 1.5c.
Deviation of modelled
$\hat{BL}$ (figure 1.5b)
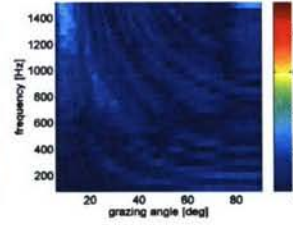from measured $\hat{BL}$

Figure 1.5d.
Modelled $\hat{BL}$ using
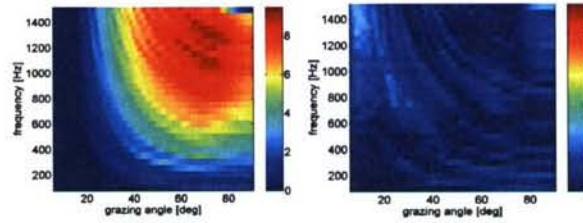DE-inverted geo-acoustic
parameters (single sediment)

Figure 1.5e.
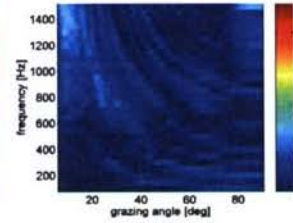Deviation of modelled
$\hat{BL}$ (figure 1.5d)
from measured $\hat{BL}$

Figure 1.5f.
Modelled $\hat{BL}$ using
DE-inverted geo-
acoustic parameters
(two sediments)

Figure 1.5g.
Deviation of modelled
$\hat{BL}$ (figure 1.5f)
from measured
$\hat{BL}$

Table 1.2. Parameters to be inverted for: two-sediment inversions of the synthetic data.

| Parameter	Search range	True value	Inversion result Best solution $E < 0.01$	Inversion result Solutions with $E \approx 0.07$
c_2 [m/s]	1400-1700	1540	1540.1 ± 0.3	1539.1 ± 0.2
ρ_2 [g/cm^3]	N.A	1.624	1.625 ± 0.001	1.622 ± 0.001
h_2 [m]	0.1-5	2.0	2.000 ± 0.007	3.006 ± 0.002
c_3 [m/s]	1400-1700	1530	1530.1 ± 0.3	1575.1 ± 0.3
ρ_3 [g/cm^3]	N.A	1.594	1.595 ± 0.001	1.714 ± 0.001
h_3 [m]	0.1-5	1.0	1.001 ± 0.007	1.3 ± 0.4
c_4 [m/s]	1500-1900	1570	1570.1 ± 0.4	1575.1 ± 0.2
ρ_4 [g/cm^3]	N.A	1.702	1.702 ± 0.001	1.714 ± 0.001
α [dB/λ]	0-2	0.05	0.051 ± 0.001	0.055 ± 0.001
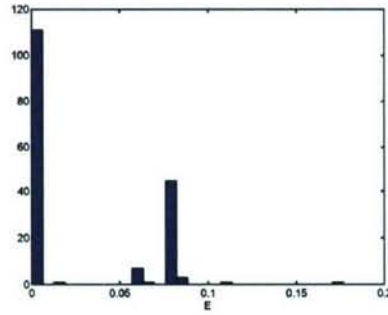
Figure 1.6. Two-sediment inversions of the synthetic data: histogram of the final energy function values obtained for the 171 successful inversions.

strongly coupled, but there is virtually no correlation between the geo-acoustic parameters and the thicknesses.

Histograms of these parameter estimates are given in figure 1.8. The corresponding mean and standard deviation for each parameter are given in table 1.2. It can be concluded that all parameters are accurately determined and that their mean values are in excellent agreement with the true values.

Next, we select the somewhat worse solutions where E is around 0.07 (see the second peak in the histogram for E, figure 1.6). Histograms of these parameter estimates are given in figure 1.9. The corresponding mean and standard deviations for each parameter are given in table 1.2. It is observed that a single layer solution is found now, i.e., a top sediment layer with a sound speed nearly equal to that of the first layer, with a thickness equal to the sum of the two sediments (being 3 m). Further, c_3 becomes equal to c_4 and, consequently, h_3 becomes undetermined. Still, this somewhat worse solution is physically
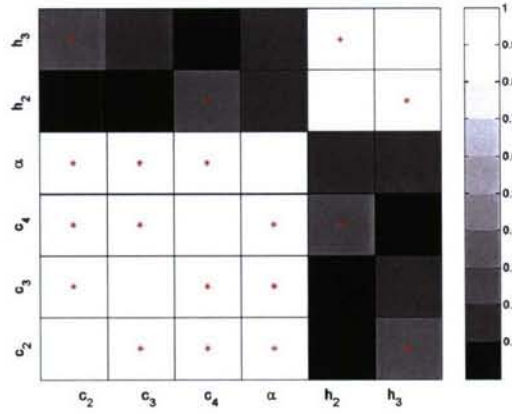
12

Figure 1.7. Two-sediment inversions of the synthetic data: magnitude of the correlation co-efficient for all parameter combinations. A red star is plotted if the correlation is statistically significant.
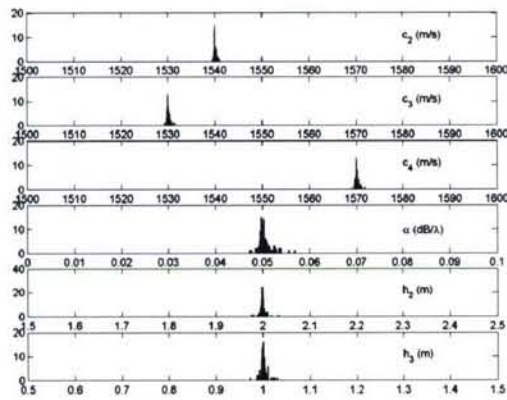

Figure 1.8. Two-sediment inversions of the synthetic data: histograms of the best estimates for each parameter ($E < 0.01$).
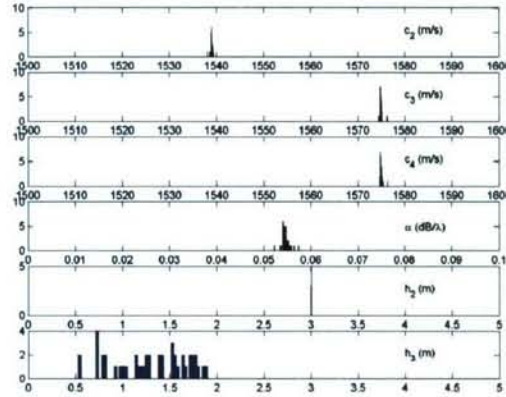
Figure 1.9. Two-sediment inversions of the synthetic data: histograms of the somewhat worse estimates ($E \approx 0.07$).

plausible. The somewhat higher sound speed found in the lower 1 m of the 3 m sediment (1540 m/s instead of the true 1530 m/s) and also below the sediment (1575 m/s instead of the true 1570 m/s) is compensated by a somewhat higher attenuation (0.055 dB/λ instead of the true 0.05 dB/λ).

The good performance of this synthetic inversion problem is promising for inversion of measured data using a two-sediment geo-acoustic model. However, the two solutions discussed also illustrate the non-uniqueness of the solution of geo-acoustic inverse problems. For this synthetic case the two solutions can clearly be distinguished by their energy. For the inversion of experimental data it is expected that it can be less obvious which solution to choose.

4.2.2   The North Elba data.   We now discuss the inversion results of the bottom loss data obtained from the North Elba ambient noise data (see figure 1.5a) assuming a two-sediment model for the seabed (see figure 1.1b). The inversion algorithm is the same as that for the synthetic inversions described in the previous paragraph. The inversion was run 200 times, of which 114 successful runs were selected. Histograms of the corresponding parameter estimates are given in figure 1.10. It seems that sediment thicknesses are not well resolved. However, for the total sediment thickness, $h_2 + h_3$, we do obtain a peaked distribution. Also, as in the synthetic case, h_2 and h_3 are correlated.

Figure 1.11 presents a plot of the estimates for h_2 plotted against those for h_3. It seems obvious to make a selection based on total sediment thickness. We chose $3.3 < h_2 + h_3 < 3.5$ m.

Histograms of the selected solutions are given in figure 1.12. (Of course, the distribution for $h_2 + h_3$ is very peaked now, but h_2 and h_3 separately re-
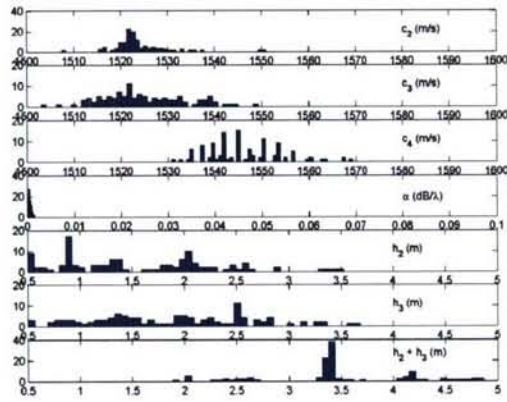
Figure 1.10. Two-sediment inversions of the North Elba data: histograms of the 114 estimates for each parameter. Note that we included the histogram for total sediment thickness.
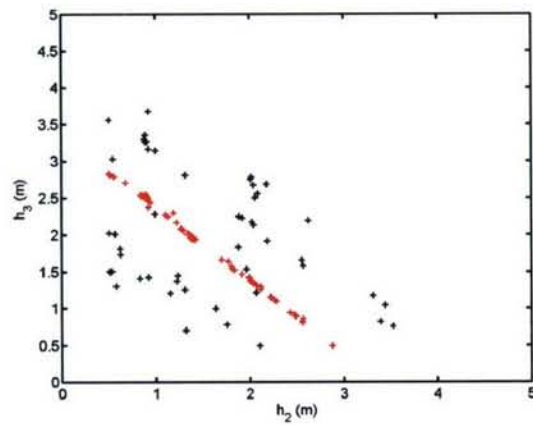

Figure 1.11. Two-sediment inversions of the North Elba data: 114 estimates for h_2 plotted against those for h_3. The selected solutions are indicated by the red symbols.
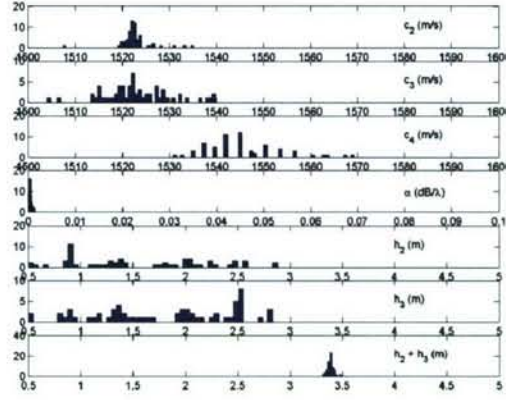
Figure 1.12. Two-sediment inversions of the North Elba data: histograms of the parameter estimates, which were selected on total sediment thickness.

main unresolved). The corresponding mean and standard deviations for each parameter are given in table 1.3. The inversion result reported in (Harrison and Simons, 2002) is also included for comparison.

Table 1.3. Parameters to be inverted for: two-sediment inversions of the North Elba data.

Parameter	Search range	Inversion result Harrison and Simons	Inversion result This work
c_2 [m/s]	1400-1700	1600	1523 ± 4
ρ_2 [g/cm^3]	N.A	1.8	1.57 ± 0.01
h_2 [m]	0.1-5	0.7	1.57 ± 0.65
c_3 [m/s]	1400-1700	1530	1523 ± 7
ρ_3 [g/cm^3]	N.A	1.75	1.57 ± 0.03
h_3 [m]	0.1-5	2.1	1.82 ± 0.65
c_4 [m/s]	1500-1900	1600	1546 ± 8
ρ_4 [g/cm^3]	N.A	1.8	1.64 ± 0.02
α [dB/λ]	0-2	0.14[1]	0.0005 ± 0.0003
$h_2 + h_3$ [m]	N.A.	N.A.	3.38 ± 0.03

For completeness, parameter coupling of the selected solutions is shown in figure 1.13, a similar behaviour as that of the synthetic inversion problem (figure 1.7). Basically, a single sediment solution is obtained, because the inversion result for c_2 equals that of c_3 and a peaked distribution is only obtained for $h_2 + h_3$ and not for h_2 or h_3 separately. Further, the solution agrees well with the single-sediment solution given in table 1.1. However, it does not agree well
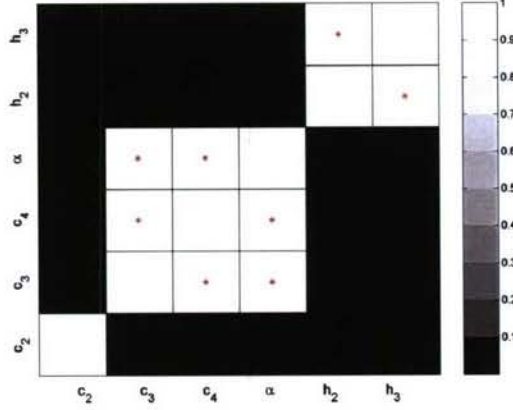
Figure 1.13. Two-sediment inversions of the North Elba data: magnitude of the correlation coefficient for the selected solutions. A red star is plotted if the correlation is statistically significant.

with the solution of (Harrison and Simons, 2002), albeit that both solutions are representative of a silt bottom.

Finally, we have calculated the beam-smeared bottom loss $\hat{BL}$ for the mean values of the inversion results as given in table 1.3, the result of which is given in figure 1.5f. The deviation from the measured (beam-smeared) bottom loss, as presented in figure 1.5a, is given in figure 1.5g. No further improvement compared to the single-sediment solution (figures 1.5d and 1.5e) is obtained, which is not surprising, as the single-sediment and two-sediment inversion results are basically the same.

5.   Summary and conclusions

An approximation of the plane wave reflection coefficient of the seabed (as a function of grazing angle and frequency) can be found by comparing the upward- and downward-going noise. In (Harrison and Simons, 2002) these were determined by beamforming the ambient noise field received on a vertical array of hydrophones. Geo-acoustic parameters were derived with a hand-searching technique that relies on inspection of the experimental reflection loss for critical angle, modulation depth and fringe spacing. In this article we inferred geo-acoustic parameters by inversion of the measured reflection coefficient with a global optimisation technique as an automatic search method. For this study we selected the North Elba data (silt bottom), one of the sites in the Mediterranean where ambient noise measurements were carried out (see (Harrison and Simons, 2002)). The measured reflection coefficient was com-

pared with calculations using models for the plane wave reflection coefficient, searching over geo-acoustic parameter space. For these inversions we assumed the seabed to consist of a single homogeneous fluid sediment layer on top of a homogeneous fluid subbottom. The data were also inverted using a seabed model comprising two fluid sediment layers on top of a homogeneous fluid subbottom. For the global search method a relatively new (but fast) technique, called "differential evolution" (Storn and Price, 1995), was applied. It was found that all parameters could be accurately determined. With the two-layer geo-acoustic model basically a single-sediment solution is obtained, which is in excellent agreement with the solution obtained with the single-sediment model. However, they do not agree well with the solution reported in (Harrison and Simons, 2002), albeit that all solutions are representative of a silt bottom. A comparison of the beam-smeared bottom loss, calculated for the geo-acoustic parameters inverted, with the measured bottom loss shows that a considerable improvement can be obtained with an automated search technique.

Notes

1. Attenuation of first sediment layer

References

E.L. Hamilton and R.T. Bachman, "Sound velocity and related properties of marine sediments", J. Acoust. Soc. Am., 72(6), December **1982**, pp 1891 - 1904

Peter Gerstoft, "Inversion of seismoacoustic data using genetic algorithms and a posteriori probability distributions", J. Acoust. Soc. Am., 95 (2), February **1994**, pp 770 - 782

Finn B. Jensen, William A. Kuperman, Michael B. Porter, Henrik Schmidt, "Computational Ocean Acoustics", American Institute of Physics, New York, **1994**

Rainer Storn and Kenneth Price, "Differential Evolution - A simple and efficient adaptive scheme for global optimization over continuous spaces, ICSI Technical Report TR-95-012, March **1995**

N.M. Carbone, G.B. Deane and M.J. Buckingham, "Estimating the compressional and shear speeds of a shallow-water seabed from the vertical coherence of ambient noise in the water column", J. Acoust. Soc. Am., 103, **1998**, pp 801 - 813

C. H. Harrison and D.G. Simons, "Geoacoustic inversion of ambient noise: A simple method", Conference on Acoustical Oceanography, Southampton UK, 9-12 April **2001**, edited by T.G. Leighton, Proc. Inst. of Acoust. 23, pp 91-98

C. H. Harrison and D.G. Simons, "Geoacoustic inversion of ambient noise: A simple method", J. Acoust. Soc. Am., 112 (4), October **2002**, pp 1377 - 1389

Camiel van Moll and Dick G. Simons, "Improved Performance of Global Optimisation Methods for Inversion Problems in Underwater Acoustics", Proc. of the 7th European Conference on Underwater Acoustics, Delft 5-8 July, 2004

Mirjam Snellen, Camiel van Moll and Dick G. Simons, "Application of Differential Evolution as an Optimisation Method for Geo-acoustic Inversion ", Proc. of the 7th European Conference on Underwater Acoustics, Delft 5-8 July, 2004

E Sub-bottom profiling with ambient noise measured on a drifting vertical array; CRETE 2005

SUB-BOTTOM PROFILING WITH AMBIENT NOISE MEASURED ON A DRIFTING VERTICAL ARRAY

Simons Dick G.[a,b], Snellen Mirjam[a], Weterings Ardien[a,b] and Harrison Chris H.[c],

[a]Delft University of Technology, Department of Earth Observation and Space Systems, Kluyverweg 1, Delft, The Netherlands
[b]TNO Defence, Security and Safety, Oude Waalsdorperweg 63, The Hague, The Netherlands
[c]NATO Undersea Research Centre, Viale S. Bartolomeo 400, 19138 La Spezia, Italy

D G Simons, TNO Defence, Security and Safety, PO Box 96864, 2509 JG The Hague, The Netherlands, fax: +31-70-3740490, email: simons@fel.tno.nl

Abstract: The angle and frequency dependent reflective properties of the seabed can be determined from beam-steered ambient noise measurements on a vertical array of hydrophones. From the up-to-down ratio the beam-smeared modulus square of the plane wave reflection coefficient is obtained. Geo-acoustic parameters can be inverted by matching the measured and modelled reflection loss assuming a certain number of sediment layers. The searching for the geo-acoustic parameters is done with fast global optimisation techniques such as differential evolution. An alternative approach is to Fourier transform the reflection coefficient producing the minimum phase impulse response, which explicitly shows layer boundaries. Spectral factorisation is applied to restore the lost phase of the reflection coefficient. This method offers the possibility of determining the number of layers and their order. Both methods were applied to reflection loss data extracted from ambient noise measurements on a drifting vertical array in the shallow waters in the Mediterranean. The results of both methods are compared showing good agreement between the two sets of sediment layering estimates. It is concluded that the methods offer a sub-bottom profiling technique without making additional sound where the array is sensing local seabed properties with a footprint of order the water depth.

Keywords: Geo-acoustic inversion, ambient noise, sub-bottom profiling

1. INTRODUCTION

In a series of recent papers, methods for deriving geo-acoustic parameters from measured ambient noise fields are presented. Carbone ([1]) measures the broadband noise coherence

with a vertically separated pair of hydrophones, which is compared with noise model calculations searching over geo-acoustic parameter space. In [2] an approximation of the plane wave reflection coefficient of the seabed (as a function of grazing angle and frequency) is determined directly from the beam-formed ambient noise field received on a vertical array of hydrophones by comparing the upward- and downward-going noise. Subsequently, model calculations for the reflection coefficient and an efficient global search technique are employed for inferring the geo-acoustic parameters ([3]). In [4] the seafloor layering is obtained in a direct manner by Fourier transforming the reflection coefficient as a function of frequency for each angle. Spectral factorization is applied for restoring the phase of the reflection coefficient.

In this paper we apply the latter two methods, both employing the measured reflection coefficient, for sub-bottom profiling. To demonstrate the methods' capabilities they are applied to real data consisting of a series of ambient noise data acquired with a drifting vertical hydrophone array.

In section 2 the method of inverting the reflection coefficient data is presented. For the global search the technique of "differential evolution" ([5]) is applied. A brief description of differential evolution is also included in section 2. In section 3 the method of Fourier transforming the reflection coefficient is described. The ambient noise experiments and the data selected for this study are described in section 4. The sub-bottom profiling results as obtained by both methods are presented, compared and discussed in section 5. Section 6 gives a summary and some conclusions.

2. SUB-BOTTOM PROFILING THROUGH INVERSION OF SHALLOW WATER AMBIENT NOISE

A beam-smeared approximation $\hat{R}$ of the bottom reflection coefficient R is obtained by determining the ratio of the downward and upward array response of the vertical array. Theoretically, this is given by ([3])

$$\hat{R}(\theta_s, f) = \frac{A_-}{A_+} = \frac{A(-\theta_s)}{A(\theta_s)} = \frac{\displaystyle\int_{-\pi/2}^{\pi/2} \frac{R(\theta,f)}{1-R(\theta,f)} \, b(\theta,\theta_s,f) \sin 2\theta \, d\theta}{\displaystyle\int_{-\pi/2}^{\pi/2} \frac{1}{1-R(\theta,f)} \, b(\theta,\theta_s,f) \sin 2\theta \, d\theta} \tag{1}$$

with A_+ and A_- the upward and downward array response, respectively. θ is the grazing angle at the seabed, θ_s the steering angle of the beam-former, f the frequency, R the true bottom reflection coefficient and b the beam pattern of the vertical array.

The real bottom loss B is given by $B = -20^{10}\log|R|$ and $\hat{B} = -20^{10}\log|\hat{R}|$ is the beam-smeared bottom loss. The effect of beam-forming is to smear out features in B, especially at the lower frequencies. The seabed is assumed to consist of a single fluid sediment layer on top of a homogeneous fluid sub-bottom (see Fig. 1). The sediment and sub-bottom are each assumed to have a
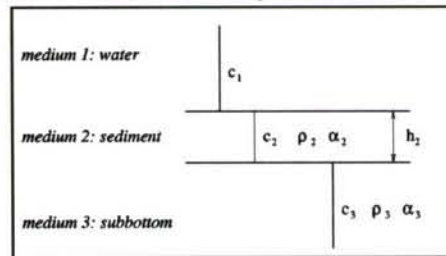

Fig. 1: The single-sediment geo-acoustic bottom model.

constant sound speed, density and attenuation. Further, the attenuation in the sediment and sub-bottom are assumed equal, i.e., $\alpha_2 = \alpha_3$.

Analytical solutions for the reflection coefficient as given by [6] are used for the forward calculations. We search with an optimisation method for the six unknown geo-acoustic parameters, $\mathbf{m} = (c_2, \rho_2, h_2, c_3, \rho_3, \alpha)$, by matching measured and modelled bottom loss $\hat{B}$ using the following energy function

$$E(\mathbf{m}) = \frac{1}{C}\sum_{\theta,f}\left(\hat{B}_{cal}(\theta,f,\mathbf{m}) - \hat{B}_{exp}(\theta,f)\right)^2 \tag{2}$$

with $\mathbf{m}$ the vector containing the unknown geo-acoustic parameters, C a normalisation constant, $\hat{B}_{cal}$ and $\hat{B}_{exp}$ the calculated and measured bottom loss in dB (including smearing effect), respectively.

For the optimization of E (Eq. 2) differential evolution (DE) is used ([5]). DE starts with an initial population of q randomly chosen parameter value combinations $\mathbf{m}$. These $\mathbf{m}$'s are improved during successive generations of constant size q, in the sense that a descendant replaces an $\mathbf{m}$, becoming its successor, if it has a lower energy. In [5] various ways to generate descendants, i.e., new $\mathbf{m}$'s, are described. Here only the following procedure is adopted. At the start of generation k the parameter vectors $\mathbf{m}_{k,1}, \ldots \mathbf{m}_{k,q}$ are given and for each of them a descendant is created, being a potential successor. To create this descendant $\mathbf{d}_{k,i}$ of $\mathbf{m}_{k,i}$ first a partner $\mathbf{p}_{k,i}$ is constructed according to $\mathbf{p}_{k,i} = \mathbf{m}_{k,i1} + F(\mathbf{m}_{k,i2} - \mathbf{m}_{k,i3})$, with three different vectors $\mathbf{m}_{k,i1}$, $\mathbf{m}_{k,i2}$ and $\mathbf{m}_{k,i3}$ chosen at random from the population and F a scalar multiplication factor between 0 and 1. The descendant $\mathbf{d}_{k,i}$ of $\mathbf{m}_{k,i}$ results from applying crossover to $\mathbf{m}_{k,i}$ and $\mathbf{p}_{k,i}$ with crossover probability p_c. A higher value of p_c leads (on the average) to more dimensions of $\mathbf{p}_{k,i}$ to be copied into $\mathbf{d}_{k,i}$, while the values for the remaining dimensions are taken from $\mathbf{m}_{k,i}$. Only if its energy is lower, $\mathbf{d}_{k,i}$ replaces $\mathbf{m}_{k,i}$, thereby becoming its successor. The setting parameters of DE are population size q, multiplication factor F, crossover probability p_c and the number of generations N_G. The global search is followed by a local search with the downhill simplex method.

3. SUB-BOTTOM PROFILING BY FOURIER TRANSFORMING THE REFLECTION COEFFICIENT

The reflection coefficient is an interference pattern as a function of frequency and grazing angle caused by the angle dependent path differences between the layer boundaries. As presented by Harrison ([4]) the impulse response for each grazing angle is derived by Fourier transforming the complex reflection coefficient. The impulse response reveals the layer boundaries of the sea-bottom.

The ratio of the downward and upward array response gives the modulus square of the reflection coefficient $|\hat{R}|$. However, the phase of the reflection coefficient can not be measured. For deducing the phase, spectral factorization is applied. The impulse response $r(t)$ now becomes

$$r(t) = \Im^{-1}\left\{\exp\left(H\left(\ln\left(\left|\hat{R}(\omega)\right|\right)\right)\right)\right\} \tag{3}$$

where $\Im$ is the Fourier transform and H is the operation of adding the through Hilbert transformation generated imaginary part and original real part.

$|\hat{R}(\omega)|$ is obtained from the data for a limited range of frequencies only, with the upper frequency (being 1500 Hz at normal incidence for our data) and lower frequency limit caused by the onset of grating lobes and by the beam angle resolution, respectively. Therefore $|\hat{R}(\omega)|$ is preprocessed before spectral factorization, Eq. (3), is used, extending the available frequency range. $|\hat{R}|$ is extrapolated between zero and the lower frequency. The extrapolated data between the upper frequency limit and 3kHz will be suppressed by using a windowing function. For this extrapolation, the modulus square reflection coefficient is written as a sum of n cosines ([4]), $|\hat{R}|^2 = \sum_{n=0} a_n \cos(\omega \tau_n)$.

4. THE AMBIENT NOISE DATA

For this study we selected data obtained using a drifting vertical array of hydrophones in the Mediterranean. The array was allowed to drift for around 12 hours and covered in this period about 5 miles near the Ragusa Ridge, south of Sicily. The experiment is described in more detail in [4]. The array consisted of 64 elements with an acoustic aperture of 62 m. Only the middle 32 regularly spaced hydrophones (aperture 16 m, element spacing 0.5 m) were used for the processing, which consisted of beamforming of the noise data. The water depth amounted to about 130 m. The resulting array responses versus angle and frequency were averaged over a series of data spanning a few minutes.
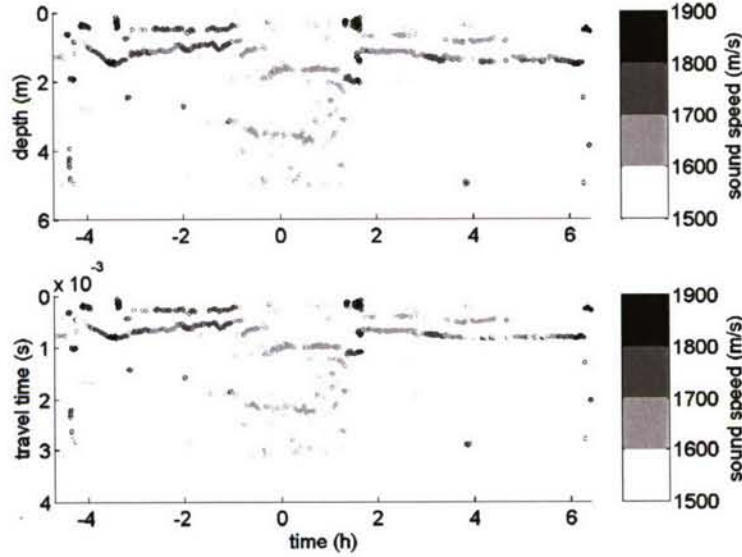

Fig. 2: a) Inverted layer thickness in meter as a function of time. The gray scale indicates the corresponding inverted sediment sound speed c_2 (m/s). b) Similar as for a) but now travel time.

5. RESULTS

5.1. Geo-acoustic parameters from inversion of ambient noise data

Fig. 2a depicts the layer depths as a function of time as obtained through inversion of the ambient noise data. Each dot in the figure corresponds to one inversion result, i.e., to one measured reflection coefficient. Also shown (in grayscale) are the corresponding sediment sound speeds. From these results it can be concluded that several layers exist. The sound speeds in the area corresponding to the left of the plot are somewhat higher than those in the area corresponding to the right of the plot. In the middle of the track the layering shows a very different behavior compared to the layering at the two ends of the track, which is probably caused by the presence of a ridge.

Fig. 2b shows the same results as Fig. 2a, but now travel times (one-way) (as derived using the inverted c_2 values) are presented. Compared to Fig. 2a the layering becomes more unique. It is concluded that some of the results of Fig. 2a correspond to local optima that differ in layer thickness and sediment sound speed but that are equal with regards to travel times. The sediment is found to have low attenuation coefficient, in general less than 0.2 dB/λ, with densities in between 1.2 and 1.8 g/cm^3.

5.2. Layer boundaries from Fourier transforming the reflection coefficient

The method of Fourier transforming the reflection coefficient is applied to the data. Fig. 3 shows the resulting profiling results constructed from the impulse responses between 80° and 90°. Several layer boundaries can clearly be distinguished. Again a change in layering can be seen at the ridge. The results of Fig. 3 show good agreement with the results presented in [4].
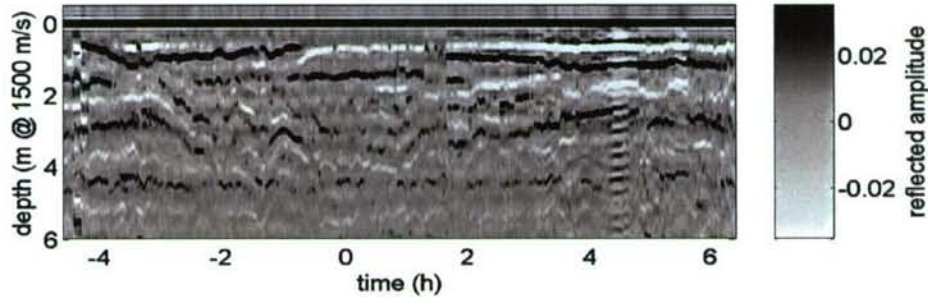

Fig. 3: Sub-bottom profile derived with Fourier transforming the reflection coefficient. Layer depth is in meters (using a sediment sound speed of 1500 m/s) and array drifting time is in hours.

5.3. Comparison of the two methods

Fig. 4 shows the comparison between the two sets of estimated layer thicknesses. The light dots present layer thicknesses as determined through inversion of the ambient noise data, valid for a sediment sound speed of 1500 m/s. The black dots indicate the first absolute

maxima of the inverse Fourier transformation results. Clearly the two methods give layer thicknesses that are in good agreement.
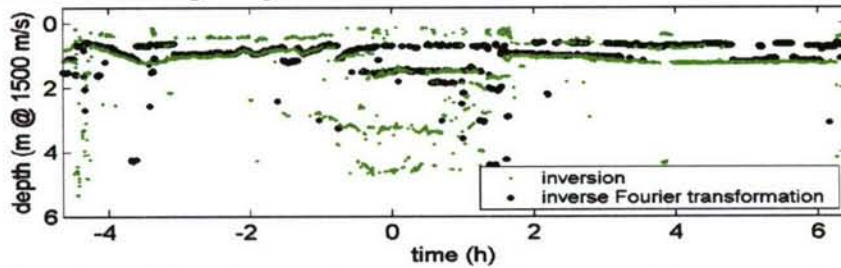

Fig. 4: Light dots: Inverted layer thickness (for a sediment sound speed of 1500 m/s). Black dots: layer thickness obtained by the inverse Fourier transformation method.

6. CONCLUSIONS

In this paper two methods for determining the seabottom layering out of ocean ambient noise have been applied to a series of data, acquired along a 5-mile track. The first method, where the reflection coefficient is modelled and a global optimisation method applied to find the maximum match between modelled and measured data, does not only provide the layering, but also allows for estimating other geo-acoustic parameters, such as sediment sound speed. The computational load of the method is large, implying computation times of a few days on a state-of-the-art PC. The second method, however, where the layering is determined directly from the data through inverse Fourier transformation, gives seabottom layering only. The computational load of this method is small, resulting in computation times of the order of minutes.

By comparison of the two sets of layer estimates it has been demonstrated that both methods give results that are in good agreement and apparently perform equally well for sub-bottom profiling. If one is interested in sediment classification, the inverse Fourier transform method could be used as a pre-processing step for the inversion, providing the number of layers and their order and an estimate for their thicknesses.

REFERENCES

[1] **N.M. Carbone, G.B. Deane and M.J. Buckingham**, Estimating the compressional and shear speeds of a shallow-water seabed from the vertical coherence of ambient noise in the water column, J. Acoust. Soc. Am. (103), pp 801-813 , 1998

[2] **C.H. Harrison and D.G. Simons**, Geoacoustic inversion of ambient noise: a simple method, J. Acoust. Soc. Am. (112), pp 1377-1389 , 2002

[3] **D.G. Simons, C.A.M. van Moll, C.H. Harrison**, Proc. Acoustics Inversion Methods and Experiments for Assessment of the Shallow Water Environment, Ischia, Italy, June 2004

[4] **C.H. Harrison**, Sub-bottom profiling using ocean ambient noise, J. Acoust. Soc. Am. (115), pp 1505-1515 , 2004

[5] **R. Storn and K. Price**, Differential Evolution – A simple and efficient adaptive scheme for global optimization over continuous spaces, ICSI Technical Report TR-95-012, 1995

[6] **Finn B. Jensen, William A. Kuperman, Michael B. Porter, Henrik Schmidt**, *Computational Ocean Acoustics*, American Inst. of Physics, New York, pp. 49-50, 1994

REPORT DOCUMENTATION PAGE
(MOD-NL)

1. DEFENCE REPORT NO (MOD-NL)	2. RECIPIENT'S ACCESSION NO	3. PERFORMING ORGANIZATION REPORT NO
TD2006-0143	-	TNO-DV 2006 A459

4. PROJECT/TASK/WORK UNIT NO	5. CONTRACT NO	6. REPORT DATE
015.31956	-	March 2007

7. NUMBER OF PAGES	8. NUMBER OF REFERENCES	9. TYPE OF REPORT AND DATES COVERED
92 (incl 5 appendices, excl RDP & distribution list)	1	Final

10. TITLE AND SUBTITLE

MFP-REA follow-up 2002-2005

11. AUTHOR(S)

Prof Dr D.G. Simons
C.A.M. van Moll, MSc

12. PERFORMING ORGANIZATION NAME(S) AND ADDRESS(ES)

TNO Defence, Security and Safety, P.O. Box 96864, 2509 JG The Hague, The Netherlands
Oude Waalsdorperweg 63, The Hague, The Netherlands.

13. SPONSORING AGENCY NAME(S) AND ADDRESS(ES)

Royal Netherlands Navy

14. SUPPLEMENTARY NOTES

The classification designation Ongerubriceerd is equivalent to Unclassified, Stg. Confidentieel is equivalent to Confidential and Stg. Geheim is equivalent to Secret.

15. ABSTRACT (MAXIMUM 200 WORDS (1044 BYTE))

Acoustic propagation in shallow water depends among others on the composition of the sea bottom. It is very desirable for the navy to use passive acoustic methods instead of active, to acquire knowledge about this composition. The intention of the Matched Field Inversion - Rapid Environmental Assessment project is to use ambient noise received on a vertical array for this bottom classification. To exploit the limited information content of ambient noise, a well chosen geoacoustic model is required, together with an efficient optimisation algorithm and an educated interpretation of the inversion results. This combination of knowledge has resulted in several articles, which are summarised in this report.

16. DESCRIPTORS	IDENTIFIERS
Underwater acoustics, ambient noise, bottom loss, reflection loss, matched field processing, geoacoustic inversion, global optimisation, differential evolution, vertical line array	

17a. SECURITY CLASSIFICATION (OF REPORT)	17b. SECURITY CLASSIFICATION (OF PAGE)	17c. SECURITY CLASSIFICATION (OF ABSTRACT)
Ongerubriceerd	Ongerubriceerd	Ongerubriceerd

18. DISTRIBUTION AVAILABILITY STATEMENT	17d. SECURITY CLASSIFICATION (OF TITLES)
Unlimited Distribution	Ongerubriceerd

Distribution list

The following agencies/people will receive a complete copy of the report.

1	DMO/SC-DR&D standaard inclusief digitale versie bijgeleverd op cd-rom
2/3	DMO/DR&D/Kennistransfer
4	Programmabegeleider Defensie ltz 1 drs. R.P.A. Dekeling
5	DMO/S&WT/HS&WT
6/8	Bibliotheek KMA
9	TNO Defensie en Veiligheid, vestiging Den Haag, Manager Waarnemingssystemen (operaties), ir. M.W. Leeuw
10	Programmaleider TNO Defensie en Veiligheid, dr. ir. J.C. Sabel
11/12	TNO Defensie en Veiligheid, vestiging Den Haag, Archief
13/24	TNO Defensie en Veiligheid, vestiging Den Haag, Business Unit Waarnemingssystemen dr. M.A. Ainslie dr. S.P. Beerens dr. ir. G. Blacquiere M.E.G.D. Colin, MSc ir. F.P.G. Driessen dr. F.P.A. Lam ir. C.A.M. van Moll (3) dr. A. Ranada Shaw dr. P.A. van Walree ing. S.P. van IJsselmuide

The following agencies/people will receive the management summary and the distribution list of the report.

4 ex.   DMO/SC-DR&D

1 ex.   DMO/ressort Zeesystemen

1 ex.   DMO/ressort Landsystemen

1 ex.   DMO/ressort Luchtsystemen

2 ex.   BS/DS/DOBBP/SCOB

1 ex.   MIVD/AAR/BMT

1 ex.   Staf CZSK

1 ex.   Staf CLAS

1 ex.   Staf CLSK

1 ex.   Staf KMar

1 ex.   TNO Defensie en Veiligheid, Algemeen Directeur,
ir. P.A.O.G. Korting

1 ex.   TNO Defensie en Veiligheid, Directie
Directeur Operaties, ir. C. Eberwijn

1 ex.   TNO Defensie en Veiligheid, Directie
Directeur Kennis, prof. dr. P. Werkhoven

1 ex.   TNO Defensie en Veiligheid, Directie
Directeur Markt, G.D. Klein Baltink

1 ex.   TNO Defensie en Veiligheid, vestiging Den Haag,
Manager Informatie en Operaties (operaties), ir. P. Schulein

1 ex.   TNO Defensie en Veiligheid, vestiging Rijswijk, daarna reserve
Manager Bescherming, Munitie en Wapens (operaties), ir. P.J.M. Elands

1 ex.   TNO Defensie en Veiligheid, vestiging Rijswijk,
Manager BC Bescherming (operaties), ir. R.J.A. Kersten

1 ex.   TNO Defensie en Veiligheid, vestiging Soesterberg,
Manager Human Factors (operaties), drs. H.J. Vink